Design of Active Trailer Steering Systems for Long Combination Vehicles using Robust Control Techniques

by

Tushita Sikder

A Thesis Submitted in Partial Fulfillment

of the Requirements for the Degree of

Master of Applied Science

in

Automotive Engineering

The Faculty of Engineering and Applied Science

University of Ontario Institute of Technology

Oshawa, Ontario, Canada,

July 2017

Dedicated to

Mom, Dad, Animesh, and Shabana

Thanks for their unremitting encouragement, robust support and unconditional love and affection.

ACKNOWLEDGEMENTS

I would like to express my sincere gratitude to my supervisors, Dr. Yuping He and Dr. Jing Ren, for their guidance, support and motivation through the entire journey of my master studies. Furthermore, I would like to thank Dr. Yuping He for giving me an opportunity to work on this interesting project.

I would also like to thank my fellow graduate students for their continuous support and assistance.

Finally, I would wish to convey my gratitude to Natural Science and Engineering Research Council of Canada (NSERC) and Ingersoll Axles for providing the financial support for this research.

ABSTRACT

The exponential growth in freightage and the ever-increasing traffic congestion has aided Long Combination Vehicles (LCVs) to emerge as an economical and pragmatic solution for freight transport compared to single unit vehicles. Despite their numerous merits, LCVs face certain stability challenges at high speeds and exhibit inferior maneuverability at low speeds. LCVs are especially susceptible to unstable motion modes, such as rollover, jack-knifing and trailer sway, which has escalated strong concerns regarding their safety. Therefore, it is imperative to develop safety systems with a focus on improving stability, and ensuring safety of LCVs. Active safety systems such as Active Trailer Steering (ATS), have been widely explored to overcome these stability challenges. So far, the design of ATS systems have utilised the Linear Quadratic Regulator (LQR) control technique. Although the LQR technique provides satisfactory results, it fails to control the system in presence of external disturbances such as sensor noise, parametric uncertainties, and un-modelled dynamics. This encourages the need of a robust control strategy. This research focuses on developing an ATS system for a B-train double using robust control techniques. The robust Linear Quadratic Gaussian (LQG) and the μ synthesis control techniques are employed for designing the ATS control system. The control techniques are analysed under a variety of tests by using numerical simulations. TruckSim and MATLAB/Simulink software packages are used for numerical simulations. The results suggest that the LQG control technique effectively controls the system in the presence of noise, whereas the μ synthesis control technique is able to achieve desired system performance in the presence of noise, and parametric uncertainties.

CONTENTS

LIST OF FIGURES

LIST OF TABLES

ABBREVIATIONS

ATS	Active Trailer Steering
ATDB	Active Trailer Differential Braking
CG	Center of Gravity
DOF	Degree of Freedom
EoM	Equation of Motions
ESC	Electronic Stability Control
KF	Kalman Filter
LCV	Long Combination Vehicle
LQG	Linear Quadratic Gaussian
LQR	Linear Quadratic Regulator
MRAC	Model Reference Adaptive Control
PFOT	Path Following Off Tracking
RWA	RearWard Amplification
SLC	Single Lane Change
SMC	Sliding Model Control
TV	Torque Vectoring

NOMENCLATURE

I	Moment of inertia of the tractor
I_1	Moment of inertia of the first trailer
I_2	Moment of inertia of the second trailer
a	Distance of front axle from the CG of the tractor
d	Distance between the CG of the tractor and the first hitch point
e	Distance between the first hitch point and the CG of the first trailer
f	Distance between the CG of the first trailer & second hitch point
m	Total mass of the tractor
u	Vehicle forward speed
v	Lateral velocity of the tractor
Y_i	Reaction force at the hitch point (i=0 to1)
C_1	Cornering stiffness of the front axle of the tractor
C_2	Cornering stiffness of the second axle of the tractor
C_3	Cornering stiffness of the third axle of the tractor
C_4	Cornering stiffness of the fourth axles (1st trailer)
C_5	Cornering stiffness of the fifth axle (1st trailer)
C_6	Cornering stiffness of the sixth axles (1st trailer)

C_7 Cornering stiffness of the seventh axle (2nd trailer)

C_8 Cornering stiffness of the eighth axles (2nd trailer)

C_9 Cornering stiffness of the ninth axle (2nd trailer)

b_1 Distance of second axle from the CG of the tractor

b_2 Distance of third axle from the CG of the tractor

h_1 Distance between the CG of the first trailer and the fourth axle

h_2 Distance between the CG of the first trailer and the fifth axle

h_3 Distance between the CG of the first trailer and the sixth axle

k_1 Distance between the CG of the second trailer and seventh axle

k_2 Distance between the CG of the second trailer and eighth axle

k_3 Distance between the CG of the second trailer and the ninth axle

m_1 Total mass of the first trailer

m_2 Total mass of the second trailer

v_1 Lateral velocity of the first trailer

v_2 Lateral velocity of the second trailer

φ Yaw rate of the tractor

φ_1 Yaw rate of the first trailer

φ_2 Yaw rate of the second trailer

δ	Steering angle for the front axle of the tractor
$f_1(\alpha_1)$	Lateral force on the first axle of the tractor
$f_2(\alpha_2)$	Lateral force on the second axle of the tractor
$f_3(\alpha_3)$	Lateral force on the third axle of the tractor
$f_4(\alpha_4)$	Lateral force on the fourth axle of the tractor
$f_5(\alpha_5)$	Lateral force on the fifth axle of the tractor
$f_6(\alpha_6)$	Lateral force on the sixth axle of the tractor
$f_7(\alpha_7)$	Lateral force on the seventh axle of the tractor
$f_8(\alpha_8)$	Lateral force on the eighth axle of the tractor
$f_9(\alpha_9)$	Lateral force on the ninth axle of the tractor

CHAPTER 1

Introduction to Long Combination Vehicles (LCVs)

1.1. Introduction

This chapter introduces the Long Combination Vehicles (LCVs) and its different configurations. Thereafter, it highlights the merits and limitations of such vehicles. The motivations behind this research are discussed. Furthermore, the thesis objectives and contributions are presented.

1.2. Long Combination Vehicles (LCVs)

LCVs are extensively preferred today for transportation of goods. LCVs are heavy road vehicles that exceed dimensions of a typical heavy truck-trailer or tractor-semitrailer combinations, in both length and weight. In Canada, any articulated heavy vehicle having an overall length of 25 meters and over is considered a LCV. A LCV comprises of a towing unit, known as a tractor, and one or more trailing units. Each of these units are connected with each other at an articulated point with the assistance of mechanical couplings, such as pintles, fifth wheels, dollies and hitches [1, 2].

The initial LCVs had a total length less than 26 meters. Such vehicles are termed as *short LCVs* and have been widely used for many years in USA, Australia, Canada, Finland, Sweden and other countries. The *intermediate LCVs* are vehicles with a maximum total length of 30 meters, and are capable of transporting four 20-feet equivalent units (TEUs). These LCVs are designed for long distance (over 400 km) cargo transport and use designated freeway network, as they are only permitted on dedicated routes [3].

Long LCVs, with a total length more than 30 meters consist of two or more trailers or semi-trailers. They are called as *Road trains* in Australia, and *Doubles* or *Triples* in USA [3]. Figure 1.1 depicts a commonly used configuration of a LCV, known as a B-train double. LCV configurations are discussed in detail in section 1.2.

Figure 1.1: Configuration of a B-train double.

In Ontario, Canada, LCVs can achieve up to 40 meters of overall length [2]. LCVs can improve the productivity of long distance road transportation by increasing the available cargo capacity per driver by 25-100% [4, 5]. Since in several countries there exist restrictions on the permissible total weight of LCVs, an increase in productivity by the volume of transported cargo is witnessed as enhanced productivity. LCVs exhibit superior fuel economy in comparison to a single unit vehicles [4-6]. With less fuel usage, they can reduce up to 11 million tons of greenhouse gas emissions entering the environment [2, 7, 8]. An investigation, conducted by a Swedish transport research institute, estimated that LCVs have the capability to reduce the fuel consumption and emissions by 15%, which can result in a 23% saving in operational costs [9, 10].

A study highlights that the probability of traffic accident occurrence increases with number of road users [7]. Since with the use of LCVs, fewer road vehicles are required to transport the same payload, the number of road users are reduced. This leads to fewer accidents, and reduction in road wear [3, 9]. In a report by Woodrooffe and Ash, it is estimated that the use of LCVs in Alberta, Canada can result in a 29% saving in shipping costs, 44% reduction in mileage, 32% reduction in fuel consumption and emissions, and 40% decrease in road wear [3, 10]. These advantages have favoured LCVs in emerging as the preferred mode of transportation in past years. However, from a safety perspective there are concerns regarding the maneuverability and stability of LCVs. This has prompted various studies in this area.

Despite numerous advantages, LCVs face certain stability challenges. At high speeds, their high centre of gravity (CG) and large size results in low lateral stability [1]. At these speeds, they are also prone to unstable motion modes, such as rollover, jack-knifing and trailer sway. Whereas, at low speeds, the path-following off-tracking (PFOT) becomes a predominant concern, resulting in inferior maneuverability [1, 11-14]. These unstable motion modes often contribute in causing fatal accidents [11-13]. Therefore, improving the safety and reliability of such vehicles is a primary concern [1, 3, 10, 13].

1.3. Configurations of LCVs

A LCV is an assembly of two or more vehicle units. These vehicle units are connected to one another at articulation points by mechanical couplings, known as fifth-wheels. LCVs comprise of two major units, the leading unit and the trailing units.

Leading units are commonly known as *tractors*. They contain the LCV's powertrain and perform the function of towing the trailing units. *Tractors* comprise of a steerable front axle that is manipulated by the driver. Figure 1.2 depicts a *tractor*.

Figure 1.2: The towing unit of the LCV, *tractor*.

Figure 1.3: The *trailer* of a LCV.

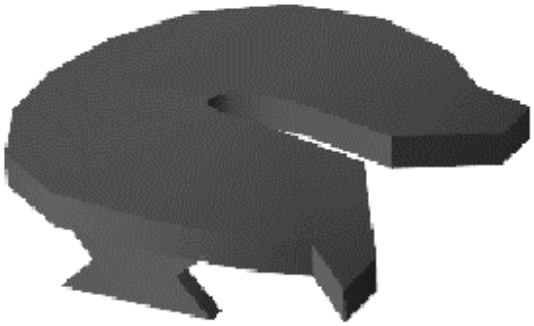

Figure 1.4: Mechanical coupling- Fifth-wheel.

Figure 1.5: Mechanical coupling –Dolly.

Trailers are categorised into full trailers and semitrailers. Full trailers contain running gear at both ends, front and rear. Therefore, are capable of fully supporting themselves vertically. Contrarily, semitrailers contain running gears only at the rear end and hence require a tractor to provide the essential vertical support at the front. Figure 1.3 depicts a semitrailer. Although a tractor can provide the front vertical support, sometimes a converter dolly is employed to *convert* a semitrailer into a full trailer. The dolly provides the functioning of a tow bar and the steerable front running gear, which are both not available on the semitrailer [15]. Figure 1.4 illustrates the fifth-wheel coupling utilised to connect the adjacent vehicle units, whereas Figure 1.5 depicts the above-stated converter dolly.

Multi-trailer trains are created by connecting one or more additional trailers to a tractor-semitrailer combination. A combination with two trailers is called a *double* and with three trailers is called a *triple*. Double trains are frequently used in North America and Australia. Triples are rare, and usually seen outside of some western states and provinces of the US and Canada, respectively, and the outskirts of Australia [15].

Vehicle trains are classified as A-, B-, or C-trains depending upon the nature of the couplings used to connect the adjacent trailers. A-trains are the most common amongst the listed configurations. They employ a converter dolly for connecting the adjacent trailers. However, A-trains exhibit high Rear-Ward Amplification (RWA), an undesirable dynamic performance measure. RWA signifies that the rearmost trailer has the tendency to exhibit the highest lateral acceleration compared to other vehicle units. In order to overcome this issue, the B-trains were introduced. B-trains utilise a combination of semitrailers in place of full trailers to reduce the number of articulation points. To accomplish this, towing trailers are equipped with an extended frame section at the rear, on which a fifth-wheel is mounted to accommodate the towed semitrailer. Although B-trains improve the dynamic performance, they exhibit practical and logistical problems as they require special semitrailers in the forward trailer positions. A-trains, on the other hand, can be created by using conventional semitrailers with the help of a converter dolly.

The C-train was developed to acquire dynamic advantages of the B-train while retaining the logistical advantages of the A-train [15]. A C-train consists of a converter dolly which has a double drawbar arrangement that joins the tractor with a pair of laterally spaced pintle hitches. This arrangement eliminates both the yaw and roll motions that are present in an A-train's pintle hitch. In addition, the C-train has the same number of yaw articulation points as the B-train. However, the geometry of the C-train dolly requires a wide spread among the rear axles of the towing semitrailer and the front of the towed semitrailer, and this geometry contributes to scrubbing of tires. C-trains usually have self-steering axles to mitigate tire scrubbing during tight corners [15, 16].

1.4. Operational Behavior of LCVs

LCVs demonstrate stability challenges at low speeds as well as at high speeds [1]. At low speeds, LCVs exhibit poor maneuverability and tire scrubbing. Whereas at high speeds, excessive RWA causes trailer swing, path deviation, rollover, jack-knifing and large sideslip [11, 13]. Such scenarios results in poor lateral stability, and are not only dangerous for the LCV itself, but to other road users and the infrastructure.

1.4.1. High Speed Stability

One of the major safety issues concerning LCVs is rearward amplification (RWA) at high speeds. *Rear-Ward amplification is the ratio of the peak lateral acceleration of the rearmost trailer's center of gravity to the lateral acceleration of the leading unit during a lane change maneuver* [17]. A lower RWA value reduces the vehicle's tendency to rollover [18]. However, for overall performance, the ideal value for RWA ratio is 1 [15].

RWA implies that the rearmost trailer has a tendency to exhibit higher peak lateral acceleration as compared to that of the tractor [15, 17]. RWA of lateral acceleration is the fundamental cause for rollover at high speeds. It is prominent when an articulated vehicle travelling at high speeds (above 80 km/h) negotiates a turn or lane change maneuver. In such situations, it is observed that the rear axle pulls outward from the steering axle's path. Moreover, in situations, where the driver performs sharp maneuvers to avoid an unexpected and sudden obstacle, the rearmost trailer exhibits a tendency to skid sideways into other traffic lanes (Off-tracking). Such a condition may also result in rollover.

Figure 1.6: The B-train double during the jackknifing scenario.

Rollover is a scenario in which a vehicle tips over onto its side or roof. Vehicle rollovers are distinctly categorized into two types, *tripped* and *untripped* [19]. External forces causes *tripped* rollovers such as a collision with another vehicle. A survey shows that 34% of the rollover accidents are caused due to collision with an object, and 60% of rollover accidents occur due to driving on an embankment [19, 20]. *Untripped* rollovers are a result of high-frequency steering inputs, speed instability, and insufficient friction with the ground.

In LCVs, inferior lateral stability and relatively low roll stability at high speeds accounts to rollover scenarios. In 1996 and 1997, the US National Highway Traffic Safety Administration recorded over 15,000 rollover accidents of commercial heavy vehicles. Of which 9400 rollovers accidents were of tractor semitrailers alone [11, 21]. Rollover accidents of heavy vehicles cause destruction to vehicle themselves and damage to property. Another research states that the majority of rollover accidents occurring in Netherlands involves articulated heavy vehicles [22].

It also mentioned that these accidents occurred in three main situations: sudden course deviation, often in combination with braking from a high initial speed; high speed while cornering; and load shift [11, 22]. Figure 1.8 illustrates B-train double exposed to a rollover scenario.

Figure 1.7: The B-train double during the rollover scenario.

Winkler et al. in their study reviewed the US accident statistics and reported a strongly negative correlation between steady-state roll stability and the average frequency of rollover accidents [2, 23]. They illustrated through their work that a slight increase in roll stability significantly reduces the frequency of rollover accidents. In particular, occurrence of rollover is highly influenced by RWA ratio [24]. In reality, it is extremely difficult for a driver to sense an impending rollover. A driver's perception of the vehicle's stability is often based on the tractor's response that he/she controls, rather than the trailers [23]. Since in LCVs, the rearmost trailer is usually the first unit to experience rollover. By the time the driver realizes the rollover occurrence, it is usually too late for the driver to take corrective action.

1.4.2. Low Speed Maneuverability

At low speeds, the primary challenge encountered by LCVs is the path following ability of its rearmost trailer. The performance measure is termed as Path-Following Off-tracking (PFOT). In LCVs, where the rearmost axle cannot be steered independently during cornering, the rear end tends to follow a different path with respect to the path of the tractor.

The complex configurations and large sizes of LCVs contribute to a poor path-following performance [25, 26]. A research conducted by [15] states that the amount of PFOT of each unit is directly proportional to the square of its wheelbase. Although it may also depend on other factors, such as vehicle forward speed. The poor path-following causes scrubbing of tires during tight cornering maneuvers and damage to the road infrastructure. Moreover, it also increases the safety concerns for the neighboring traffic, by intruding the nearby lanes [27]. Such scenarios are witnessed during lane change maneuvers and cornering.

PFOT can be defined as the maximum radial offset between the path of the tractor's front axle center and that of the trailer's rear axle center during a specific maneuver [28]. A research based on the traffic accidents provide substantial evidence that PFOT is a crucial measure for safe vehicle operations [24]. Due to PFOT, the design of pavements, roads, and trucking yards requires more land areas to ensure the safe operations of LCVs.

PFOT is a result of unbalanced centrifugal forces [29]. Although, PFOT is prominent at low speeds, it may also occur at high speeds. At high speeds, the rearmost trailer deviates from its intended path and does not follow the path of the tractor. The relationship between truck size and weight and its propensity towards high RWA value is complex and hard to predict.

However, such factors are deemed as significant contributors to PFOT. For example, a vehicle with low RWA ratio can perform poorly in high-speed transient off tracking (as with the trucks carrying dense cargo). A PFOT scenario can be observed in Figure 1.9, where the vehicle intended path is deviated while cornering.

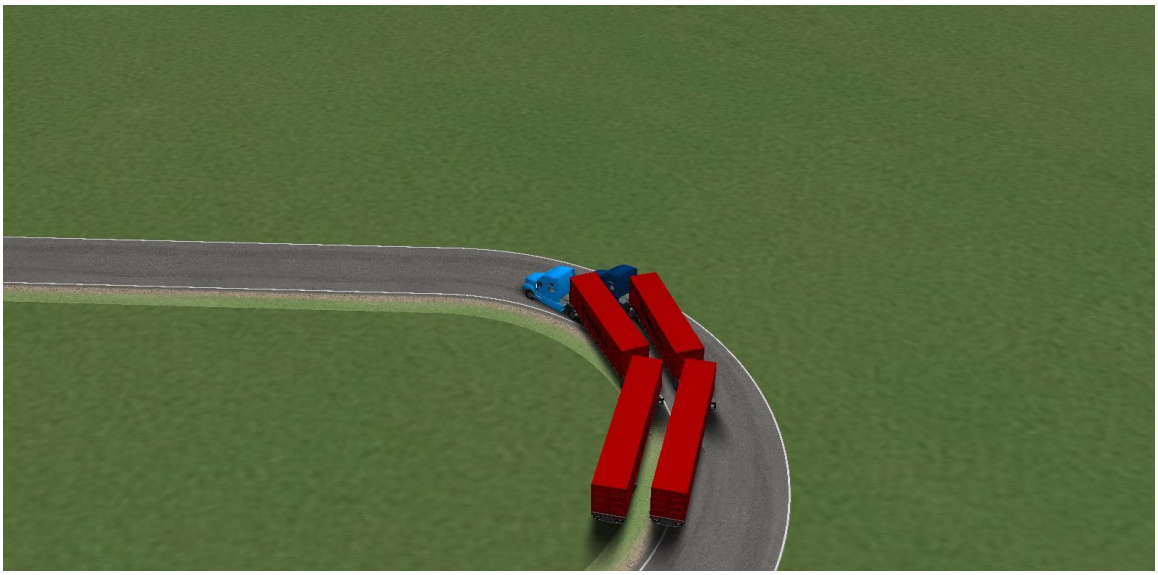

Figure 1.8: The B-train double during the Path Following Off-Tracking (PFOT) scenario.

1.5. Motivations

Over the past few decades, safety of heavy vehicles has risen an alarming concern internationally. The severe consequences of accidents involving heavy vehicles and their strong representation in traffic fatalities has captured the attention of the researchers around the world. Heavy vehicles are integral to the goods transportation system. In fact, the drastic increase in the amount of transported goods, and the growing traffic congestion problem demands the use of LCVs than the conventional tractor-semitrailer combinations [10].

The advantages of LCVs are not only limited to the reduction of the congestion problem, but also include economic and environmental benefits. This provides a compelling motivation for enhancing the LCV's driving characteristics and their stability in critical conditions. However, enhancing the dynamic performance of a complex vehicle such as LCV requires complex active safety systems. This has escalated the demand for active safety systems such as ATS.

So far, most of the researches conducted in a view to increase stability of LCVs with ATS have implemented LQR based control strategies. LQR controllers are comparatively simple to synthesize, and they work as a feedback controller, which enables them in delivering superior performance. Therefore, LQR controllers are preferred at the design stage for building a controller.

However, such controllers do not exhibit robustness in the presence of parameter uncertainties, un-modelled dynamics and external disturbances. In addition, while modeling the LQR controller vehicle forward speed and system parameters (e.g. cornering stiffness) are assumed as constants. The LQR control design also assumes availability of full-state vector feedback. However, it is inefficient and expensive to measure all states of the system. Such assumptions contradict the real life scenarios. This encourages an investigation into robust control strategies such as Kalman filtering with an LQR controller, and μ synthesis. A Kalman filter (KF) works as a state estimator for estimating the states of the parameters based on the previously collected data and the system model. Thus, a combination of KF and LQR controller can overcome certain limitations of the LQR control technique. The μ synthesis technique addresses the robustness concerns and effectively deals with systems' uncertainties.

1.6. Thesis Objectives and Contributions

So far, most of the research conducted has focused on designing ATS in LCVs using the LQR controllers. This study anticipates to broaden the current research by offering a reliable comparison of the mentioned control strategies for implementing ATS. Although, the LQR based controllers provide satisfactory results, in the presence of the disturbance such controllers are unable in achieving optimal performance. A prime objective of this research is to design a robust controller that is capable of controlling the system in the presence of external disturbances such as noise and parametric uncertainties.

To augment the robustness of the LQR controller, a Kalman Filter (KF) is used. KF aids the LQR controller in dealing with noise. So far, the combination of a LQR control with KF, also known as LQG (Linear Quadratic Gaussian) controller, has not been applied to ATS systems for a B-train double configuration.

Additionally, the robust μ synthesis technique is employed to design the ATS control system. The μ synthesis control technique has not been explored for a B-train double with an ATS system, with the purpose of improving robustness. This study also presents a comparison between the mentioned control strategies, LQR, LQG and μ synthesis for designing ATS systems in LCVs.

Numerical simulations are performed while considering the presence of sensor noise. Moreover, the impact of noise on the efficacy of the control system is evaluated, another aspect that has been insufficiently addressed. Furthermore, the simulation results of the synthesised controller are validated using TruckSim and MATLAB co-simulation. All controllers are designed to address the high-speed stability concerns of LCVs.

1.7. Thesis Organization

Chapter 1 outlines a brief introduction of LCVs and its configurations, it also highlights the motivation of this thesis. Furthermore, it describes the objectives and contributions of this research. The rest of the thesis is organized as follows.

Chapter 2 constitutes a literature review of the LCVs with ATS. It also highlights the different control systems used for implementing ATS for LCVs. Further, it discusses the control strategies such as LQR, LQG and μ synthesis that are used in this research for designing the ATS control system.

Chapter 3 introduces the vehicle system modelling, validation and stability analysis. It begins with a brief introduction of a hand derived 4-DOF linear model based on Newton's equations for motion. Further, the model validation is conducted by using models generated by Equation of Motion (EoM) software and the TruckSim software. It also describes the selection rationale for choosing the appropriate active axles for implementing ATS in a B-train double. Finally, chapter 3 presents the Eigenvalue stability analysis of the B-train double over a range of vehicle forward speeds and changing payloads.

Chapter 4 discusses the synthesis of various controllers presented in this work. Moreover, it illustrates the relevant control theory. Chapter 5 presents the simulation results of the ATS system's performance using the three control strategies. This sections aims at establishing the efficacy of the controllers, LQR, LQG and μ synthesis. In Chapter 6, conclusions are drawn regarding the proposed control strategies for implementing ATS in B-train double, and the future work related to the above-mentioned study is presented.

CHAPTER 2

Literature Review

2.1. Introduction

This chapter introduces the design methodology of the ATS systems for LCVs. A survey will aid in illustrating the research performed in past decades in order to find viable solutions to overcome the difficulties of inferior maneuverability and lateral stability in LCVs. It includes a review of the related control strategies, which are considered for this research, the LQR technique, the LQG technique and the μ synthesis technique.

2.2. Vehicle Control Systems

The past few decades has witnessed numerous technological advancements within the automotive industry. This has led to a significant improvement in dynamic characteristics and safety of the road vehicles. These advances can be attributed to the introduction of vehicle stability control systems. United States Government has established FMVSS 126 vehicle standard that mandates all vehicles sold after 2012, in North America to include an electronic stability control (ESC) system [30, 31]. An ESC system is an emergency safety system, which detects the discrepancies between the intended path of the vehicle and the actual path of the vehicle. To rectify the erroneous path deviation, the system produces a yaw moment by applying the brakes to allow safe operation, and additionally aids the driver in maintaining the intended path. Simulations and tests reported in the paper [32] demonstrate that the ESC systems can effectively enhance vehicle stability and path-following performance under emergency maneuvers at high lateral accelerations.

The prime objective of stability control systems is to inhibit vehicles from going beyond the stability limits. Such systems safeguard the driver from losing control and thereby, ensures their safety. With the advance in control technologies, it is now possible to actively control and enhance dynamic performance and safety of vehicles. Such active systems are based on similar control principles as ESC systems. However, they aim to enhance the vehicle's performance throughout its operation rather than only intervening in emergencies [33].

2.3. Active Safety Systems (ASSs) in LCVs

Until now, numerous studies have been conducted to overcome the design related issues of LCVs. Primarily, active control techniques such as Torque Vectoring (TV), Active Differential Braking Systems (ADBS) and ATS have been investigated [34]. LCV's complex structure, large size, and high center of gravity results in inferior maneuverability and lateral instability. This inhibits them to effectively negotiate common maneuvers such as single lane change, double lane change and so on. Moreover, it makes them susceptible to unstable motion modes.

In order to negotiate these maneuvers safely, it is vital to improve LCV's stability in different operating conditions [35]. Traditionally, LCVs comprise of non-steerable trailer axles. The non-steerable axles are simple, economical, and demonstrate reasonable performance. However, while cornering LCVs with non-steerable axles, tend to scrub the tires against the road, and exhibit poor handling characteristics such as jack-knifing and trailer sway [12, 13, 35]. To reduce tire scrubbing and to enhance the low speed maneuverability, passive steering systems (PSS) are proposed. These systems steer the trailer axles according to a geometrical relationship or force-moment balance [10, 11, 36].

However, PSS has a detrimental effect on the high speed performance of LCVs, resulting in poor handling, higher lateral acceleration and high-speed off-tracking [11, 13, 36]. Moreover, PSS are designed to work in steady-state circular motion, and generally cannot provide the correct steering inputs for transient maneuvers [13].

Figure 2.1: The B-train double configuration with Active Trailer Steering system (ATS).

Active control techniques offer viable solutions by acknowledging LCVs conflicting design problem. To address the off-tracking in transient low-speed maneuvers, Active Trailer Steering (ATS) systems have been proposed. They work similar to passive steering systems by steering the trailer axles. However unlike the PSS, the steering angle of each trailer axle is not completely dependent on the simple geometric relationship or force-moment balance. The ATS system considers the vehicles current states [13, 36] to calculate the optimal steering angle. Figure 2.1 demonstrates the functioning of an ATS system in a B-train double configuration.

Hata et al., [37] proposed a feedforward control design for an ATS system in trucks, which focused on reducing the tail sway. The presented design, improved path following ability at low speeds and successfully reduced the swept path without introducing any tail sway. Gohring et al., [38] and Pfung et al., [39] performed similar research on trucks. Notsu et al., [40] presented a research investigating the cornering behavior of a tractor-semitrailer

with a steerable axle. Here, the designed control system aimed at improving the path following ability of the trailer at low speed and during gentle curve negotiations. Notsu et al., in continuation of the above study, proposed a control strategy denoted as the *coupling point path follow control*. In this strategy, the semitrailer's rear end was manipulated to follow the path of the fifth-wheel. However, the idea was not pursued further due to a number of limitations of the controllers, which required further evaluation for it to become a practical proposition [13].

In 2009, the Cambridge Vehicle Dynamics Consortium (CVDC) developed an active steering system for tractor-semitrailers to improve the path-following ability. The developed steering control strategy steered the wheels of the semitrailer, such that the trailer rear end follows the trajectory of the fifth-wheel at all speeds [11, 41]. This strategy improves maneuverability and reduces scrubbing of tires at low speeds, while improving stability, dynamic response and handling at high speeds. The proposed controller is nonlinear, where it relies on a look-up table to account for the information propagation delay caused by the length of the trailer unit.

Since then, ATS has been widely investigated to improve the maneuverability [4 ,11,13, 28, 34] and lateral stability at high speeds [10, 43, 44]. The trade-off between maneuverability and lateral stability has also been widely studied [11, 13, 44-46].

2.4. Control Systems for ATS Implementation

2.4.1. LQR Technique

The linear quadratic regulator (LQR) technique is a popular design method that provides practical feedback gains. The past two decades has seen numerous applications of LQR-based technique for implementing the ATS systems for LCVs [44, 47].

The LQR controller for ATS systems in LCVs focuses on improving both low-speed maneuverability and high-speed stability [11, 14, 28, 29, 44, 45]. Many published numerical simulation results show that ATS systems can achieve acceptable levels of RWA ratio and PFOT [29, 45, 47, 48].

Cheng et al. used the LQR technique for building a path-following controller, which was capable of minimizing the path-tracking error in steady state maneuvers using ATS [11]. In addition, they focused on building a roll stability controller using the LQR technique. The ATS controller ensured improved roll stability in transient maneuvers, while maintaining the path-tracking deviation within an acceptable range. Palkovics and El-Gindy proposed an active steering control system to improve the tractor's handling behavior [49]. The system focused on minimizing the tractor's states, the yaw rate and the sideslip angle. El-Gindy et al. [17] and Hac et al. [50] further followed this idea of state minimization by using an LQR controller.

Rangavajhula et.al [28] developed an active trailer steering controller of articulated vehicles with a tractor and three full trailers. They used a LQR controller to minimize the RWA ratio and the off-tracking at the same time. It is noteworthy that the LQR technique is the most widely studied control strategy for implementing ATS [13, 25, 29, 42-45].

A survey shows that the LQR technique provides the analytical solution with relatively simple design and low computational time [47]. Therefore, the LQR technique is often used as a platform for building ATS systems for LCVs. However, in designing the LQR controllers, few unrealistic assumptions are made, such as the vehicle model parameters and operating conditions are constant.

In reality, the vehicle system parameters vary with different operating conditions. For example, the payload of a trailer and vehicle forward speed may vary and these factors may contribute to huge variations in performance. In addition, the LQR technique does not consider the external disturbances. The result of the optimization process of the LQR technique is in a form of feedback controller that provides constant gains to all states under all operating conditions. This may not be the ideal method for dealing with system uncertainties, as for the robustness we require different gains for different states. Hence, the conventional LQR controllers often face difficulties in predicting the true behavior of the vehicle [30, 47, 51]. Therefore, there exists a necessity to develop a robust controller that is capable of dealing with such system uncertainties.

2.4.2. Robust Controllers

It is crucial for a control system design to be robust. In reality, engineering systems are vulnerable to external disturbance and measurement noise. There are always differences between mathematical models used for designing the controller and the actual system [52]. The concept of robust control was developed in early 1980s and soon a number of techniques were established for dealing with uncertainties in the system. A robust controller explicitly deals with uncertainties that cannot be dealt with conventional controllers like the LQR controller.

A well-established robust control technique is H∞. It was developed by Duncan McFarlane and Keith Glover. The H∞ technique effectively rejects disturbances, which means that the system will experience minimal deviation from the expected behavior in spite of the present disturbances [53]. The H∞ optimization approach can achieve robust stability against system perturbations. However, it guarantees robustness only for nominal system. Moreover, the H∞ technique does not always ensure robust stability and robust performance of the closed loop system [52]. In order to achieve robust stability and robust performance, design methods based on the structured singular value μ is used [52].

Sliding Mode Control (SMC) method is another widely preferred robust control technique. It is simple in design and performs well while dealing with complex nonlinear dynamic plant with uncertainties. The SMC design provides a systematic approach for a problem related to maintaining system stability [34, 47, 54, 55]. However, the SMC controller is susceptible to a phenomena known as chattering [54], a tendency to exhibit high frequency control output, which poses risk of damaging the mechanical actuators (brakes, steering etc.). ATS systems using the SMC technique in LCVs are limited [34].

Model Reference Adaptive Control (MRAC) is another technique, preferred for linear systems [46]. Although it provides additional flexibility under wide range of vehicle operating conditions, it is unable to produce satisfactory results in presence of external disturbances such as unreliable measurement data [30]. When dealing with inaccurate system model and external disturbances, the MRAC controller may exhibit inferior robustness [30, 51].

Fuzzy logic controller exhibits good performance while dealing with uncertainties in non-linear systems. However, to achieve optimal performance it is crucial to tune the controller well, which is a highly intricate and complex process. So far, only few studies have incorporated the fuzzy logic control technique in LCVs for implementing ATS [14, 34, 45].

Another widely explored method is the Linear Quadratic Gaussian (LQG) technique. It was developed to overcome the shortcomings of the LQR control technique. An LQG controller is the combination of a LQR controller and a Kalman filter (KF). In a LQR controller, it is assumed that the entire state vector is measured at all times. In reality though, only a few states are measured and there always exists disturbances in measurements and processes, which significantly affect the controller's performance. Thus, using a filtering technique is imperative. Often the Kalman filter along with LQR is used to filter the noise and thereby increase the robustness of the system [52, 56, 57].

2.4.2.1. Kalman Filter (KF)

Certain control strategies require the full feedback of vehicle states, which in many cases cannot be measured or extracted easily. The KF is known as an effective mathematical tool that is capable of estimating the states of a dynamic system from a series of incomplete and noisy measurements. Presently, the KF plays a vital role in many engineering applications as it allows incorporation of real world sensing in our systems [58, 59]. Since its introduction in 1960's, KF has been the subject to extensive research, especially in the fields of assisted navigation or autonomous vehicles [58]. Moreover, given its design simplicity and robustness, KF has been used for motion prediction [59].

The role of KF with linear vehicle model is to estimate unknown vehicle states, which are required by the controller. The KF can be used with limited sensor information like steering wheel angle, yaw rate, roll rate, and lateral velocity or acceleration as inputs. It is seldom that the optimal conditions exist, and yet the filter performs well for many applications [60, 61]. The KF estimates the process states, which are used to calculate the control inputs, and then obtain feedback from the system [62-64].

2.4.2.2. Linear Quadratic Gaussian (LQG) Technique

As stated earlier, while dealing with the LQR technique, it is assumed that the vehicle parameters are constant. This is unrealistic as system parameters vary when exposed to different operating conditions, at least there is always some measurement noise present [30, 47]. In some studies, filtering techniques are used to analyze the effectiveness of the LQR control design. LQG is a combination of two concepts, Linear Quadratic Regulators (LQR) for full state feedback and KF for state estimation. A research presented by Dinc et al. depicts the application of LQR controller with a Kalman filter for controlling the longitudinal flight motion of an Unmanned Air Vehicle (UAV). The simulation results show improvements in comparison with classical design. The combined approach offers design flexibility and ability to circumvent the sensor noise [62]. Another study performed by Chingiz et al. [56] for an altitude controller showed the similar results. In case of the disturbances, Kalman filter accurately estimated the values of the states for the LQR controller and thereby increased the effectiveness of the control system.

In a research conducted by Cheng et al., a Kalman filter was used to estimate sideslip angles, required by the LQR controller for constructing an optimal control for tractor semitrailer ATS system. The presented design was equipped to improve the roll stability

in transient maneuvers while keeping the path-tracking deviation of trailer's rear end within the acceptable range [13]. Labane et al. compared the two controllers, LQR and LQG, for its effectiveness in achieving the stability of lateral and longitudinal flight dynamics of an aircraft. The LQR controller demonstrated expectable performance, when the system was not subjected to external disturbance. However, the LQG controller demonstrated an excellent following of the outputs of plant with a steady shift error [65].

Today the LQG design technique is deeply rooted in optimal stochastic control theory and holds sustainable solutions for many applications in the modern world these range from flight navigation, missile navigation control systems, medical processes controllers and even nuclear power plants [53, 58].

2.4.2.3. μ synthesis Technique

In a control system, it is critical to acknowledge the effect of external disturbances, signal noise and modeling inaccuracies [52]. Systems that are capable of tolerating such variability and uncertainty are called robust. This problem of stabilizing the uncertain linear dynamic systems has been studied for almost three decades. The challenge encountered by every control engineer is to tackle the difference between the actual system and its mathematical model used in control system designing [66]. In the traditional control theory, a typical system model assumes few parameters and considers few as constant. In addition, the robustness, of these single input single output systems (SISO) is achieved through the proper designing of maximum phase and gain margins [52]. However, in realty, the plant or the system to be controlled is non-linear and consists of multiple inputs and multiple outputs (MIMO). A real-world system is vulnerable to various types of uncertainties such as non-ideal sensors, actuators, external noises, parametric uncertainties, un-modelled non-

linearities and many others [66]. Non-linear control techniques, such as SMC, Fuzzy logic, exist but they are often difficult to tune for good results. Moreover, to an extent it is mandatory to linearize the non-linear systems around pre-defined operating points for better results.

Often linear control methods are used to control non-linear systems [67]. H∞ and μ synthesis techniques are such linear control methods that can be used to control MIMO systems. From its introduction since 1980s, considerable advance has been witnessed in the field of μ synthesis. The μ synthesis technique is capable of addressing robustness issue of systems with uncertainties and external disturbances [30, 51, 68-73]. So far, most of the published μ synthesis controllers are designed for single unit vehicles. Limited attention has been given for designing the controller for a LCV. A part of its credit can be given to difficulties faced in the selection of the weighing functions.

The weighting functions are a form of lead and lag signals that compensates the effects on the performance and robustness of the systems. Traditionally, these functions are chosen using the tedious and time-consuming, trial and error method. A research shows the effectiveness of a μ synthesis controller in achieving lateral stability and path-following with ATDB system for a car-trailer combination [28]. Further, to track the trajectory of the vehicle, a reference yaw-rate model is added. This ensures that the vehicle maintains the intended path.

The μ synthesis technique overcomes the effect of the disturbances in the system and achieves robustness of the closed-loop system for all possible plant uncertainties [52].

4.5. Summary

This chapter describes the importance of vehicle control systems in today's world. A specific safety system concerned with LCVs, ATS is discussed. A literature review is presented which indicates that the ATS systems can effectively assist in achieving superior lateral stability and maneuverability for LCVs. Various linear control methods have been used for incorporating ATS in LCVs. The most popular method is the LQR technique. Other control strategies such as fuzzy logic and SMC are rarely employed as they require the complex tuning of the controllers. Traditional control techniques like the LQR controller fail to exhibit robustness in presence system uncertainties. Several research studies have recommended the use of robust control strategies in order to achieve robustness under uncertainties.

Control strategies like LQG and μ synthesis are explored with the purpose of enhancing the robustness of the ATS control system. The LQG technique is utilised to overcome the shortcomings of the LQR controller. A LQG controller is a combination of a LQR controller and a Kalman filter, where Kalman filter assists in rejecting the systems disturbance and upsurges the robustness of the system. The μ-synthesis enables to overcome the effect of the disturbances in the system output and to achieve robustness of the closed-loop system for all possible plant uncertainties [52].

CHAPTER 3

Vehicle Systems Modelling, Validation and Stability Analysis

3.1. Introduction

This chapter deals with the modelling, validation and stability analysis of the vehicle system. First, a linear 4-DOF yaw plane model for a B-train double LCV configuration is presented. The EoM [74, 75] software is used to generate a comparative vehicle model. Thereafter, TruckSim is used to validate the 4DOF linear model. This chapter presents the selection rationale for the active trailer axles of the B-train double. The ATS axles that demonstrate the highest influence on the vehicle's stability are considered as the suitable axles for further research. Finally, the stability of the vehicle system is analyzed using Eigenvalue analysis method under vehicle parameters such as change in forward speed, change in payload, cornering stiffness, moment of inertia and so on.

3.2. Vehicle System Modelling

3.2.1. 4-DOF Yaw Plane Model of a B-train double

As mentioned in chapter 2, vehicles are complex nonlinear systems. However, for analyzing such a complex system, simplified vehicle models are required. This section presents the modeling of a linear 4-DOF vehicle model. The model is developed by defining governing equation of motions, based on the Newton's second law of motion. The modelling approach is adopted from Ellis [76], and has been previously implemented in [1, 34, 35].

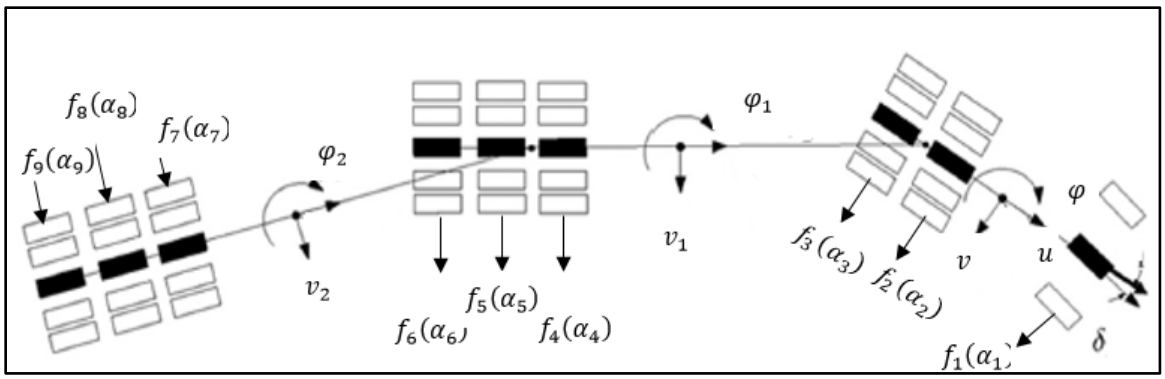

Figure 3.1: Schematic diagram of a B-train double showing the forces and moments.

Figure 3.1 show the schematic configuration of the B-train double. The vehicles comprise of a tractor and two trailers. The tractor consists of one front axle and two rear axles. Both the trailers shown consist of three axles each. The vehicle units are connected to each other using fifth-wheel couplings.

The following assumptions are made during the design synthesis of the 4-DOF model [1].

1. Each axle is represented by a single tire.

2. The vehicle's forward speed u is constant. Also, u and the steering angle δ are known.

3. The articulated angles between the adjacent units are small.

4. The pitch and roll motions, braking forces, and the aerodynamic forces are neglected.

5. The relation between the lateral force of a tire and the sideslip angle is linear ($f_i(\alpha_i) = C_i$ where i =1 to 9).

The model is developed using the body-fixed coordinate system. The 4-DOF model consider four independent motions, tractor's lateral velocity and yaw rate, first trailer's and second trailer's articulation motions. In the vehicle model, the articulation motion of the two trailer is depicted as yaw rates. The governing equation of motions for each vehicle unit, the tractor, first trailer and second trailer are defined below.

The governing equations of motion of the tractor are expressed as:

$$m(\dot{v} + u\varphi) = f_1(\alpha_1) + f_2(\alpha_2) + f_3(\alpha_3) - Y \tag{3.1a}$$

$$I\dot{\varphi} = af_1(\alpha_1) - b_1 f_2(\alpha_2) - b_2 f_3(\alpha_3) + dY \tag{3.1b}$$

The governing equations of motion of the first trailer are formulated as

$$m_1(\dot{v}_1 + u\varphi_1) = f_4(\alpha_4) + f_5(\alpha_5) + f_6(\alpha_6) + Y - Y_1 \tag{3.2a}$$

$$I_1\dot{\varphi}_1 = -h_1 f_4(\alpha_4) - h_2 f_5(\alpha_5) - h_3 f_6(\alpha_6) + eY + fY_1 \tag{3.2b}$$

The governing equations of motion for the second trailer are defined as

$$m_2(\dot{v}_2 + u\varphi_2) = f_7(\alpha_7) + f_8(\alpha_8) + f_9(\alpha_9) + Y_1 \tag{3.3a}$$

$$I_I\dot{\varphi}_2 = -k_1 f_7(\alpha_7) - k_2 f_8(\alpha_8) - k_3 f_9(\alpha_9) + jY_1 \tag{3.3b}$$

The sideslip angles of the axles are:

$$\alpha_1 = \frac{v+a\varphi}{u} - \delta,\ \ \alpha_2 = \frac{v-b_1\varphi}{u},\ \alpha_3 = \frac{v-b_2\varphi}{u},\ \alpha_4 = \frac{v_1-h_1\varphi_1}{u},\ \alpha_5 = \frac{v_1-h_2\varphi_1}{u},\ \alpha_6 = \frac{v_1-h_3\varphi_1}{u}$$

$$\alpha_7 = \frac{v_2-k_1\varphi_2}{u},\ \alpha_8 = \frac{v_2-k_2\varphi_2}{u},\ \alpha_9 = \frac{v_2-k_3\varphi_2}{u}$$

The velocities and the accelerations at each articulation point are calculated. The kinematic constraint equation for acceleration at the first fifth wheel between the tractor and first trailer is defines as:

$$\dot{v}_1 + e\dot{\varphi}_1 = \dot{v} - d\dot{\varphi} + u\varphi - u\varphi_1 \tag{3.4a}$$

The kinematic constraint equation for acceleration at second fifth wheel between the first and second trailer is expressed as:

$$\dot{v}_2 + j\dot{\varphi}_2 = \dot{v}_1 - f\dot{\varphi}_1 + u\varphi_1 - u\varphi_2 \tag{3.4b}$$

By eliminating the reaction forces at the fifth-wheels and substituting the values of the sideslip angle in Equations (3.1) to (3.3), the 4-DOF B-train double model can be described in the following state space form.

$$\dot{x} = Ax + B\delta \tag{3.5}$$

where, x is the state variable vector which is defined as $x = [\, v \;\; \varphi \;\; v_1 \;\; \varphi_1 \;\; v_2 \;\; \varphi_2 \,]^T$

A is the state matrix; B is the input matrix and δ is the input. Matrix A and B are provided in Appendix 1.

3.2.2. Linear Vehicle Model using Equation of Motion (EoM) Software

Generally, the EoM software is employed to generate linear equation of motions for mechanical systems. The software runs in MATLAB or Octave software. The input for the software is a simple function file that describes the system, whereas the output is the state space form of the equations. While analyzing a multibody system, EoM first gathers the information from the input data, and then generates the necessary stiffness and constraint Jacobian matrices. These matrices are required to find all the load and constraint forces present. Once they are known, the stiffness matrices are updated with the tangent stiffness terms [74]. First, the kinematic differential equations constituting the position and velocity are formed. Then, these equations are linearized to generate the second set differential equations based on the Newton-Euler method. In the first-order form, the linearized equations are written as follows [75],

$$\begin{bmatrix} I & 0 \\ 0 & M \end{bmatrix} \begin{Bmatrix} \dot{\delta p} \\ \dot{\delta w} \end{Bmatrix} + \begin{bmatrix} V & -I \\ K & C \end{bmatrix} \begin{Bmatrix} \delta p \\ \delta w \end{Bmatrix} = \begin{Bmatrix} 0 \\ \delta f_c + \delta f_a \end{Bmatrix} \tag{3.6}$$

where matrix V is the result of linearization of the kinematic differential equations, and the matrix C comprises of the viscous damping matrix and terms due to inertia forces. The matrix K is the stiffness matrix. Mass matrix M is the result from the Newton-Euler equations. The vector p represents the global locations and small angle orientations. While vector w represents the body fixed linear and angular velocities. The force fa is the acting actuator force, and fc is the acting constraint force. Generally, the constraint forces are eliminated by using a coordinate reduction. After the successive calculations, finally the output is expressed in the state space form of equation.

In EoM, each component of a system is defined as an *item*. The most basic type of item is a *body*, which signifies a rigid body. The other types of items are attached to one or more rigid bodies by ridged or flexible connectors. Available types of items used in EoM are *rigid_point*, *flex_point*, *nh_point*, *sensors* (output) and the *actuator* (input) [74].

The 4-DOF B-train double model consists of three rigid body and two fifth wheels. The fifth wheels allow only yaw motion between the two connected units. The tractor has a non-holonomic constraint with the ground. Tires are modeled as spring with damping coefficient proportional to the cornering stiffness of the tires. Moreover, the tires are fixed between two points, the ground and the respective vehicle unit.

Once the EoM software has generated the equations of motion, a number of linear analyses are automatically conducted. First, by analyzing the eigenvalues, the stability and natural frequencies of the motion are computed. The eigenvalue is a complex number; if the real part of it is positive, then the motion is considered unstable, whereas if it is negative the motion is stable. The imaginary part controls the oscillatory frequency of the motion. If the imaginary part is zero, there will be no oscillation in the unforced motion [74].

3.2.3. Non-Linear TruckSim Model

TruckSim is an efficient software package utilised for simulating the performance of multi-axle vehicles. It enables the users to build complex scenarios and test event sequences. TruckSim has an intuitive user interface and powerful analysis tools. It is preferred tool for analyzing vehicle dynamics, developing active controllers, analyzing a truck's performance characteristics, and designing active safety systems. The TruckSim package has been extensively validated using experimental data [1, 77, 78]

In this research, TruckSim is employed to validate the 4-DOF linear model and the linear EoM model. In TruckSim, a 3-D nonlinear model of the B-train double is developed. The B-train's configuration is defined as S_SS+SSS+SSS. Where the 'S' stands for the solid axels while the '_' sign indicates a connection between the two axles of a vehicle unit having no load equalization linkages. The '+' sign represents the fifth wheel between the adjacent units. The configuration is in accordance with the 4-DOF model (see Figure 3.1).

3.3. Model Validation

In this study, open-loop dynamic simulation technique has been used to validate the hand derived linear 4-DOF model and the EoM model. The emulated test procedure is a single-lane change maneuver, as specified by the SAE J2179 Standard [79]. Where the B-train double travels at a vehicle forward speed of 88 km/hr. The steering input to the front axle of the tractor is a single-cycle sine wave with a frequency 0.4 Hz and an amplitude of 0.0248 rad as illustrated in Figure 3.2. Islam et al. utilised this maneuver to validate a 4-DOF B-train double model in their research [1]. To validate the linear model, their dynamic response is compared with the nonlinear TruckSim model.

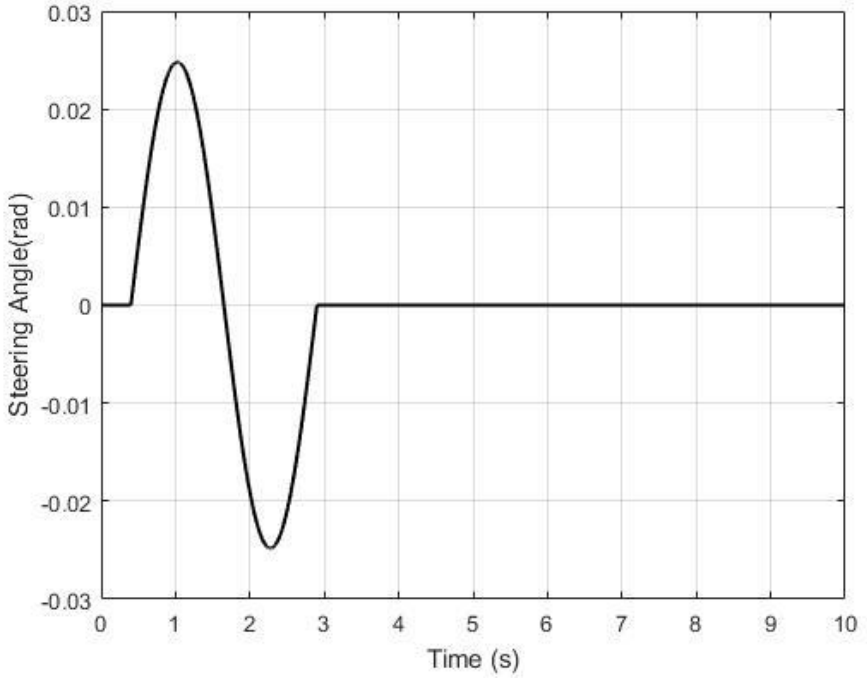

Figure 3.2: Steering angle input as recommended by SAE J2179 [79] standard.

3.3.1. Results

Figure 3.3 illustrates the comparison between the lateral acceleration curves of the 4-DOF model, the EoM model and the TruckSim model in response to the steering input. As predicted the curves of all three models follow a similar sequential path, where the tractor is followed by first and the second trailers respectively. It can be noted that in all the models, the lateral acceleration of the tractor is the highest followed by trailer 1 and trailer 2 respectively.

The curves of the EoM and TruckSim model demonstrate similarities in terms of amplitude and tendency at the beginning of the procedure. In addition, the 4-DOF model shows similar behaviour as the TruckSim model. However, variations can be observed at the end of the procedure for both the EoM and the 4-DOF models, when compared with TruckSim. These dissimilarities arise due to the nonlinearity of the TruckSim model. The result also

suggest that the TruckSim model comparatively takes longer to stabilize. Altogether, the lateral acceleration curves of the EoM and 4-DOF models demonstrate good agreement with the TruckSim model.

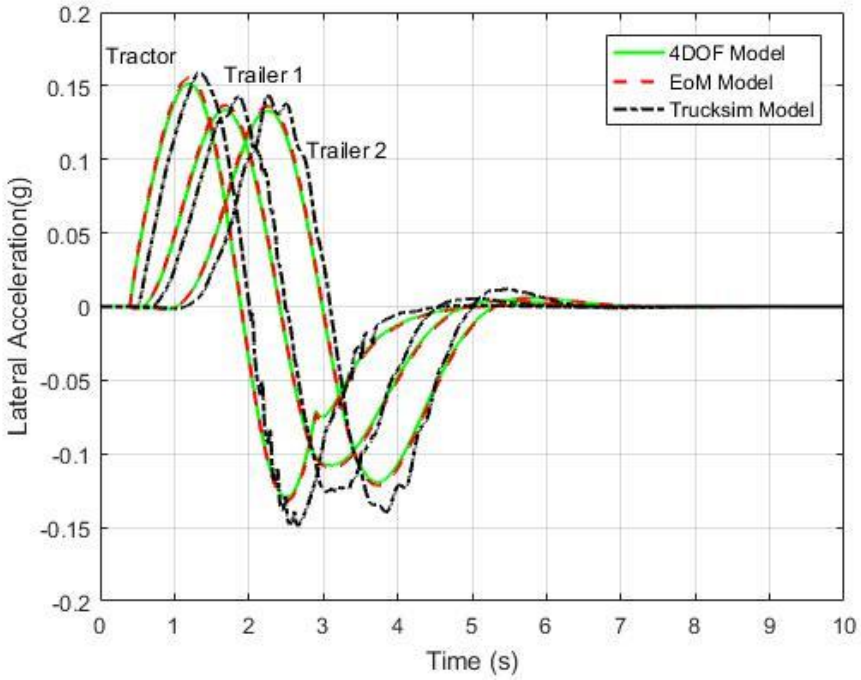

Figure 3.3: Time history of lateral accelerations of the 4-DOF, EoM and TruckSim models.

Figure 3.4 illustrates a comparison of yaw rates for the three models. Similar to the lateral acceleration curves, all the models follow predicted trajectory. At the beginning of the procedure the tractor and trailer 1 curves of the EoM and 4-DOF model, have similar tendency and peak yaw rate compared with the Trucksim model. However, this trend changes for trailer 2, where the peak yaw rate in the beginning of the cycle is higher for the TruckSim model. Similar characterstics can be observed at the end of the procedure where the tractor and trailer 1 show good agreement with Trucksim model, whereas, trailer 2 demonstrates a notable difference in yaw rate. Unlike the lateral acceleration curves, the curves of the yaw rates for Trucksim model are linear.

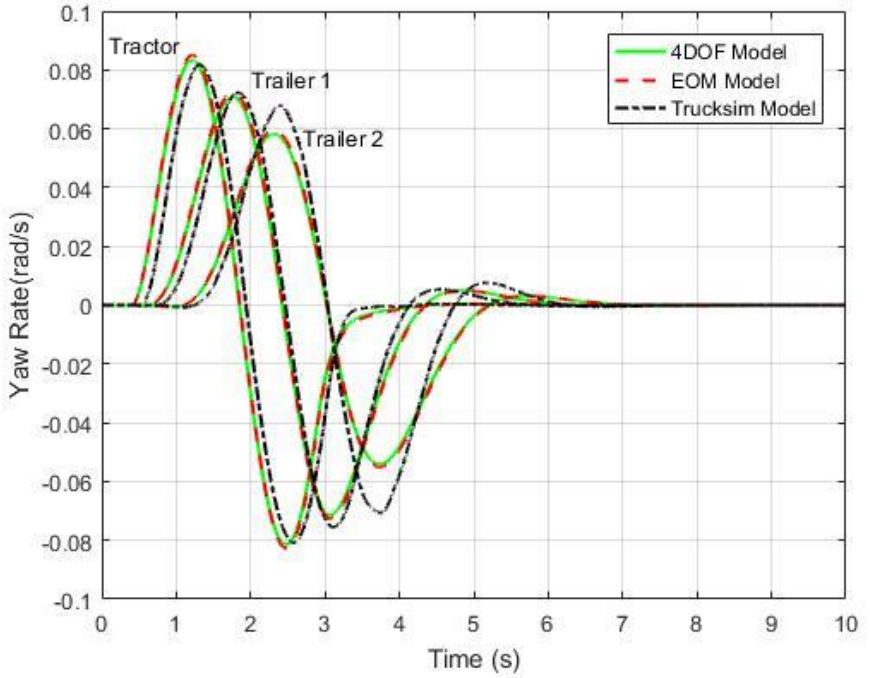

Figure 3.4: Time history of yaw rates of the 4-DOF, EoM and TruckSim model.

3.4. Selecting Rationale of the Most Active Axles for the Vehicle's Dynamic Behaviour.

Most studies concerning ATS systems assume that all trailer axles are active axles. However, in reality this is not economically feasible. Although a B-train double with an all axle ATS will ensure superior performance, such an ATS system will be highly complex. In this research, each trailer has been incorporated with only one ATS axle. The ATS configuration can be referred as a two-axle ATS system. Since, the B-train double consists of 6 trailer axles, the most suitable axles must be selected for incorporating the ATS system. This section focuses on the selection of the ATS axles.

The axles that influence the vehicle's lateral stability the most are selected. The LQR control technique has been utilised to calculate the required trailer steering angles for the following axle selection procedure.

The LQR controller is introduced in chaper 2 and synthesized in chapter 4. In the design of the LQR controller for this section, the control input is not penalized and weighting matrices Q and R remain the same during all conditions. The high-speed test procedure discussed in section 3.2 is used for the simulations.

ATS axles with the highest control demand have been considered as the most *active* axles. Since, the control demand for these *active* axles is the highest, it is logical to assume that these axles have the highest influence on the vehicle's dynamic behavior. Hence, such axles have been incorporated in the vehicle system for further study.

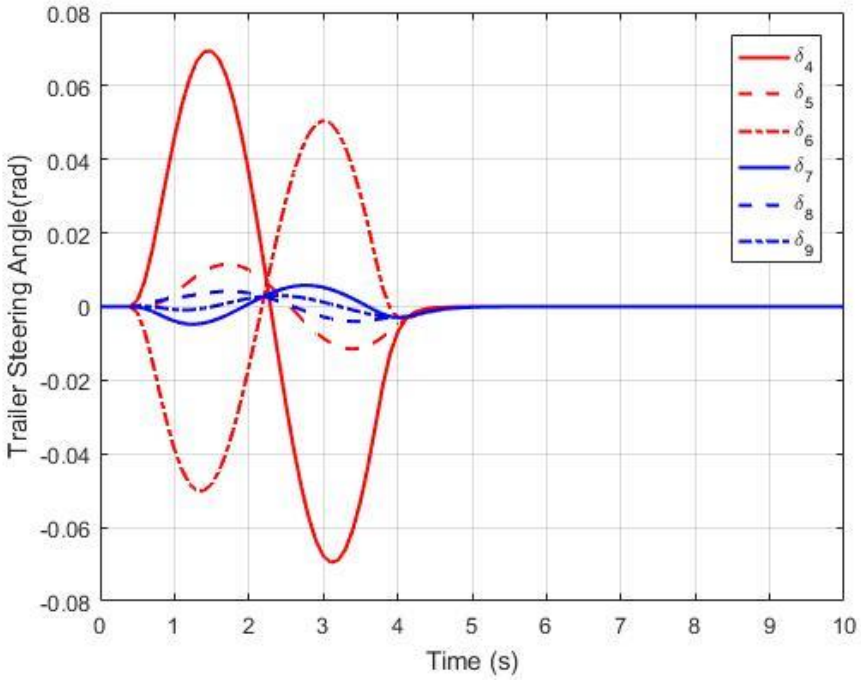

Figure 3.5: Time history of the steering angles of axles 4-9 using an all-axle ATS system.

Figure 3.5 demonstrates the trailer steering angles for an all axle ATS configuration of the B-train double. Red lines represents the active axles of the first trailer, whereas blue curves depicit the second trailer axles. The axles are numbered according to their position in the B-train double configuration.

Axles 1, 2 and 3 are located on the tractor, whereas axles 4-9 are located on the trailers. Axles 4-6 are located on the first trailer and axles 7-9 on the second trailer. Since, axles 1-3 are situated on the tractor, they do not qualify as ATS axles. Hence, the results are presented only for the trailer axles, axles 4 to 9. Figure 3.5 illustrates that axle 4 and axle 6 have the highest control demand. Thus, for a two-axle ATS axle 4 and axle 6 are the most suitable. However, as mentioned above the two-axle ATS system configuration mandates that each trailer must have one *active* axle. Since axle 4 has a higher control demand than axle 6, axle 4 is chosen as the ATS axle for the first trailer. Conversely, the second trailer axles demonstrate similar control demands. Specifically, axles 7 and 9. Hence, further evaluation is required to select the suitable *active* axle for the second trailer.

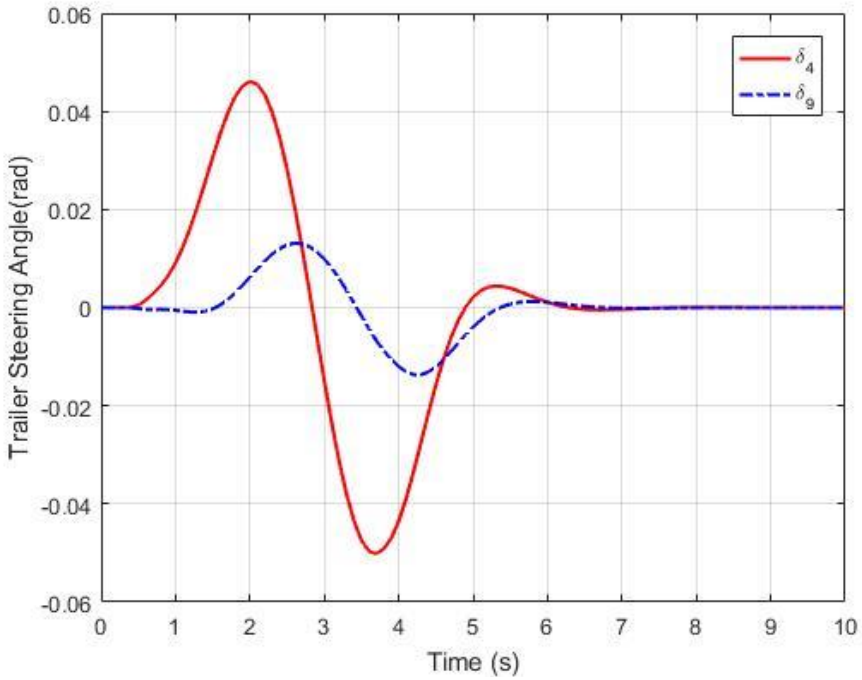

Figure 3.6: Time history of the steering angles of axles 4 and 9 using a two-axle ATS system.

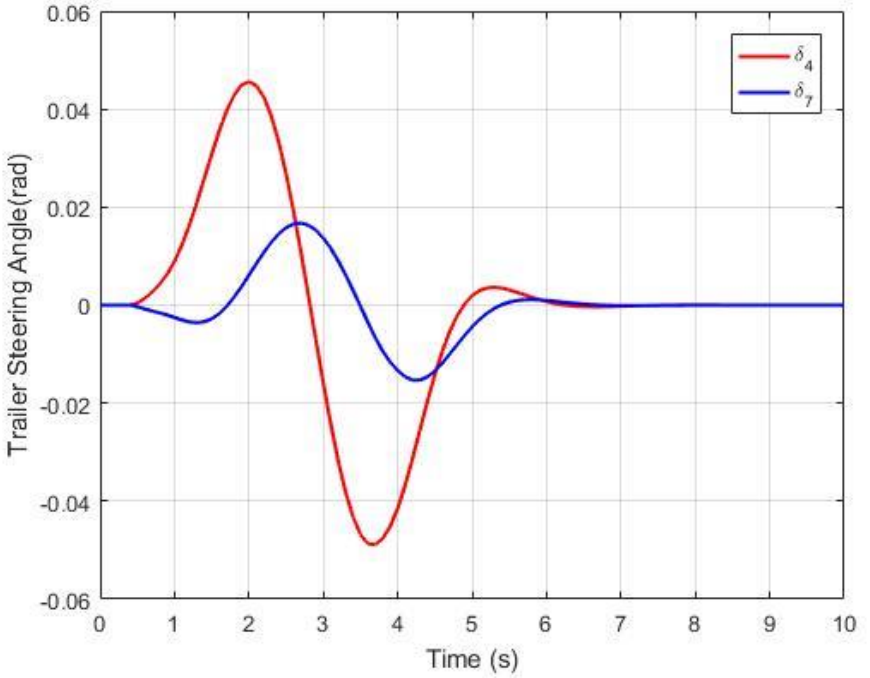

Figure 3.7: Time history of the steering angles of axles 4 and 7 using a two-axle ATS system.

To select the suitable *active* axle for the second trailer, the two-axle ATS system is employed. Both axle 7 and axle 9 are combined separately with axle 4 to formulate the configuration. Figures 3.6 and 3.7 illustrate the trailer steering angles of axles 4 and 7 and axles 4 and 9 respectively. A thorough comparison of both figures suggest that axle 7 has a higher control demand in comparison to axle 9. Moreover, the figures indicate that axle 7 reduces the control demand on axle 4. Hence, axle 7 is selected as the active axle for the second trailer.

In this research, the dynamic performance of the B-train double is evaluated using the two-axle ATS system. Based on the results obtained in this section, the two-axle ATS system will comprise of axle 4 and axle 7.

3.5. Eigenvalue Analysis

This section presents the eigenvalue analysis for the B-train double model. The eigenvalue analysis is employed to predict the stability of the vehicle system. Moreover, it is used to estimate the critical speeds of the B-train double model. Critical speed is the maximum forward speed at which the vehicle remains stable without any external inputs (steering input etc.). The hand derived 4-DOF linear yaw-plane model in section 3.1, is employed to perform the eigenvalue analysis. The system matrix *A* of the 4-DOF model is used to compute the systems eigenvalues.

Each pair of the eigenvalue is a complex number and can be expressed as

$$S_{1,2} = R_e \pm j\omega_d \tag{3.7}$$

where, R_e is a real part and $j\omega_d$ represents imaginary part. Based on the eigenvalues the damping ratio ξ is calculated. Damping ratio is a function of the vehicle's forward speed. If the damping ratio shows a negative value, the vehicles is rendered unstable [1]. Equation (3.8) illustrates the relationship between eigenvalues and damping ratio.

$$\xi = \frac{-R_e}{\sqrt{R_e^2+\omega_d^2}} \tag{3.8}$$

Each mode of the damping ratio corresponds to a specific state of the model. The mode that depicts close proximity to negative region indicates impending unstable vehicle behavior. If the mode curve reaches the negative region, the vehicle may exhibit unstable motion mode. As stated in chapter 2, to synthesize a robust controller, it is necessary to determine the critical vehicle parameters and their influence on its dynamic performance. Since an LCV is often subjected to different load configurations, in this section the B-train double's stability is evaluated under a variety of payloads.

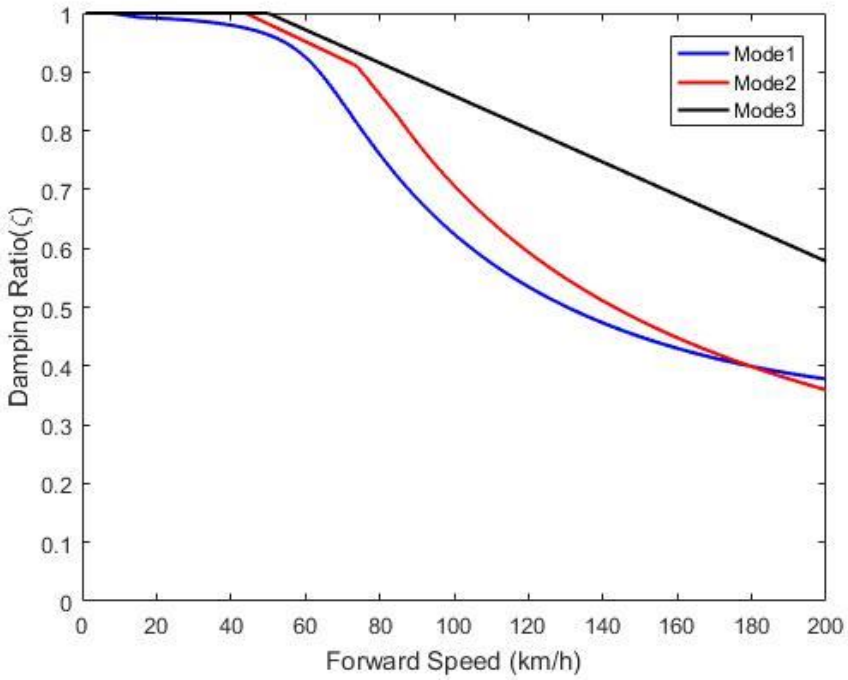

Figure 3.8: Damping ratio with respect to the vehicle forward speed without payload.

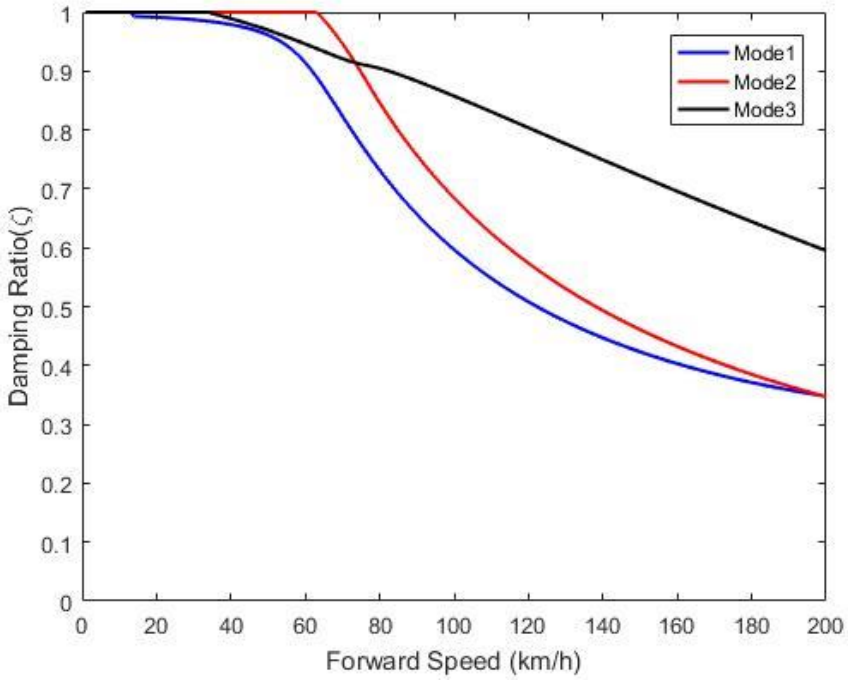

Figure 3.9: Damping ratio with respect to the vehicle forward speed with 5000kg payload.

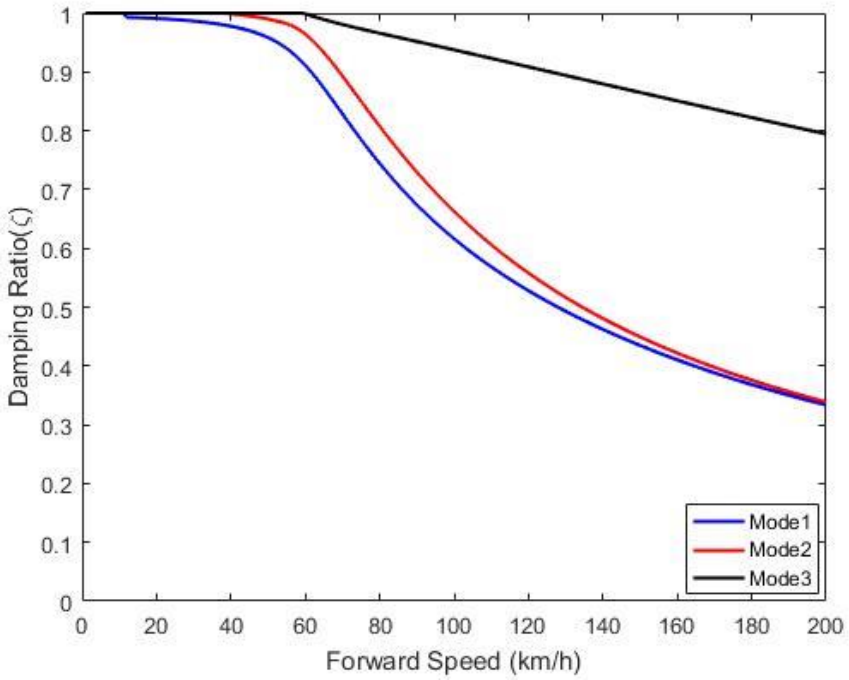

Figure 3.10: Damping ratio with respect to the vehicle forward speed with 10000kg payload.

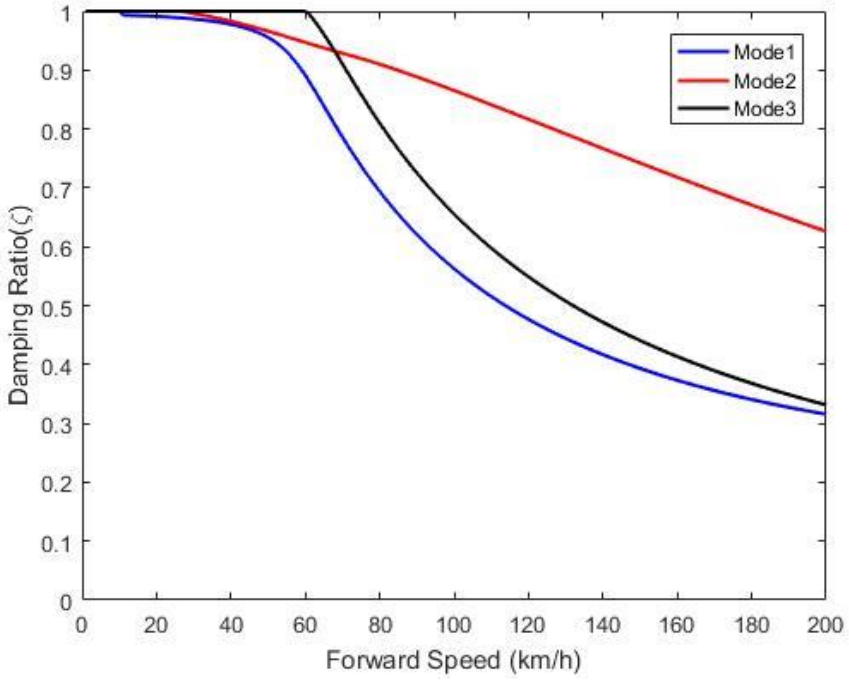

Figure 3.11: Damping ratio with respect to the vehicle forward speed with 15000kg payload.

The stability of the vehicle is evaluated under trailer loads of mass 0kg, 5000 kg, 10000kg and 15000 kg. Payload for the trailers may vary with respect to the density and quantity of the freight carried. Moreover, system parameters such as cornering stiffness, moment of inertia etc. are directly influenced by the payload. The behavior of the vehicle's parameters with different payloads with changing vehicle forward speed is studied.

Figures 3.8 - 3.11 illustrate the damping ratio of the B-train double with changing payloads. It is evident the damping ratio for different modes decreases with increase in vehicle forward speed. The mode(s) farthest from the negative region depicts the most stable performance. All figures suggest that the vehicle never experiences instability. Since in eigenvalue analysis the system's instability is evaluated without any external input, the system shows stable performance at forward speeds beyond 150 km/h.

However, close examination of the figures illustrates different behavior of the vehicle system under varying payload. The curves for payload 15000kg is comparatively lower with respect to the curves of the payload 0 kg, 5000kg and 10000kg, indicating that the vehicle is more susceptible to unstable modes at high speeds with a (higher) payload of 15000 kg.

3.6. Summary

In this chapter, Newton-Euler method was used to model the 4-DOF linear B-train double model. Moreover, the Equation of Motion (EoM) software was employed to generate a comparative linear vehicle model. Trucksim software package was used to validate the models under a high-speed single lane change maneuver.

A comparison was performed to evaluate the fidelity of the generated vehicle models. The simulation results show a reasonable agreement between the two linear models and the non-linear TruckSim model. The linear model, specifically the 4-DOF B-train double model is employed in subsequent chapters for designing control systems.

Moreover, this chapter discussed the all-axle ATS and two-axle ATS systems. Since all-axle ATS systems are not feasible for practical use, the two-axle ATS system approach was chosen for with the B-train double model. Axle 4 (1^{st} trailer) and axle 7 (2^{nd} trailer) were established as the most *active* axles, and were choosen for two-axle ATS system. Eignevalue analysis was also conducted to evaluate the effects of varying payload on the vehicle stability. The vehicle system demonstrated stability under a variety of changing payload (0 kg, 5000kg, 1000kg and1500kg) and vehicle forward speeds.

CHAPTER 4

Controller Design

4.1. Introduction

This chapter discusses the synthesis of LQR based ATS controller for the vehicle model developed in chapter 3. Additionally, it includes the synthesis of two robust control strategies for implementing ATS, namely, LQR with Kalman filtering, also known as LQG (Linear Quadratic Gaussian) and μ synthesis. This chapter focuses primarily, on discussing the control theory and mathematical laws governing the implementation of above stated control strategies. Simulation results are discussed in chapter 5.

4.2. Linear Quadratic Regulator (LQR) Technique

The ATS system for the B-train double is initially designed using the LQR control technique. In LQR design, the nominal plant is defined as an infinite horizon continuous-time system, where the system state feedback law, $u = -kx\ (t)$ minimizes the quadratic cost function J .

The system can be defined in state-space form as specified below (Equation 4.1):

$$\dot{x}(t) = Ax(t) + Bu(t) \tag{4.1}$$

$$J = \int_0^\infty [\, x^T(t)Qx(t) + u^T(t)Ru(t)]\, dt \tag{4.2}$$

where, $Q = Q^T \geq 0$, $R = R^T \geq 0$, $x^T(t) = Mx(t)$

In Equation (4.2), $x^T(t)$ is the linear combination of the state vector $x(t)$. The matrix M may be defined by the user. The matrices Q and R are called the weighting matrices. The weighting matrices allow the designer to define the impact of each state and control input on the controller response.

The LQR provides the solution using the Algebraic-Riccati Equations (ARE), (4.3)

$$A^T S + SA - SBR^{-1}B^T S + Q = 0 \tag{4.3}$$

$$k = R^{-1}B^T S \tag{4.4}$$

k is determined using Equation (4.4), it represents the optimal control gain for state-feedback equation $u = -kx\ (t)$. The system matrix A maybe modified using the control gain k. The modified system matrix A_{LQR} can be determined as shown in equation 4.5

$$A_{LQR} = A - Bk \tag{4.5}$$

There is no direct systematic approach for selecting Q and R matrices in Equation (4.2). Generally, the values are tuned using the trial and error method in order to obtain satisfactory performance of the controller. The matrix Q is a state-weighting matrix and relies on the reduced order system. States, which gives high participation in the critical mode, are given higher weights. The parameter R is the input-weighting matrix, which determines the system response [69, 80]. A small value of R, speeds up the controlled system response [81], and enhances the system's controllability. However, a very large control signal sometimes cannot be generated by the hardware.

4.3. Linear Quadratic Gaussian (LQG) Technique

The Kalman filter (KF) uses state equations (state space matrices) and initial values to calculate the residual and gain values, this aids KF to estimate the real signal value. The Kalman estimator provides the optimal solution for continuous or discrete estimation problems. Continuous Kalman filter is used when the measurements are continuous functions of time. A thorough study of the optimal estimation must include the continuous KF. However, in a modern control application, discrete KF is usually used [81].

With the help of the KF theory, the state estimate $\hat{x}(t)$ can be generated. The KF estimates the states in the form of a feedback controller, where the filter estimates the process state at some time and then obtains a feedback in the form of the measurement noise. KF works with two sets of Equations (4.6 and 4.7), namely time update equations and measurement update equations. The time update equations are responsible for projecting (forward in time) the current state. The measurement update equations are responsible for the feedback i.e. for incorporating a new measurement into the estimate to obtain an improved a posteriori estimate. The time update equations is a predictor equation, while the measurement update equations are corrector equations. The KF algorithm resembles a combination of a predictor-corrector algorithm for solving numerical problems [58].

KF can be expressed for the given state space equations

$$\dot{x}(\mathrm{t}) = Ax(t) + Bu(t) + Gw(t) \qquad \text{(State equation)} \qquad (4.6)$$

$$y(t) = Cx(t) + Du(t) + Hw(t) + v(t) \qquad \text{(Measurement equations)} \qquad (4.7)$$

$$E(w) = E(v) = 0 \qquad E(ww^T) = Q \qquad E(vv^T) = R$$

In Equations (4.6) and (4.7), u is the input, w is the process noise and v is the measurement noise. With the help of the KF, the state estimate $\hat{x}(t)$ of the state $x(t)$ can be determined using a filter whose structure is similar to a conventional state estimator/observer, mentioned below.

$$\dot{\hat{x}}(t) = A\hat{x}(t) + Bu(t) + K_f(y - C\hat{x}(t) - Du(t)) \tag{4.8}$$

The estimated state $\hat{x}(t)$ is used to minimize the covariance error mentioned in equation (4.9)

$$P_f = \lim_{T\to\infty} E[(x(t) - \hat{x}(t))(x(t) - \hat{x}(t))^T] \tag{4.9}$$

$\hat{x}(t)$ is used to replace the actual state variables $x(t)$ such that the original LQR problem can be reduced to an ordinary linear quadratic problem. P_f is symmetric unique positive semi-definite matrix that solves the algebraic Riccati Equations (ARE). The optimal value of Kalman gain K_f is obtained by solving ARE

$$P_f = P_f^T \geq 0 \tag{4.10}$$

$$K_f = P_f C^T R^{-1} \tag{4.11}$$

As mentioned in section 4.1, The LQ optimal state feedback control consist of determining optimal control to the LQR problem by minimizing the performance index J of LQR. Therefore, from the above set of equations we can redefine the LQR controller, with optimal control input as $\hat{u} = K_c\hat{x}(t)$ where K_c is the optimal state feedback matrix, $K_c = R^{-1}B^TS$ and S is a unique positive semi-definite matrix, $S = S^T \geq 0$ and satisfies the ARE (4.12) [80].

$$A^T\mathrm{S} + AS - \mathrm{S}B^TR^{-1}BS + MM^TQ = 0 \tag{4.12}$$

The Q and R mentioned in the Equation (4.12), are known as the process and measurement noise covariance matrixes respectively, commonly estimated through trial and error method. Where Q reflects the uncertainty in the assumed state model, un-modelled dynamics of the states or any sort of unknown random input [82]. R is associated with accuracy of detection of the error. The values of Q and R are extremely crucial as they regulate the value of observer gain matrix K_c.

Figure 4.1 show a schematic diagram of the synthesized controller, where δ is the steering input, u is the control signal generated by the K. $\hat{x}$ is the state estimation of the input states x, w is the white process noise, v stands for the measurement noise, y and y_v is the output measurement and measurement noise respectively.

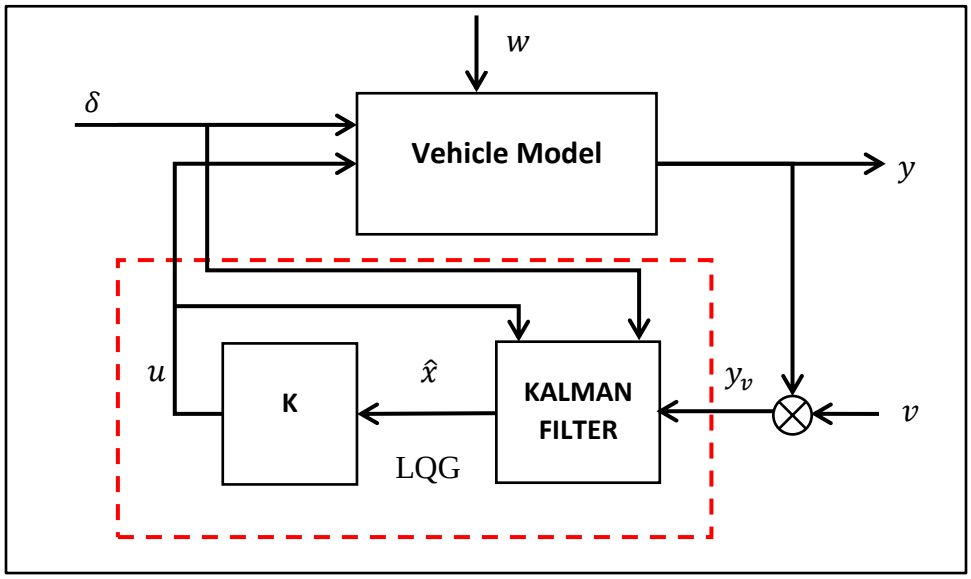

Figure 4.1: Block diagram of a LQG controller.

4.4. Noise Modelling

As motioned in the chapter 2, the noise has a detrimental effect on the closed loop performance of a control system. Noise can be categorised as process noise and measurement noise [58]. In control theory, process noise depicts the un-modelled dynamics or the discrepancies between the mathematical model and the physical system. Whereas, measurement noise is the external disturbance which corrupts the true measurement of the system. Techniques such as KF are employed to counteract the detrimental effect of process noise and measurement noise [58, 82]. However, for simplicity, in this study only the measurement noise is considered.

In chapter 5, the LQR, LQG and μ synthesis controllers are evaluated in the presence of measurement noise. Hence, it is essential to develop a realistic noise model. In numerous studies involving numerical simulations, white noise is used to model the external measurement noise.

In signal processing, white noise is a random signal having equal intensity at different frequencies, giving it a constant power spectral density. White noise refers to a statistical model for signals and signal sources, rather than a specific signal. Additionally, it is assumed that white noise is Gaussian distributed [82]. Although in reality, physical systems never encounter white noise, it provides a useful theoretical approximation of the errors.

In the simulations result presented in chapter 5, the control system's performance is examined using Gaussian–distributed white noise generated in the Matlab/Simulink environment. Suitable intensity of noise power spectral density is selected to evaluate the control system under realistic errors.

4.5. μ synthesis Technique

In reality, physical parameters of a vehicle may not be accurately known. Moreover, difficulties can arise in measuring these parameters, as they may vary under different operating conditions. For instance, in a B-train double, the mass and yaw moment of inertia of the trailers may vary significantly depending on the payload on the trailers. Hence, this research focuses on building a robust controller that is capable of dealing with such system uncertainties and controlling the dynamic behaviors of the B-train double to maintain safe operation. The primary purpose of the robust controller is to ensure the stability and performance of the closed-loop system in the presence of uncertainties.

As previously discussed, to augment the robustness of the LQR controller, a KF is added to the control system, a combination known as LQG. The KF effectively rejects the system noises and predicts the system states. Although it is considered effective in rejecting the measurement noise, it has an insubstantial impact on the process noise. As previously mentioned, process noise in a system may arise due to numerous reasons, one of which includes parametric uncertainties. Moreover, process noise can cause the system to deviate from its desired performance. Thus, the LQG control design cannot guarantee robustness.

It is commonly known, that for a LCV the payload is subject to change. As discussed in detail in section 3.4, a change in payload of the trailers induces a change in other vital vehicle parameters such as cornering stiffness of the axles, yaw moment of inertia, etc. These parametric changes have a significant influence on the vehicle's dynamic behaviour. In other words, the stability characteristics of the vehicles vary drastically with change in payload.

Thus in this research, a μ synthesis controller accounts for the parametric uncertainties directly related to change in payload. The parameters subjected to uncertainties are mass of the first trailer and the second trailer, yaw moments of inertia of the two trailers, cornering stiffness of two rear axles of the tractor and each axle of the two trailers. Additionally, the vehicle forward speed is considered an uncertain parameter ranging from 50 km/h to 105 km/h. In total, there are 13 uncertain parameters.

The schematic diagram of the synthesized μ controller is shown in Figure 4.2. Where, *Plant* depicts the nominal plant model with uncertainties. K stands for the controller and Δ is the perturbations in the plant. w represent the external inputs; z denote the output errors; yun and $Pert$ are the input and output signals of the dynamic uncertainties respectively. y is the feedback signals whereas u are the control signal.

The design goal of the controller, is to find a optimum control gain K, which stabilizes the closed loop system and satisfies Equation (4.13) for all uncertainties [52, 69].

$$\| F_U[F_L(P,K),\Delta] \|_\infty < 1 \tag{4.13}$$

For the robust performance of the system, a performance test is performed with the arbitrary value of K over the linear functional transformation F_L(P, K) with respect to the uncertain structure Δ_P[52, 69].

where, $\Delta_P \stackrel{\text{def}}{=} \left\{ \begin{bmatrix} \Delta & 0 \\ 0 & \Delta_F \end{bmatrix} : \Delta \in \Delta, \Delta_F \in C^{n_w * n_z} \right\}$ (4.14)

Δ is parametric uncertainty and Δ_F is a fictitious complex (unstructured) uncertainty.

The μ synthesis aims to minimize the peak value of the structure singular value μ_{Δ_P} of the corresponding closed loop transfer function matrix $F_L(P,K)$ for all uncertainties over the set of all stabilizing controllers, as shown in Equation (4.15)[52, 69].

$$\min_{\text{k stabilizing}} \max_{\omega} \mu_{\Delta_P}(F_L(P,K)(j\omega)) \tag{4.15}$$

the system will achieve robust performance and stability if the value of μ_{Δ_P} satisfies the following Equation (4.16)

$$\mu_{\Delta_P}(F_L(P,K)(j\omega)) < 1 \tag{4.16}$$

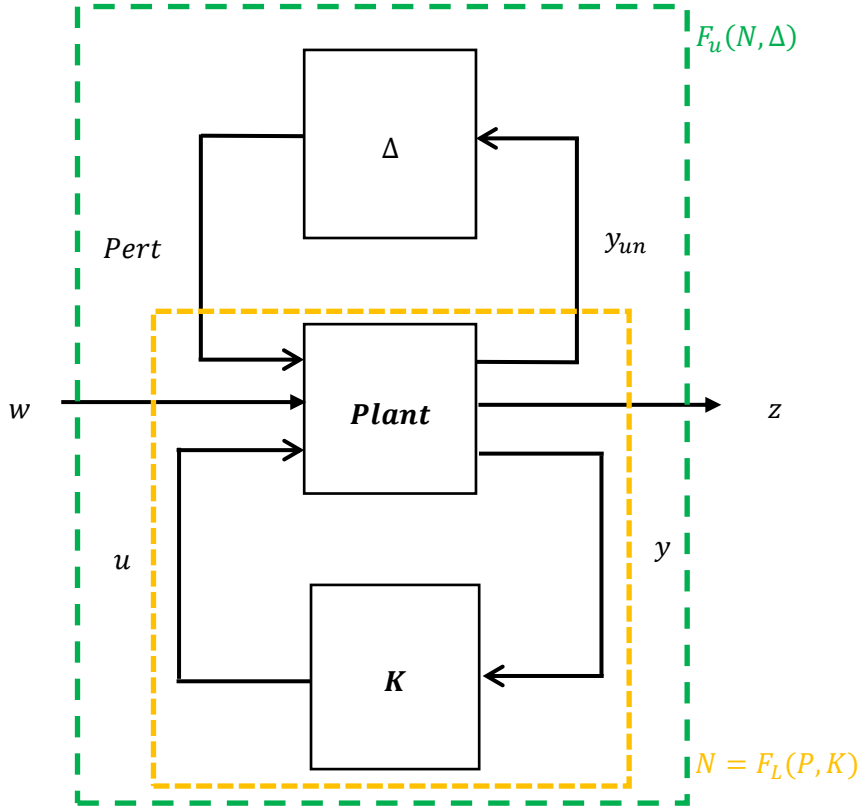

Figure 4.2: Block diagram of a μ synthesis control scheme.

4.5.1. Optimization using Genetic Algorithm (GA)

An optimal controller requires suitable values of the weighting functions. The selection of weighting functions parameters is limited by their application, and are selected from proper, minimum phase transfer functions of low or high pass filters. Traditionally, to fine-tune the weighting functions, trial and error method is used. However, this is tedious and time-consuming method. In order to generate optimal weighting functions for the μ synthesis controller, GA is introduced in this research as an optimization tool.

Solving an optimization problem within a specified period is both complex and difficult to achieve. GA is a stochastic evolutionary algorithm inspired by the natural evolution technique [29, 38, 83]. GA is initiated using a set of random values. It further continues to select the most suitable values from the set of random values; this process is termed as *selection*. After which the algorithm uses two mathematical methods, namely crossover and mutation, to *regenerate*. In regeneration, the new set of values are produced from the selected most suitable values. For running GA, i.e. initializing the population, selection and regeneration, no subsequent set of information is required. Only the evaluation of the objective function and the possible constraints are required for attaining the most suitable or the *fittest value*. Such a merit makes the GA capable of dealing with problems having complex objective function, where it is difficult to obtain the derivatives. Moreover, the random nature of GA provides it with the capabilities of escaping the local optima. The selection of the fittest value is crucial for the GA, as it enables it to find the global optima for the problem [30, 51, 83].

The role of GA in design optimization is to find optimal values of the design variables in order to minimize the objective function.

$$J_{cost} = \left\| \begin{bmatrix} W_p S_o G & -W_p S_o G K W_n \\ -W_u K S_o G & -W_u K S_o W_n \end{bmatrix} \right\|_\infty < 1 \tag{4.17}$$

where, $S_o = (I + GK)^{-1}$

is the output sensitivity function and K is the optimal control gain matrix generated by using MATLAB [52]. The weighting functions for the μ synthesis controller derived using the GA are listed in Table 4.1.

The weighting function $\mathbf{W_n}$ serves to model sensor noises d_1, d_2 and d_3 at the measurements of yaw rate of the tractor, first trailer and the second trailer, respectively. The control input u is weighted according to the input limitation by the weighting function $\mathbf{W_u}$. The weighting function matrix $\mathbf{W_p}$, is applied on the system outputs, which are the respective yaw rates of the vehicle units. Figure 4.3 demonstrates the system diagram.

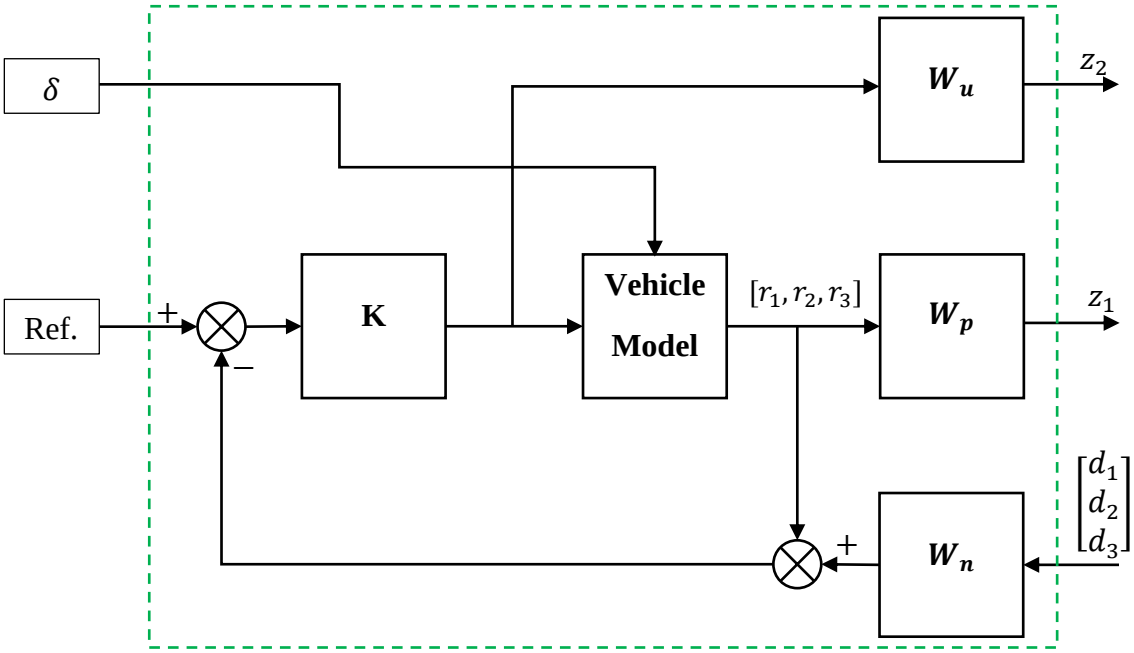

Figure 4.3: System diagram depicting a μ synthesis control scheme.

Table 4.1: Weighting functions parameters for μ synthesis controller

Weighting Functions	Parameters	
$\boldsymbol{W_p}$	$\boldsymbol{W_{p1}}$	$\left[\frac{0.9879s + 3.072}{s + 1.809e4}\right]$
	$\boldsymbol{W_{p2}}$	$\left[\frac{0.9238s + 3.003}{s + 1.809e4}\right]$
	$\boldsymbol{W_{p3}}$	$\left[\frac{1.134s + 3.347}{s + 1.809e4}\right]$
$\boldsymbol{W_u}$	$\boldsymbol{W_{u1}}$	$\left[\frac{0.00122s + 0.002464}{0.07061s + 1}\right]$
	$\boldsymbol{W_{u2}}$	$\left[\frac{0.08732s + 0.1706}{0.5092s + 1}\right]$
$\boldsymbol{W_n}$	$\boldsymbol{W_{n1}}$	$\left[\frac{0.008107s + 0.1083}{1.002s + 1}\right]$
	$\boldsymbol{W_{n2}}$	$\left[\frac{0.006775s + 0.1}{0.3546s + 1}\right]$
	$\boldsymbol{W_{n3}}$	$\left[\frac{0.1568s + 0.4766}{0.1416s + 1}\right]$

4.5.2. Reference Yaw Rate Model

The controller enhances the lateral stability of the vehicle by controlling the motion of the vehicle through minimizing the peaks of lateral acceleration and yaw rate curves. However, if the controller minimizes the yaw rate without considering the vehicle's intended path, the driver action and controller action will conflict. This eventually would hamper the vehicle motion and deviate it from its intended path. Therefore, a suitable reference model is essential, which can provide the desired yaw rate for a given set of parameters [28].

Moreover, the control system K requires a suitable reference signal in order to generate the optimal corrective yaw moment. As a result, the steady-state response of the yaw rate of the B-train double with respect to the steering input is used. Equation (4.18) describes the relationship between steady-state yaw rate of the tractor and the steering input

$$r_{ss} = \left(\frac{u}{l+k_t u^2}\delta\right) \tag{4.18}$$

where, r_{ss} is the steady-state yaw rate of the tractor, u the forward speed of the tractor, l is the wheelbase, k_t is the understeer coefficient of the LCV combination, and δ the steering input. Additional information is provided in Appendix 2.

The linear 4-DOF model's steady state yaw rate response $\frac{r_{ss}}{\delta}$ is used to generate the desired yaw rate. Moreover, a suitable time delay [30] was added as described in Equation (4.19). The first order time delay allows control over the vehicle yaw response through the yaw rate time delay t_{yaw}.

$$R_{desired} = \left(\frac{1}{1+t_{yaw}s}\right) r_{ss} \tag{4.19}$$

4.6. Summary

In this chapter, the control theory behind, LQR, LQG and μ synthesis controllers was presented. The state feedback law for the designed LQR and LQG controller for this research is same. However, LQG controller is based on LQR control theory but is assisted with KF, that provides a full states feedback to the LQR controller. This enhances the performance of the LQR controller in the LQG controller.

Since KF is integral to LQG control, its design synthesis was discussed. Moreover, the tuning methods for the three control techniques were discussed. In this study, the LQR and LQG controller are tuned using the widely used trial and error method. Whereas, the designed μ synthesis controller is tuned using GA. Moreover, the reference yaw rate model used for the μ synthesis controller was discussed. A reference yaw rate model ensures enhanced dynamics performance and simultaneously minimizes the path deviation.

CHAPTER 5

Results and Discussions

5.1. Introduction

To perform the numerical simulations, two frequencies of the steering inputs i.e. 0.2 Hz and 0.4 Hz are used. Figure 5.1 shows the two steering inputs. In literature [39], it is stated that the value of RWA (Rear-Ward amplification) ratio increases drastically at these frequencies. This signifies that the LCV's tendency to exhibit unstable motions such as rollover is high in such frequencies. Therefore, this research focuses on considering these two frequencies while performing the simulations, which would help in evaluating the dynamic behavior of the LCV with ATS in different operating conditions.

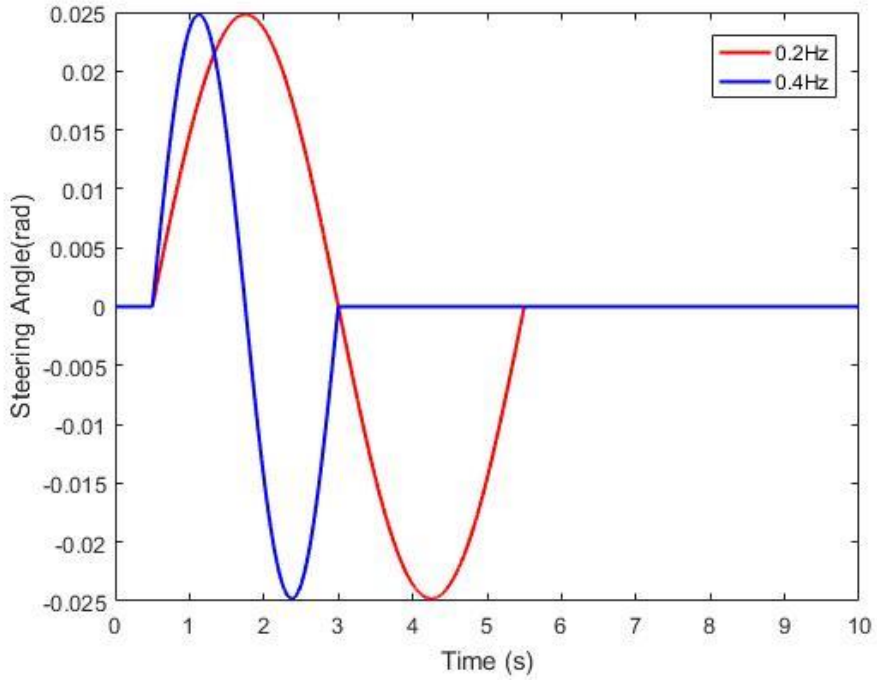

Figure 5.1: Steering input for frequencies of 0.2 and 0.4 Hz.

5.2. Performance of the LQR Controller

5.2.1. Performance of the LQR Controller without System Noise

For examining the dynamic performance of the LQR controller, a comparison is made between the baseline 4-DOF B-train double model and the LQR controlled B-train double model. Vehicle forward speed for both controlled and uncontrolled vehicle models is maintained at 88 km/h with a steering input frequency of 0.2 Hz. Figures 5.2 and 5.3 illustrate the lateral acceleration and yaw rate response of the two vehicle models. The curves of the three-vehicle units, tractor, trailer 1 and trailer 2 follows each other in the same sequence (see Figure 5.2) for every figure presented hereafter. From the figures 5.2 and 5.3, it is apparent that the LQR based ATS controller can successfully reduce the peak values of lateral accelerations and yaw rates of the vehicle system.

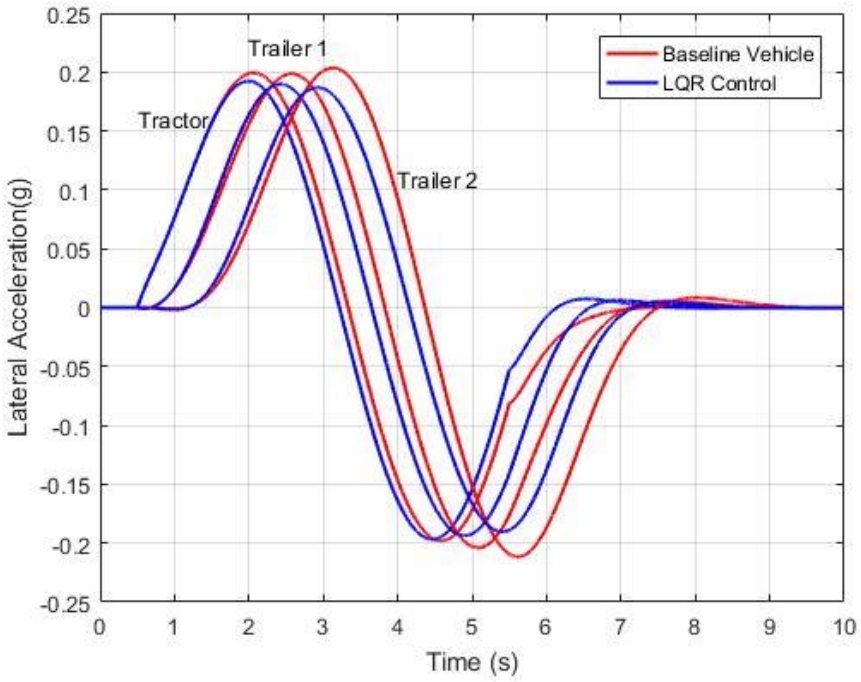

Figure 5.2: Time history of lateral accelerations for the 4-DOF model with and without the LQR based ATS.

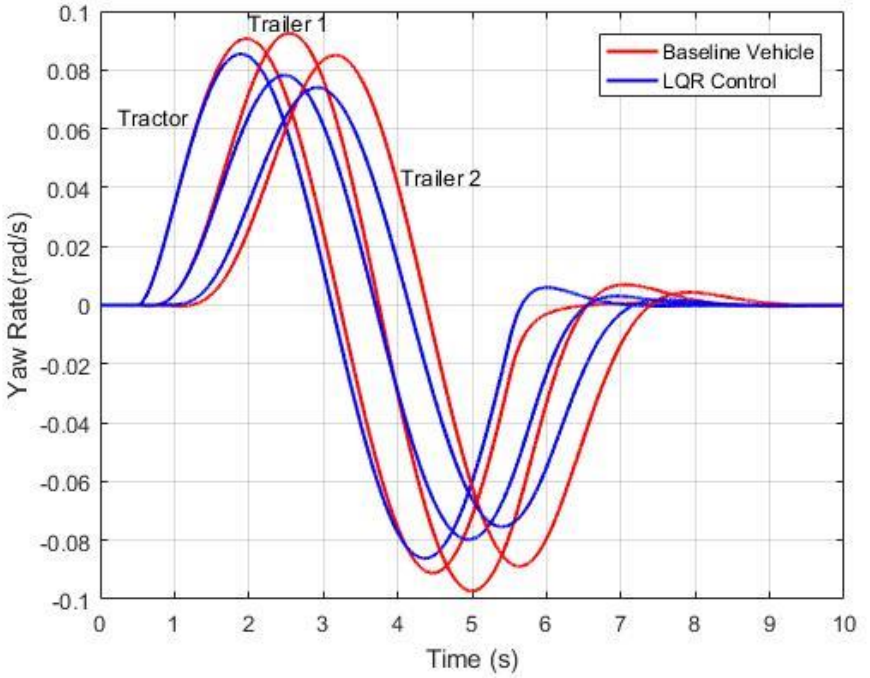

Figure 5.3: Time history of yaw rates for the 4-DOF model with and without the LQR based ATS.

It is noted that the peak value of the lateral acceleration corresponding to the rearmost trailer (trailer 2) is reduced, indicating a reduction in the RWA ratio. Trailer 2's peak lateral acceleration demonstrates a reduction of 11%, reduced from 0.21g to 0.185g, compared to the baseline model. This ensures improved lateral and yaw stability of the B-train double.

5.2.2. TruckSim MATLAB Co-simulation

To validate the designed LQR controller and its effect on the vehicle system's dynamic performance, co-simulations are performed using the MATLAB/Simulink and TruckSim environments. The dynamic response of the 4-DOF model and the TruckSim model is compared. Figure 5.4 shows the co-simulation environment between MATLAB and TruckSim software packages.

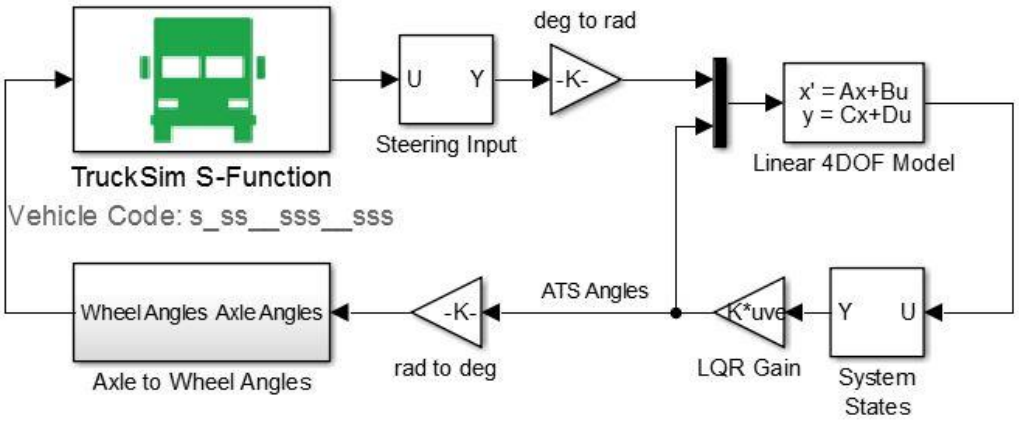

Figure 5.4: The co-simulation environment with MATLAB and TruckSim using the LQR Controller.

As illustrated in Figure 5.4, the steering input is received from TruckSim and acts as the input to the 4-DOF model. To calculate the desired ATS angles, the 4-DOF model runs parallel with the TruckSim vehicle model. The generated ATS angles are sent to TruckSim to achieve controlled performance.

Figures 5.5 and 5.6 compare the dynamic performance of the TruckSim models, with and without ATS. The figures suggest that the ATS controlled vehicle model enhances the vehicle's stability by reducing the peak lateral accelerations and yaw rates of the vehicle. Furthermore, the response of the controlled TruckSim vehicle model is similar to the response of the controlled 4-DOF baseline model. Figures 5.7 and 5.8 illustrate the lateral acceleration and yaw rate response of the TruckSim and the 4-DOF vehicle models. It is evident from the lateral acceleration and yaw rate response that TruckSim and the 4-DOF vehicle show are in good agreement

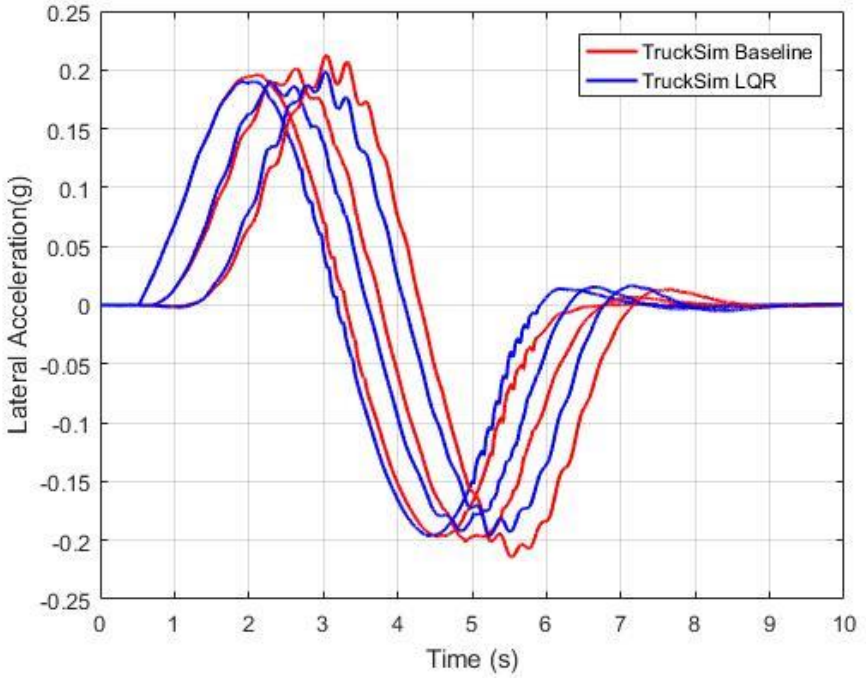

Figure 5.5: Time history of lateral accelerations for the TruckSim model with and without LQR based ATS.

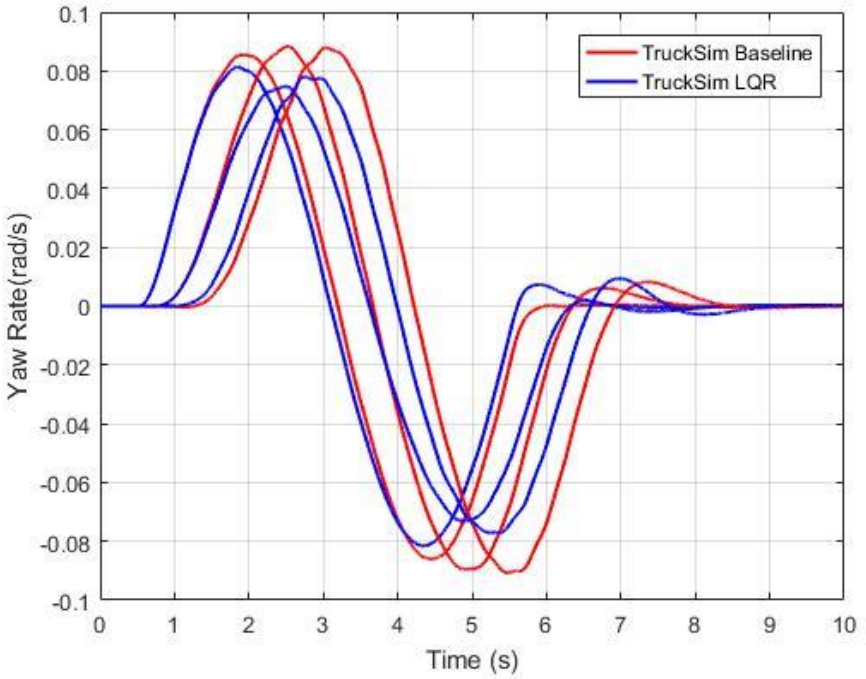

Figure 5.6: Time history of yaw rates for the TruckSim model with and without the LQR based ATS.

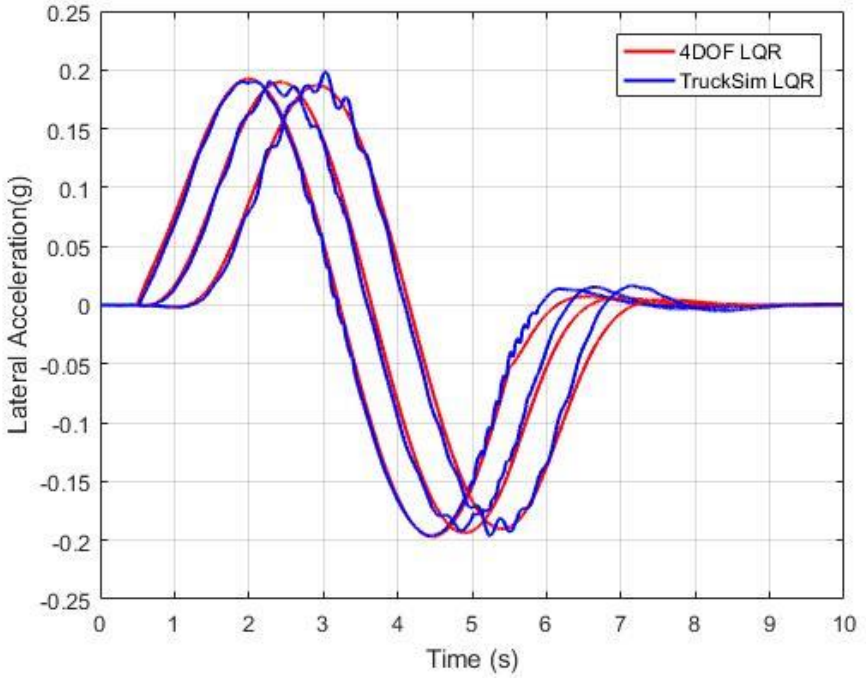

Figure 5.7: Time history of lateral accelerations for the TruckSim and 4DOF models with LQR based ATS Model.

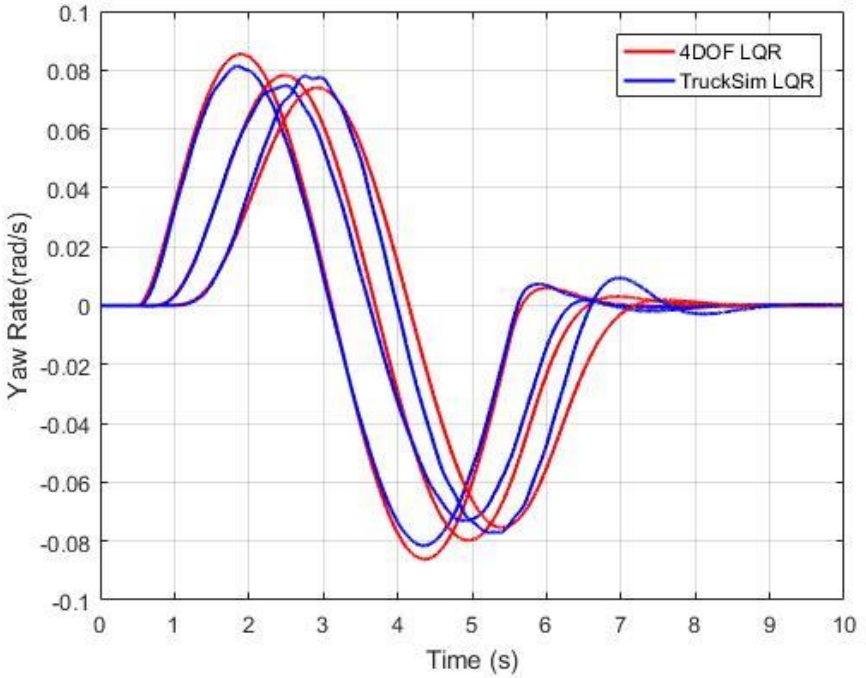

Figure 5.8: Time history of yaw rates for TruckSim and 4DOF Models with the LQR based ATS.

5.2.3. Performance of the LQR Controller with System Noise

As shown in the sections 5.2 and 5.3, the LQR based ATS controller demonstrates improved lateral and yaw stability in the absence of the system noise. However, the LQR controller may not deliver the same performance in the presence of system noise. Figures 5.9 and 5.10 show a comparison between the lateral acceleration and the yaw rate measurements of the 4-DOF model with and without measurement noise. The red curves correspond to the actual lateral acceleration and yaw rate outputs of the vehicle model without sensor noise. Whereas the blue curves represent the measured outputs in the presence of the noise. As stated in section 4.4, the term noise denotes the measurement noise.

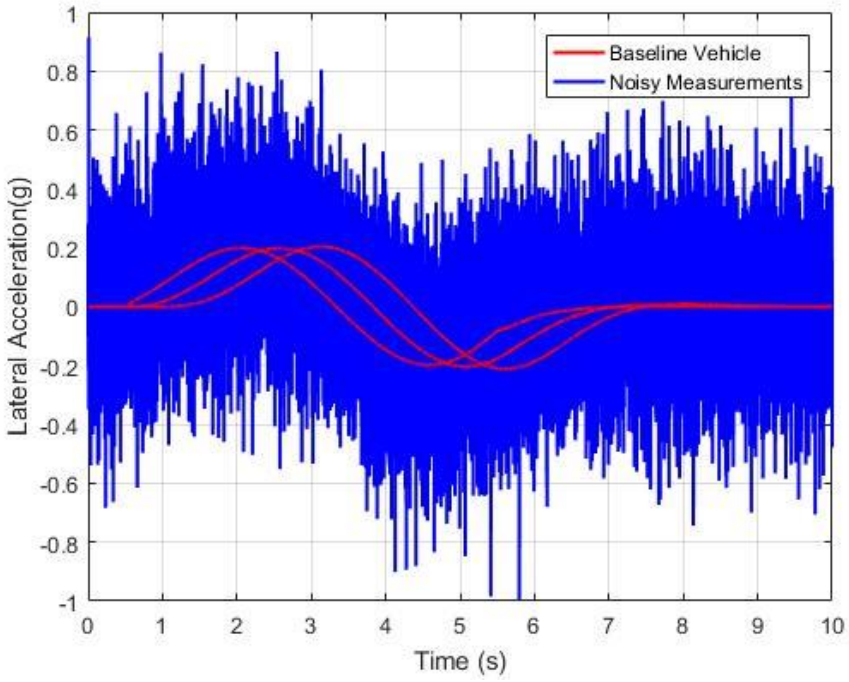

Figure 5.9: Time history of lateral acceleration measurements with and without sensor noise.

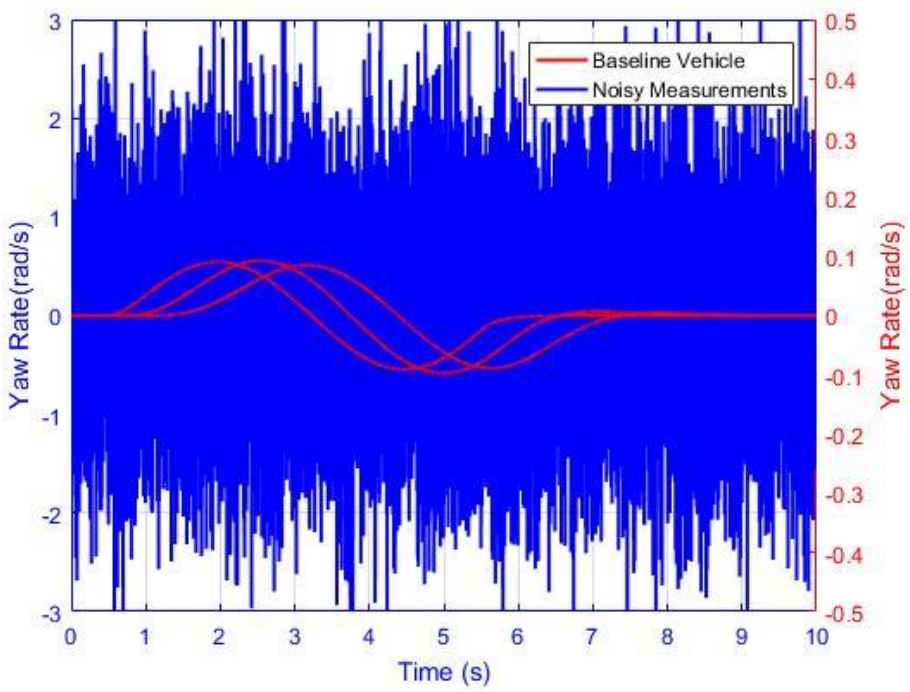

Figure 5.10: Time history of yaw rate measurements with and without sensor noise.

Figures 5.9 and 5.10 suggest that the system finds it difficult to track the true behavior of the vehicle in the presence of measurement noise. A considerable deviation is observed in the tracked values. Note that for Figure 5.10, the scale for the baseline model is on the right hand side, while the scale for the noisy measurements is on the left hand side.

In order to illustrate the performance of the closed-loop LQR controller in the presence of system noise, Figures 5.11 and 5.12 compare the baseline 4-DOF B-train double model, the LQR controlled model in absence of system noise and the LQR model in presence of noise. It is observed that the LQR controlled model is unable to track the system's true behaviour in the presence of noise. Moreover, the controller generates a control signal, which has a severely detrimental effect on the dynamic characteristics of the vehicle. In such a scenario, it is possible that the vehicle will suffer instability.

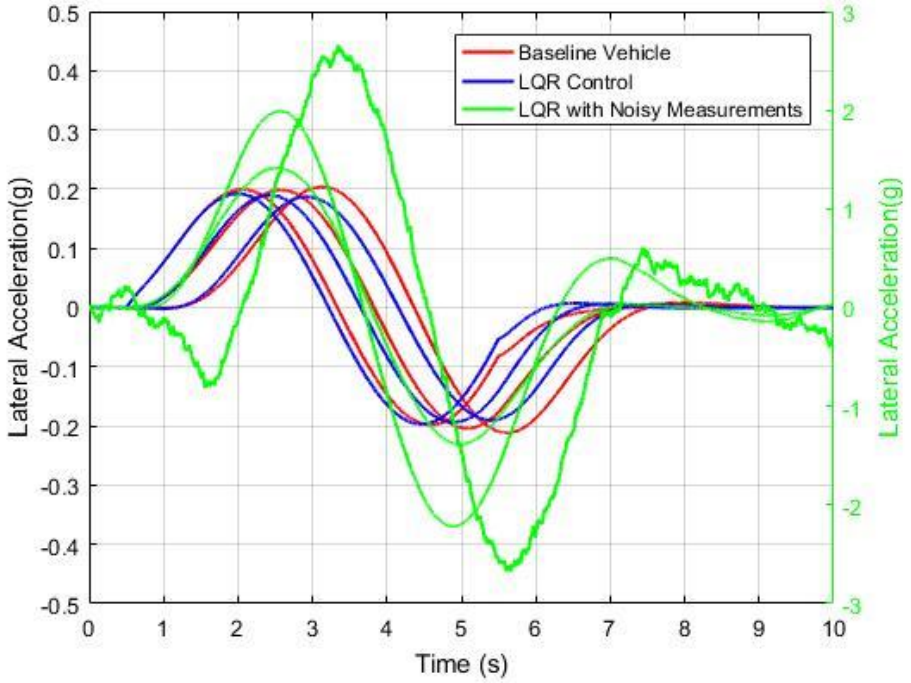

Figure 5.11: Time history of lateral accelerations for baseline vehicle, nominal LQR control and LQR control with noisy measurements.

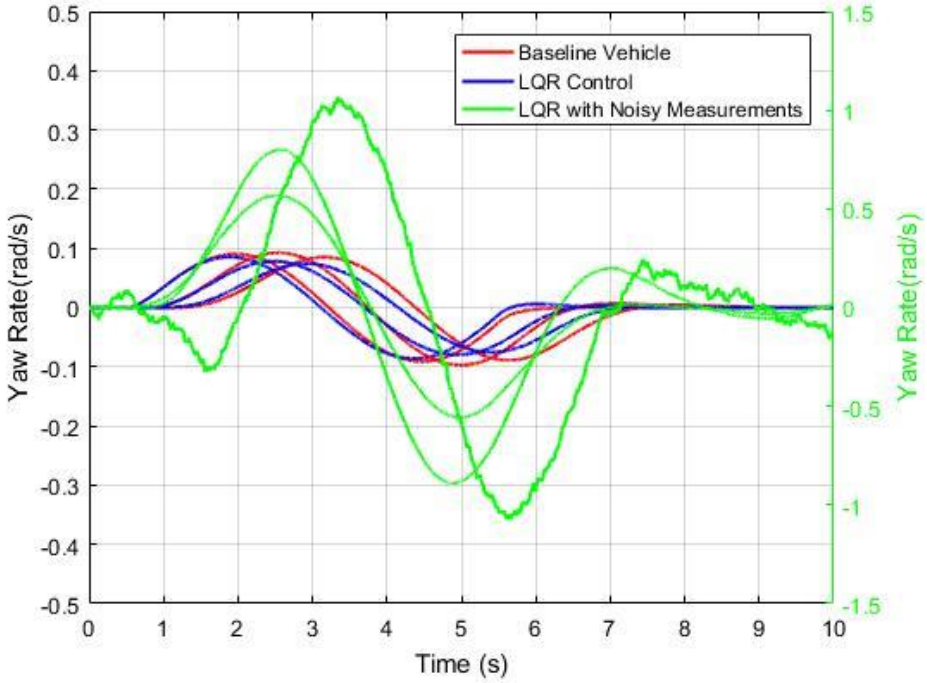

Figure 5.12: Time history of yaw rates for baseline vehicle, nominal LQR control and LQR control with noisy measurements.

The LQR controller requires full state feedback in order to generate control signal, i.e. to generate the optimal value of the trailer steering angle, it requires the measurement data of all the states [85]. Moreover, as shown in Figures 5.11 and 5.12, the controller is unable to control the vehicle in the presence of noisy measurements. In order to overcome the above-stated concerns, a state estimator is required that can estimate all the system states and predict the system's true behaviour in the presence of measurement noise. Hence, a KF is integrated with the LQR controller, to assist the LQR controller by estimating the system states and by rejecting the measurement noises to provide a robust tracking performance.

5.3. Performance of the LQR Controller with KF (LQG Controller)

To overcome the robustness concerns of the LQR controller, a KF is integrated in the closed-loop system. KF rejects the system noises and assists the LQR controller in tracking its true behavior. The combination of the LQR controller and KF is termed as the LQG controller.

Figures 5.13 and 5.14 compare the actual outputs of the baseline 4-DOF B-train model and Kalman filter's estimations of the outputs in the presence of noise. The results establish KF's effectiveness as a state estimator. KF can accurately estimate the lateral acceleration and yaw rate response of the B-train double. It should be noted that the inputs to the KF are the known steering input and the noisy measurement signals, as shown in Figures 5.1, 5.9 and 5.10. In these simulations, the vehicle forward speed is 88kph with a steering input frequency of 0.2 Hz.

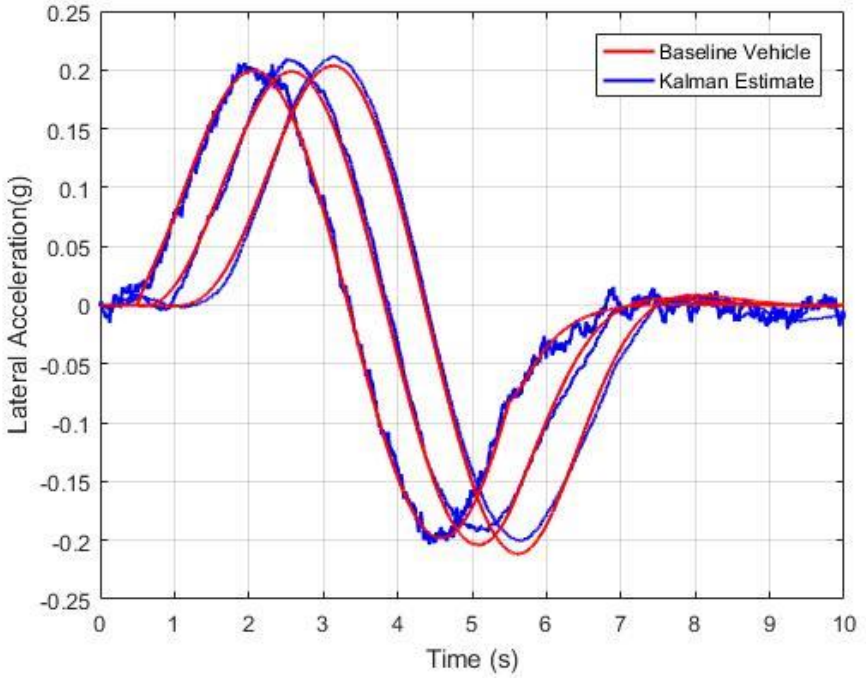

Figure 5.13: Time history of lateral accelerations for the baseline vehicle and estimation by the Kalman Filter.

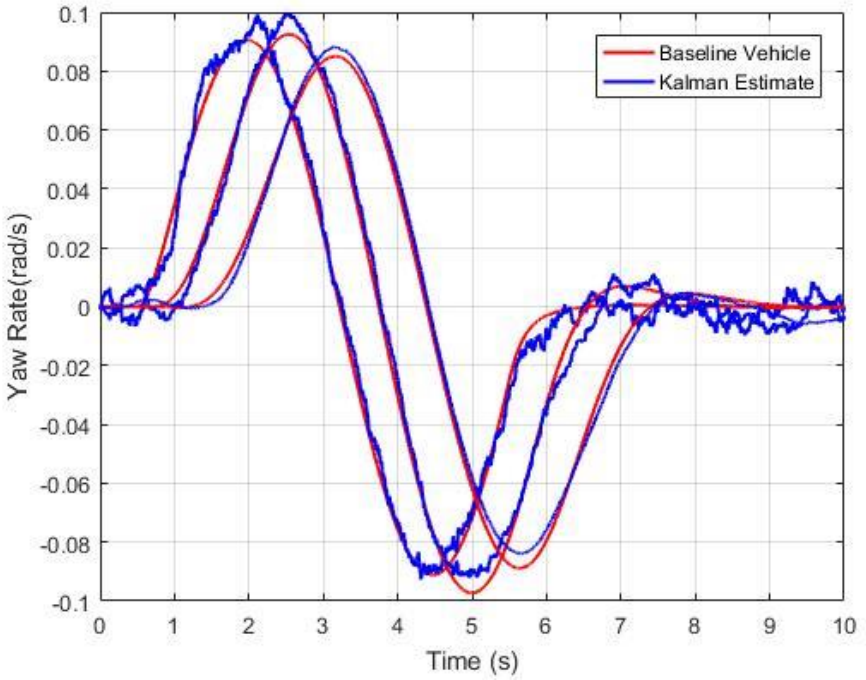

Figure 5.14: Time history of yaw rates for the baseline vehicle and estimation by the Kalman Filter.

In Figures 5.13 and 5.14, the efficacy of KF as a state estimator is established. Hence, KF can be integrated with the LQR controller to accurately predict the system's outputs in presence of noise. Moreover, the combination of KF and LQR controller can ensure optimal system performance despite the presence of noise. As previously mentioned, the combination of KF and LQR controller is termed as LQG controller. In the following paragraphs, the performance of LQG controller is evaluated.

The performance of the LQG controller is examined in Figures 5.15 and 5.16, by comparing the lateral acceleration and yaw rate response of the vehicle units with the nominal LQR control system without noise. It is evident that the LQG controller accurately predicts the dynamic characteristics of the vehicle model. This indicates that the KF is capable of effectively rejecting noise and thereby successfully augments the robustness of the LQR control system. Moreover, the system achieves optimal performance by utilising the LQG controller.

Although the LQR and LQG controllers successfully enhance the vehicle's stability, they have a detrimental effect on the vehicle's trajectory. Figure 5.17 compares the trajectories of the three vehicle units: tractor, first trailer and the second trailer for the baseline vehicle model and LQR controlled vehicle model. The figure indicates a notable deviation (> 1m) in the lateral displacement achieved by the baseline and LQR controlled vehicle models. Since SLC is an open-loop maneuver, the driver or driver model cannot intervene to correct the intended trajectory. Moreover, LQR controllers generally do not employ a reference yaw-rate model, which ensures that the driver's intention and vehicle's response are synchronised.

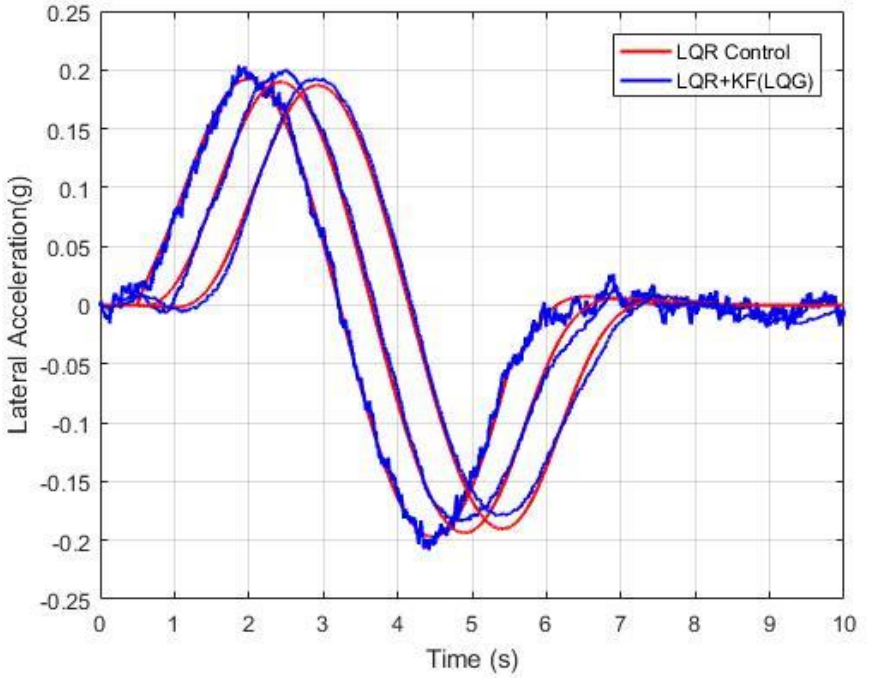

Figure 5.15: Time history of lateral accelerations for the nominal LQR control and the LQG (LQR+KF) control.

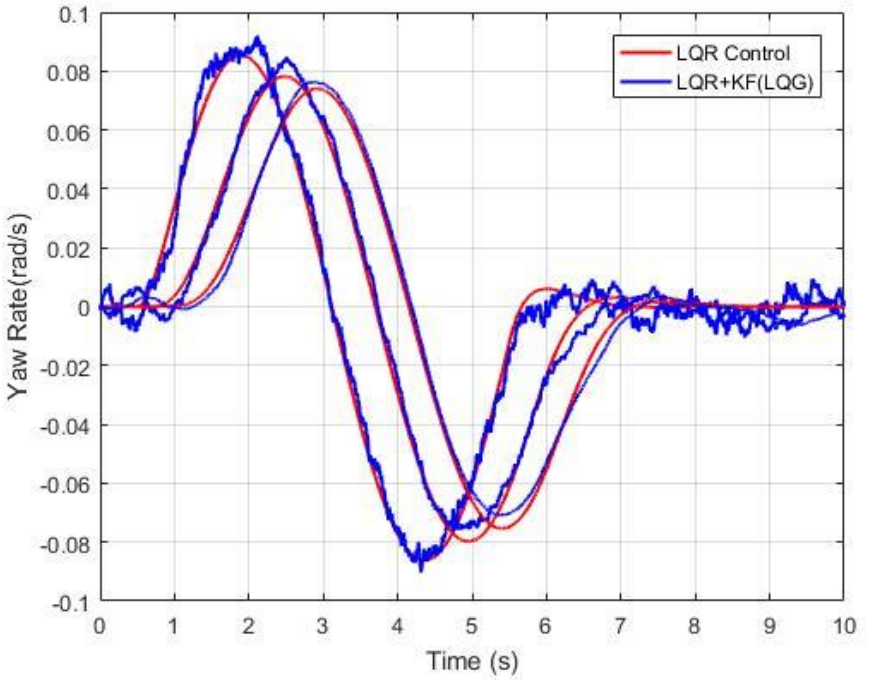

Figure 5.16: Time history of yaw rates for the nominal LQR control and the LQG (LQR+KF) control

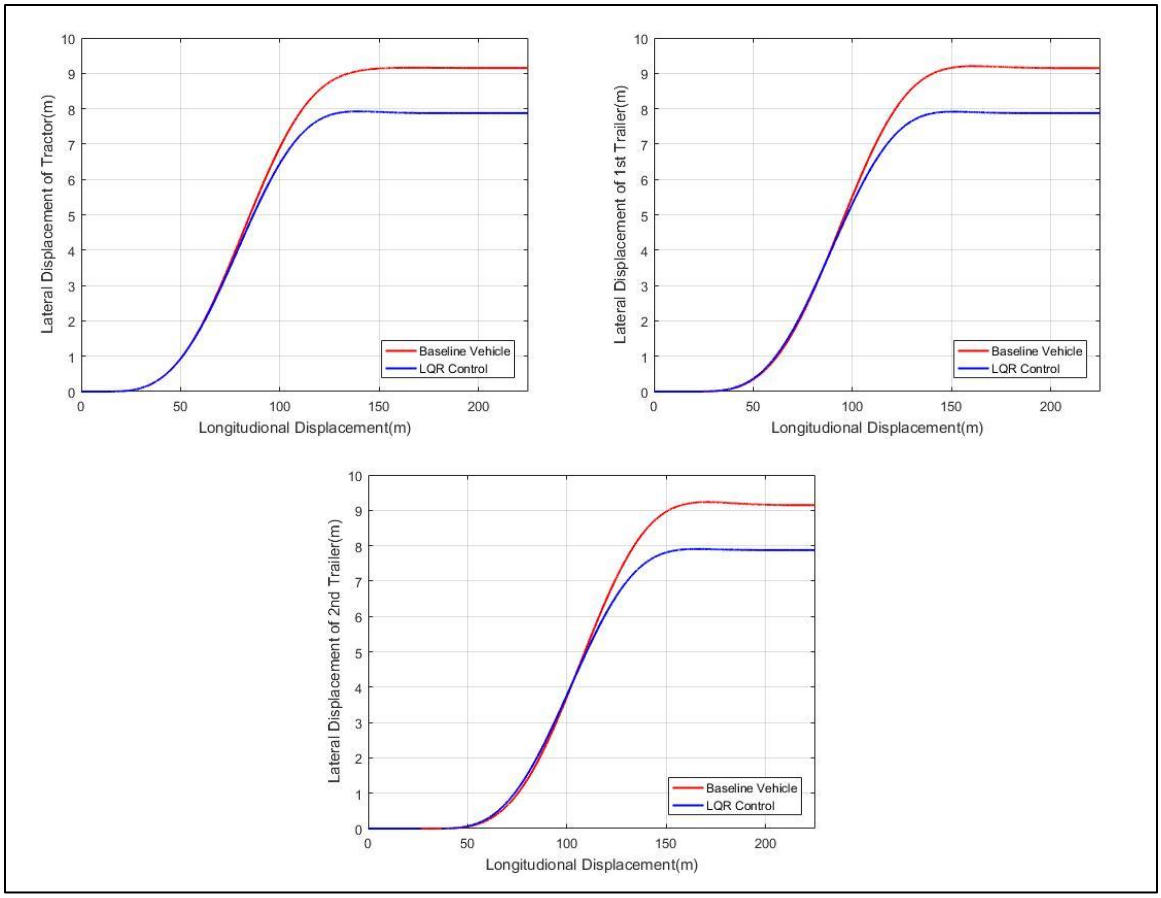

Figure 5.17: Trajectories of the vehicle units for the baseline vehicle model and LQR controlled vehicle model.

5.4. Performance Limitations of LQR Controller

5.4.1. Performance of the LQR Controller with Varying Steering Input Frequency

As mentioned at the beginning of this section, the frequency of steering input has a drastic effect on the vehicle's dynamic performance. Thus, a comparison is conducted to evaluate the LQR controller's performance with a steering input frequency of 0.4 Hz.

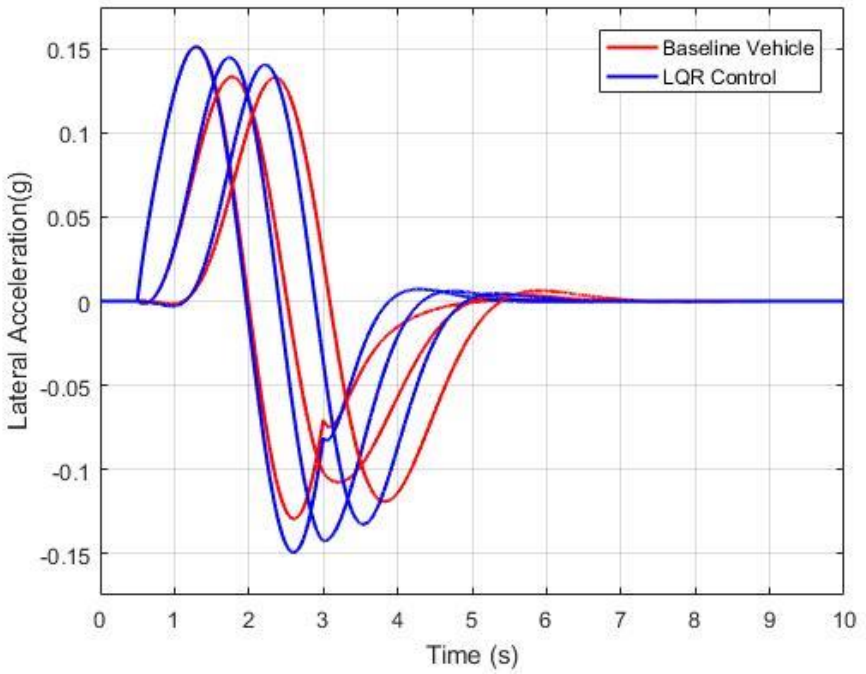

Figure 5.18: Time history of lateral accelerations for the baseline vehicle with and without the LQR controller with the steering input frequency of 0.4Hz.

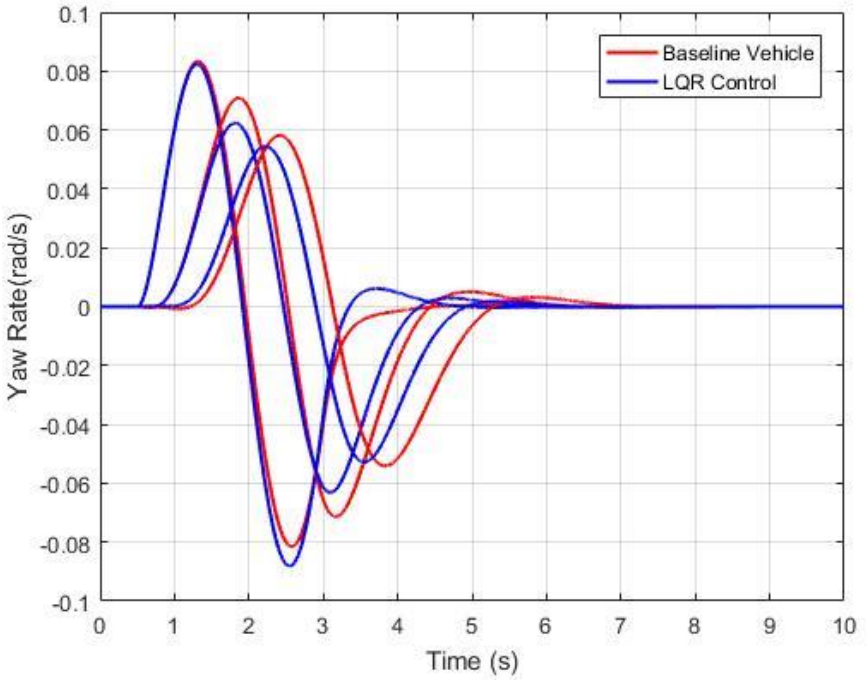

Figure 5.19: Time history of yaw rates for the baseline vehicle and the LQR controller with the steering input frequency of 0.4Hz.

Figures 5.18 and 5.19 demonstrate the lateral accelerations and yaw rates response of the B-train double models respectively. It is evident that the LQR controller is unable to reduce the peak lateral acceleration of the vehicle during the 0.4 Hz steering input SLC maneuver. In fact, the peak values of lateral acceleration are even higher than the baseline values. Conversely, Figure 5.19 shows a reasonable reduction in yaw rates of first and second trailers in comparison with the baseline vehicle model.

Results indicate the limitations of the LQR controller. The figures illustrate that the LQR controller's performance varies with the change in steering input. Moreover, attaining the optimal performance will require retuning the weighting matrices Q and R.

5.4.2 Performance of the LQR Controller under Parametric Uncertainties

Figures 5.20 and 5.21 show the lateral acceleration and yaw rate response of the vehicles with and without the LQR controller in the *worst case*. The *worst case* is a random combination of 13 parametric uncertainties as mentioned in section 4.2.3. A random combination of these parameters are considered *worst* for the dynamic performance of the vehicle. These parameters are listed in Appendix 2.

It is apparent that the baseline vehicle exhibits instability in the *worst case* scenario. Although the LQR controller prevents the system from becoming unstable, it cannot effectively control the lateral acceleration and yaw rates of the vehicle. Figure 5.22 provides further insight into the LQR controller's performance. The figure depicts the trajectories of the vehicle units. It is clear that the LQR controller cannot manipulate the lateral displacement to reach a reasonable value. The lateral displacement reaches a very large value of 60 meters before stabilizing.

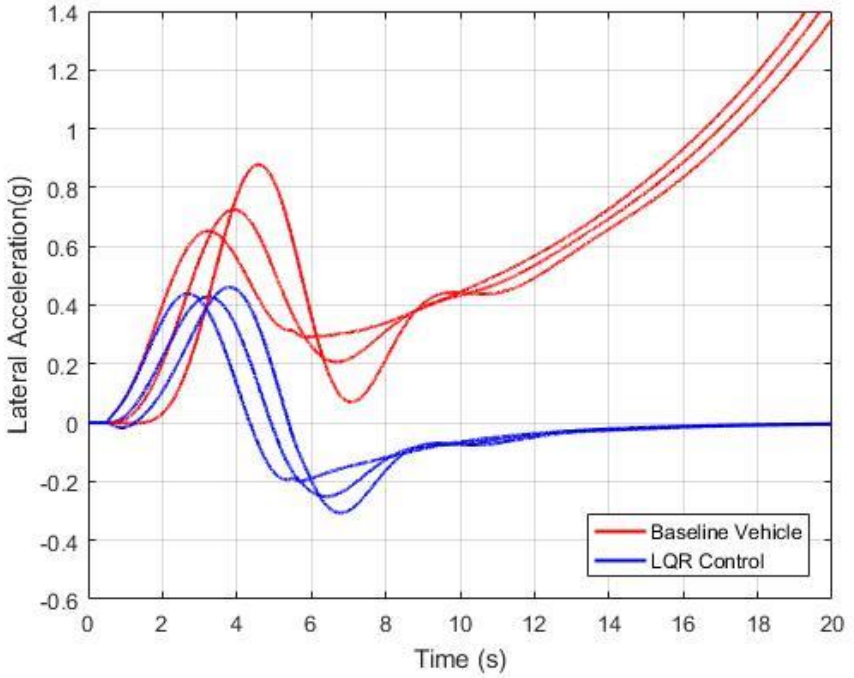

Figure 5.20: Time history of lateral accelerations for baseline vehicle and the LQR controller for the worst-case scenario.

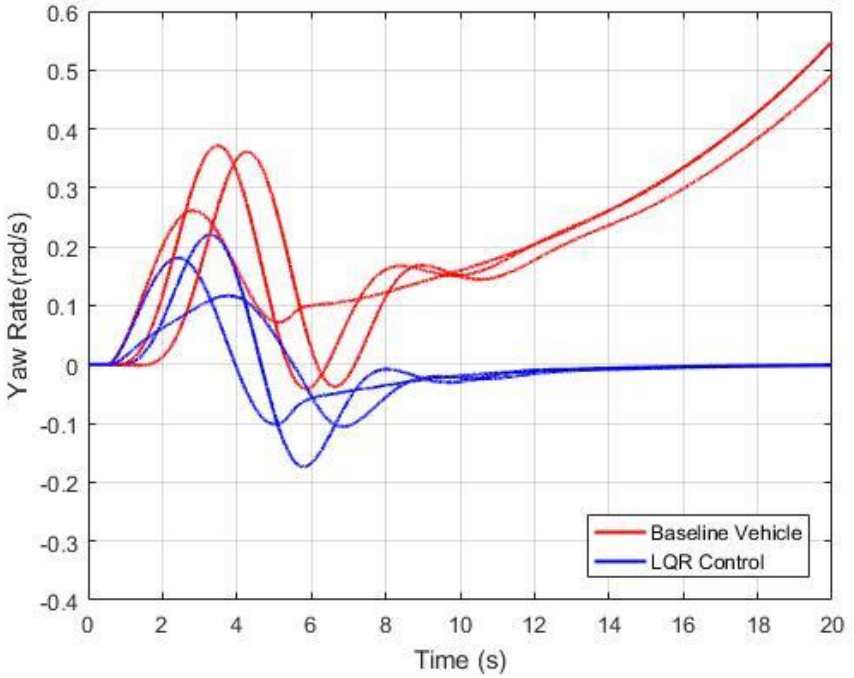

Figure 5.21: Time history of yaw rates for baseline vehicle and the LQR controller for the worst-case scenario.

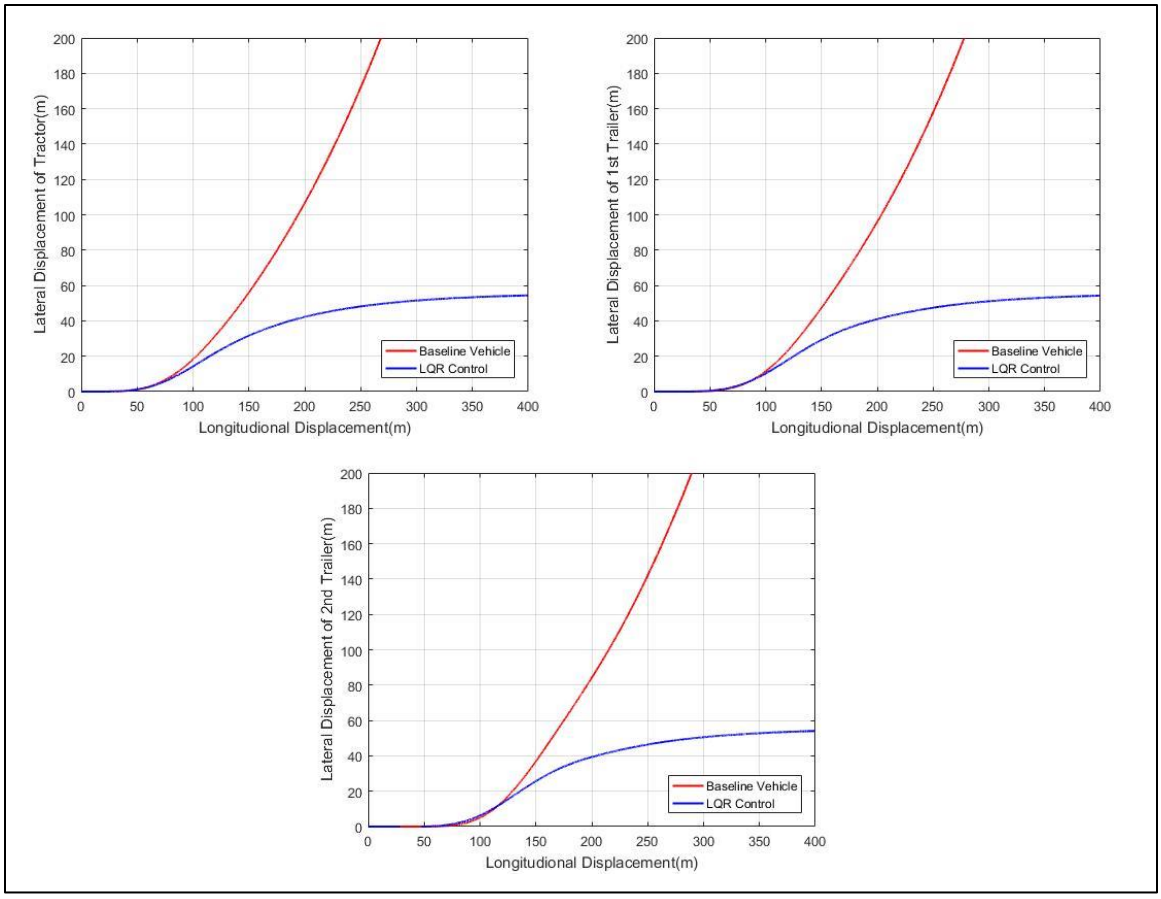

Figure 5.22: Trajectories for baseline vehicle with and without the LQR controller for the worst-case scenario.

The results presented in section 5.4.1, suggest that the LQR Controller requires retuning in order to produce optimal performance during the 0.4 Hz SLC maneuver. In real life, retuning of the control system is not always possible. Moreover, the LQR Controller's performance in the *worst case* scenario clearly indicates its limitations. Thus, a robust control technique is required that is capable of improving the dynamic performance of the vehicle without being interrupted by changing parameters. The controller must be capable of effectively controlling the lateral accelerations and yaw rate of the vehicle in order to deliver a robust dynamic performance of the vehicle.

5.5. Performance of the μ synthesis Controller

5.5.1. Performance of the μ synthesis Controller without System Noise

To examine the effectiveness of the robust μ synthesis controller, the vehicle model with and without the controller are compared. Figure 5.23 and 5.24 show the dynamic responses of the vehicle model with and without the μ synthesis controller under the single lane-change maneuver with 0.2Hz steering input as defined in Figure 5.1.

It is evident that the vehicle with the μ synthesis controlled vehicle model exhibits superior performance than the baseline vehicle model. The maximum peak values of the lateral acceleration of the tractor, the first trailer and the second trailer with the μ synthesis controller are 0.166g, 0.169g, and 0.175g reduced by 16.3%, 17% and 17.3% from the baseline values of 0.198g, 0.204g and 0.212g, accordingly (Figure. 5.23).

Moreover, the maximum peak values of the yaw rates are reduced by 11.2%, 18.5% and 14.9% from the baseline values of 0.091 rad/s, 0.097 rad/s and 0.088 rad/s to the controlled values of 0.081 rad/s, 0.079 rad/s and 0.076 rad/s, respectively.

Since, the μ synthesis controller employs a reference yaw-rate model to enhance the vehicle's dynamic performance. It is essential to see the controller tracking performance. Figure 5.25 depicts the reference yaw rate tracking performance of the μ synthesis controller. The reference signal is generated as described in section 4.5.2. The figure shows that the μ synthesis controller effectively tracks the reference yaw rate. In fact, the controller demonstrates excellent agreement specifically with the reference signal of the second trailer. This can be attributed to the fact that ATS systems have the most influence on the yaw motion of the rearmost (second) trailer.

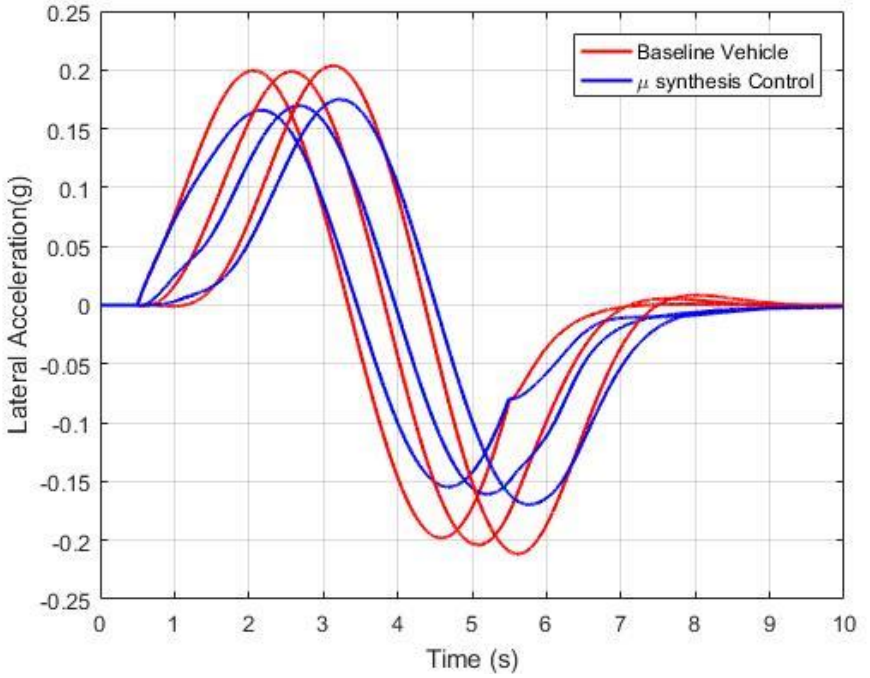

Figure 5.23: Time history of lateral accelerations for vehicle with and without μ synthesis controller for steering input of 0.2 Hz.

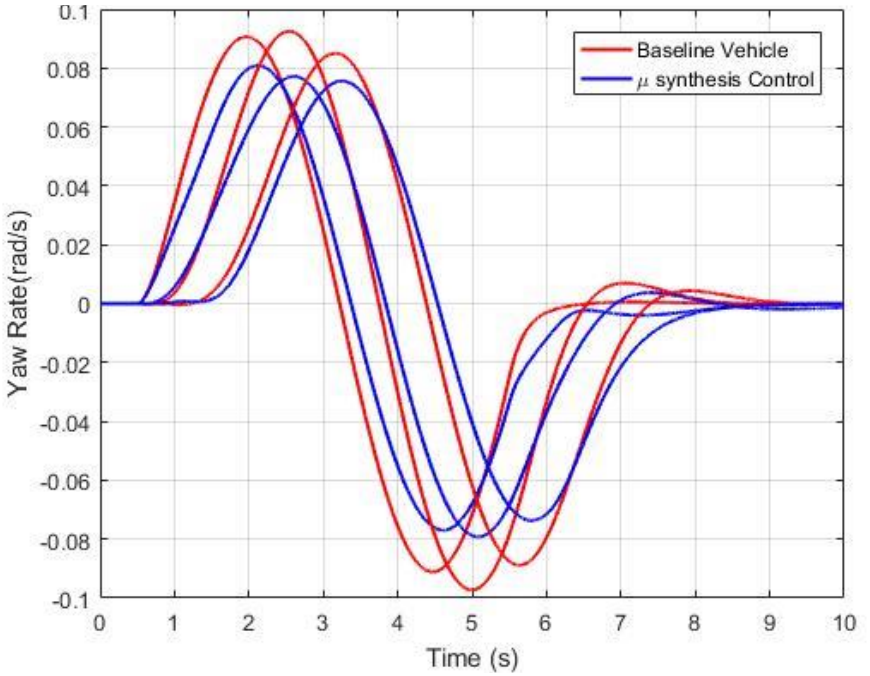

Figure 5.24: Time history of yaw rates for vehicle with and without μ synthesis controller for steering input of 0.2 Hz.

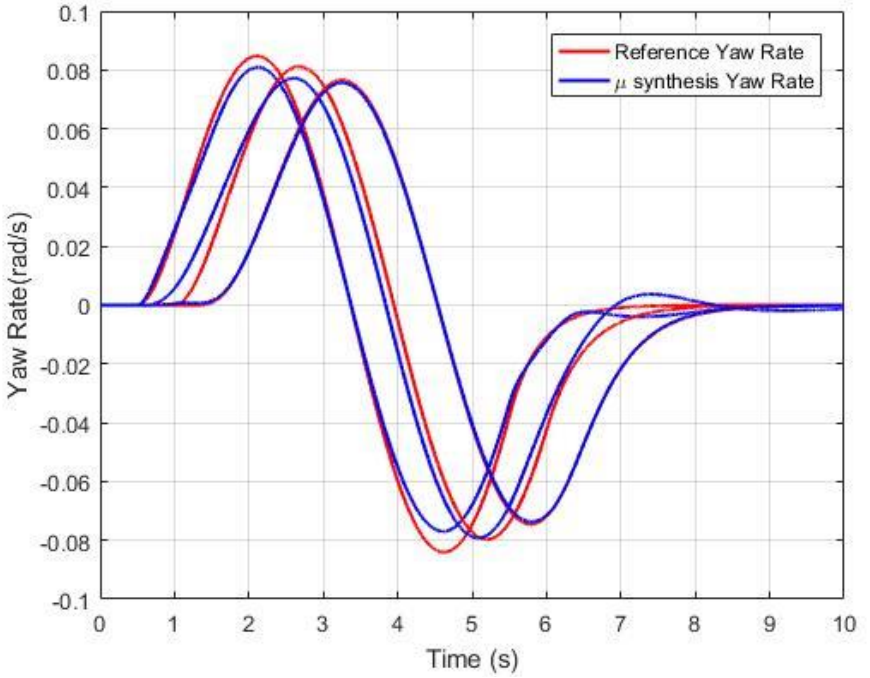

Figure 5.25: Time history of yaw rates of reference model and μ synthesis controller

5.5.2. TruckSim MATLAB Co-Simulation

Furthermore, to validate the designed μ synthesis controller, co-simulations are performed using MATLAB/Simulink and TruckSim environments. The co-simulation environment is same as that defined in section 5.2. Here, the LQR controller is replaced with the μ synthesis controller. Figure 5.26 shows the co-simulation environment between MATLAB and TruckSim software packages.

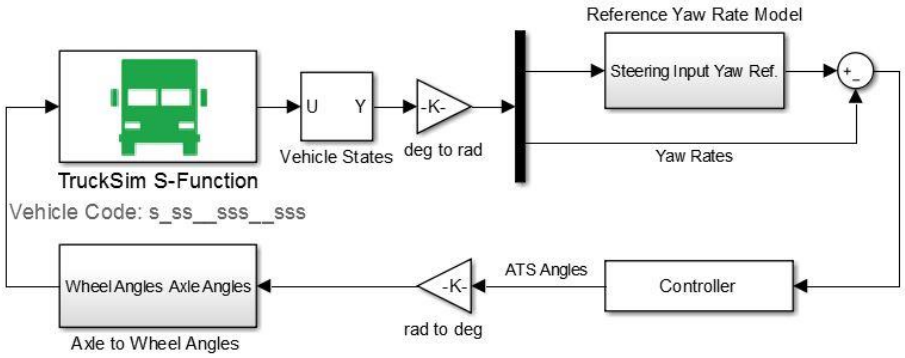

Figure 5.26: The co-simulation environment with MATLAB and TruckSim using the μ synthesis controller.

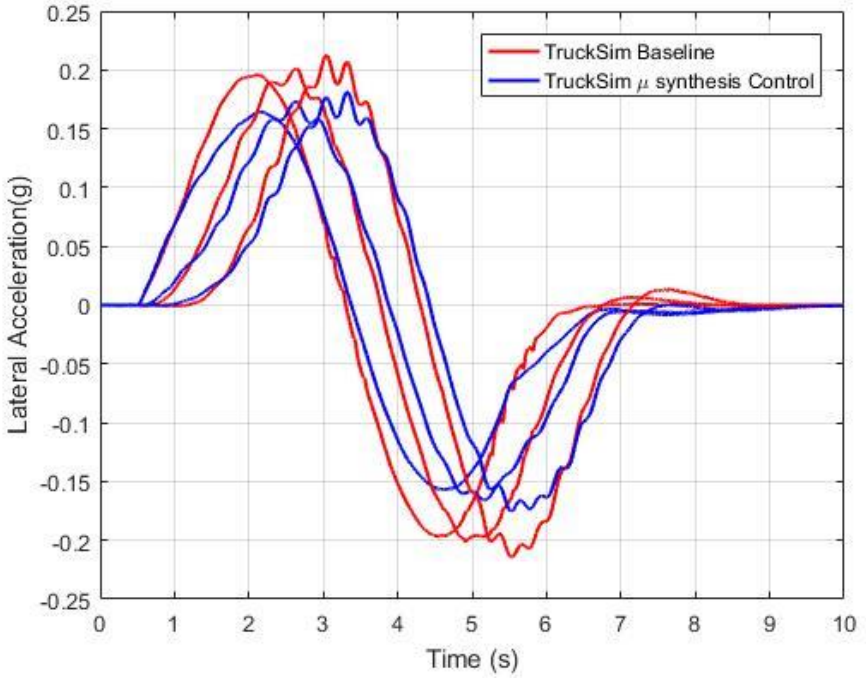

Figure 5.27: Time history of lateral accelerations of the TruckSim model with and without the μ synthesis controller.

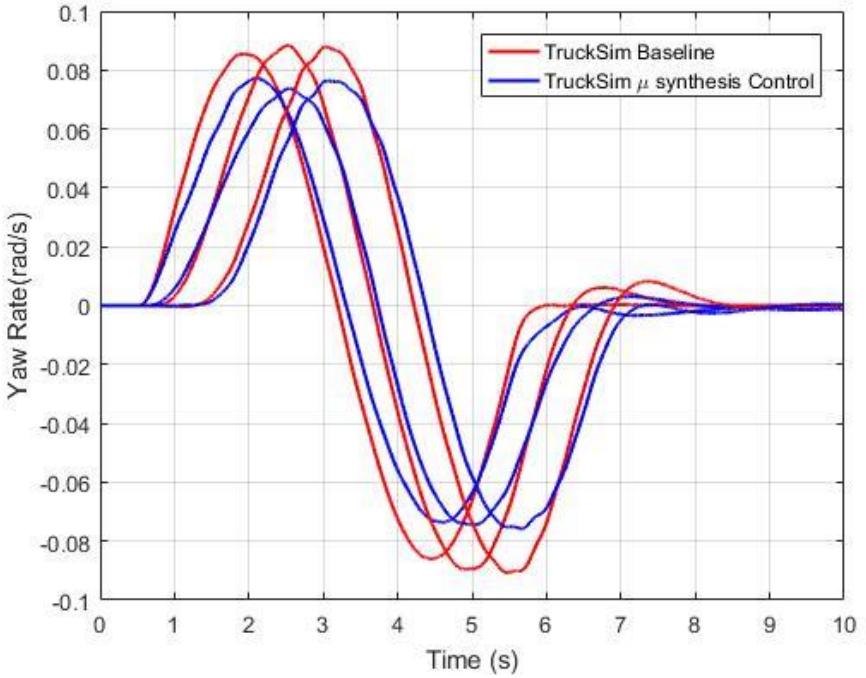

Figure 5.28: Time history of yaw rates of the TruckSim model with and without the μ synthesis controller.

Figures 5.27 and 5.28 compare the lateral acceleration and the yaw rate response of the TruckSim model with and without the μ synthesis controller. It can be observed, that the ATS controlled vehicle model successfully reduces the lateral acceleration peaks of the tractor, first trailer and second trailer, and therefore enhances the vehicle stability. Identical results are observed for the yaw rate behavior of the vehicle units.

Figures 5.29 and 5.30 compare the μ synthesis controlled 4-DOF and the TruckSim vehicle models. Despite the minor discrepancies in the yaw rates of the two vehicle models, the figures indicate excellent agreement between the lateral acceleration responses. The noted discrepancies in yaw rate can be attributed to the innate non-linearities of the TruckSim model.

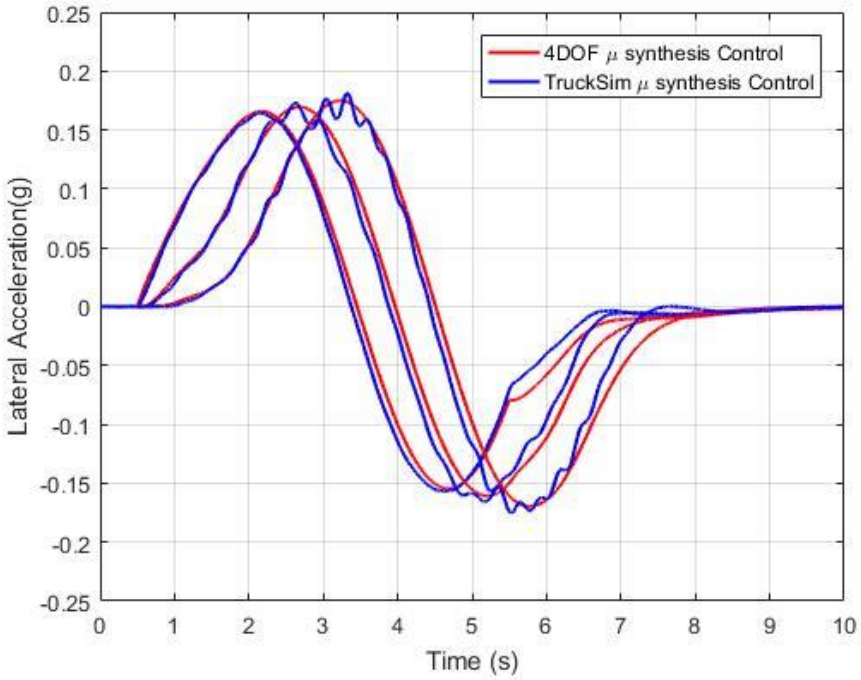

Figure 5.29: Time history of lateral accelerations of the 4-DOF and TruckSim model with μ synthesis controller.

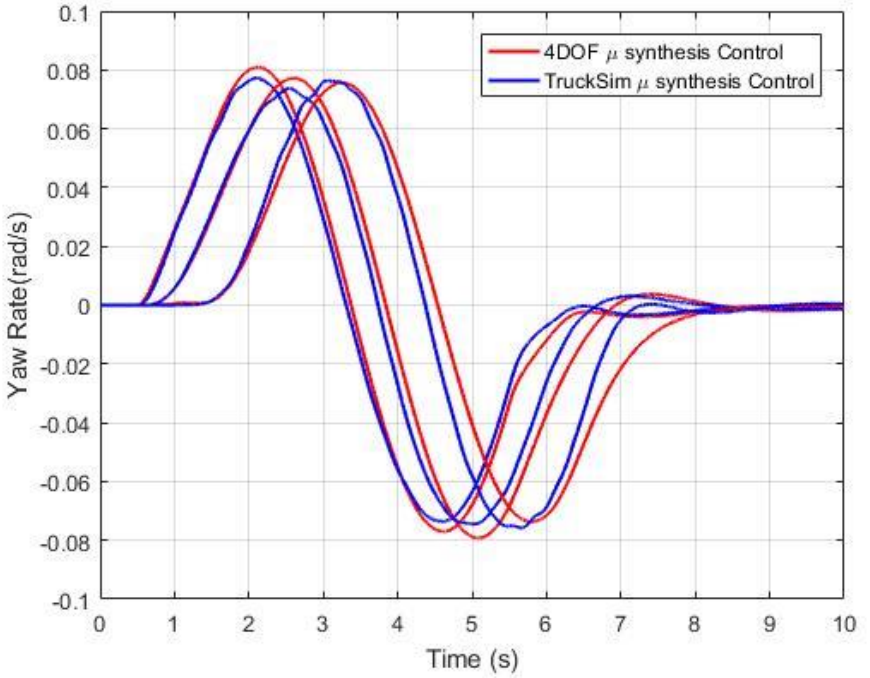

Figure 5.30: Time history of yaw rates of 4-DOF and TruckSim model with μ synthesis controller.

5.5.3. Robust Performance of the μ synthesis Controller

To establish that a controller is robust, a measure is required which quantifies the systems robustness. The robustness of the μ synthesis controller is assessed in terms of the achieved μ value. A robust performance analysis is conducted to evaluate the closed-loop vehicle system, subjected to parametric uncertainties as described in section 4.5. Figure 5.31 illustrates the achieved μ value over a range of frequency. As seen in this figure, the peak μ value is 0.935, which is less than 1 and satisfies the robust performance condition expressed in Equation (4.16).

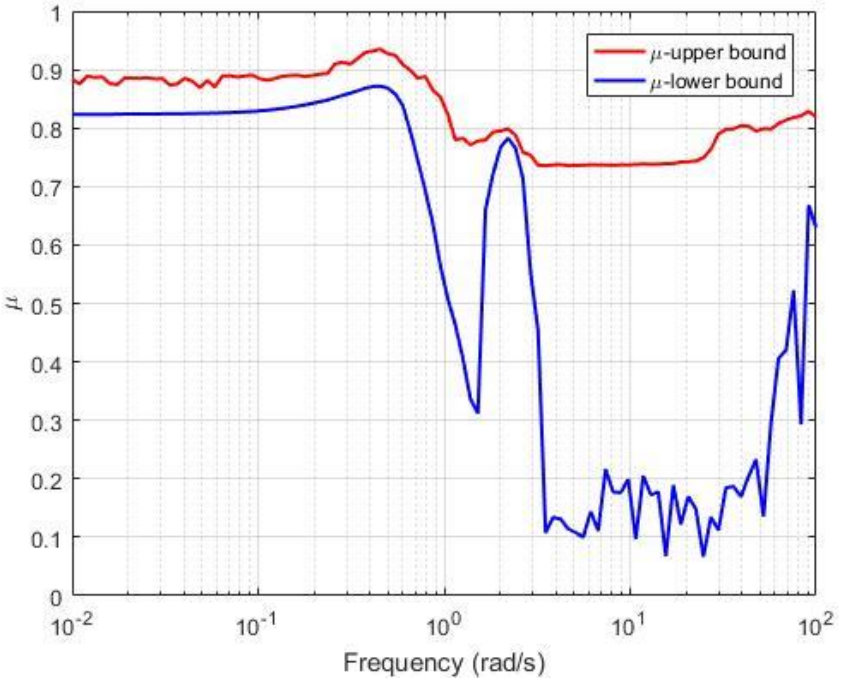

Figure 5.31: Frequency response of μ.

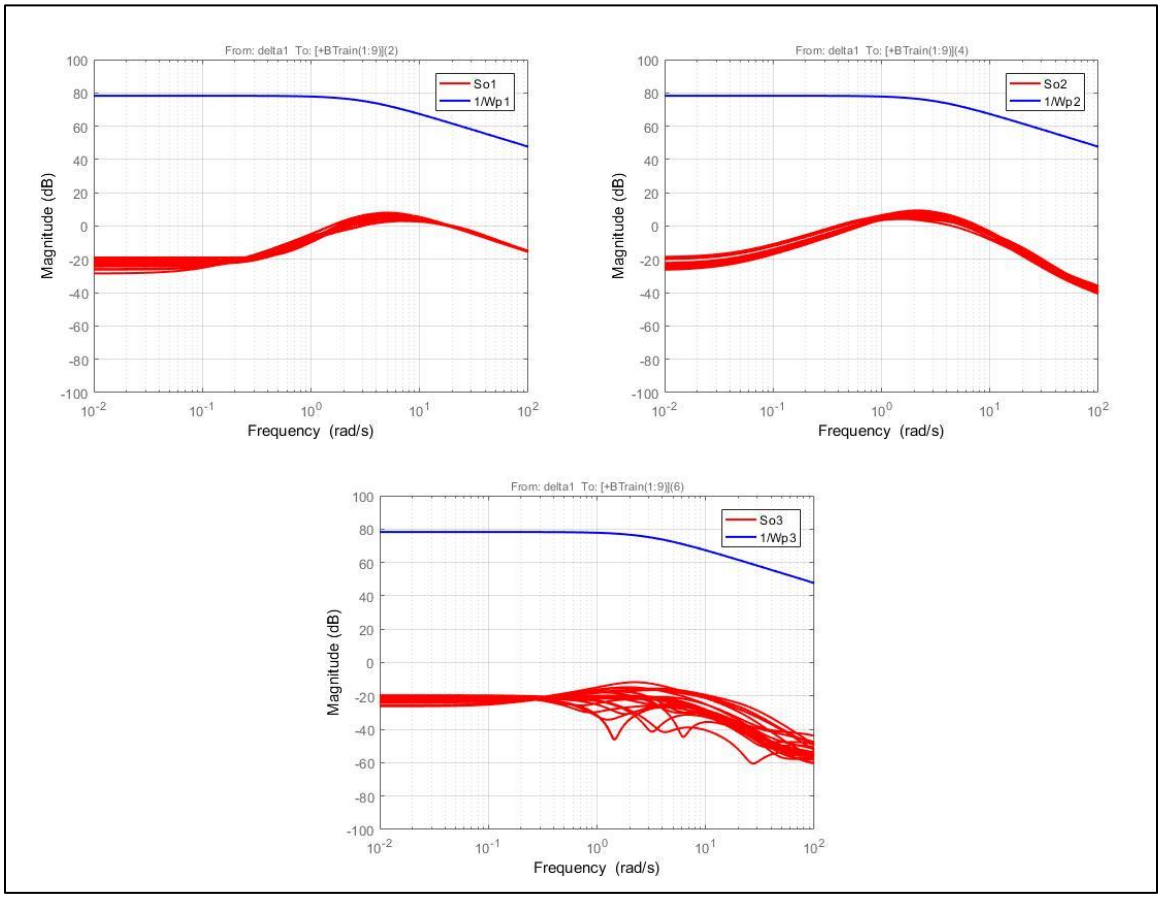

Figure 5.32: Frequency response of the output weighting functions.

To satisfy the performance criterion shown in Equation (4.16), it is necessary that the magnitude responses of the output sensitivity function with system uncertainties lie below the magnitude responses of the inverse of the performance weighting functions in the whole frequency range [19, 26]. Figure 5.32 indicates that the respective output sensitivity function lies below the corresponding inverse of the performance weighting function of the tractor, first trailer and second trailer yaw rates respectively.

5.5.4. Performance of the μ synthesis Controller with System Noise

As discussed in section 5.4, the behaviour of the LQR controller varies significantly in the presence of the system noise, and therefore the LQR controller cannot guarantee robust performance in such situations. Hence, it is necessary to evaluate the performance of the μ synthesis controller and its behaviour in the presence of system noise.

Figure 5.33 displays the yaw rate measurements of the 4-DOF vehicle model with and without measurement noise. It can be observed that the true behavior of the vehicle cannot be assessed by using the noisy measurements. As indicated in the figure, only yaw rates are considered, as they are only measured sensor outputs for the μ synthesis control system. Figure 5.34 shows a comparison of yaw rates of the vehicle models equipped with the μ synthesis controller with and without the system noise. It is evident that the μ synthesis controller can very well reject the system noises and track its true outputs. In the μ synthesis controller, the noise weighting functions, described in section 4.5.2, aid the control system to reject measurement noise and maintain optimal performance.

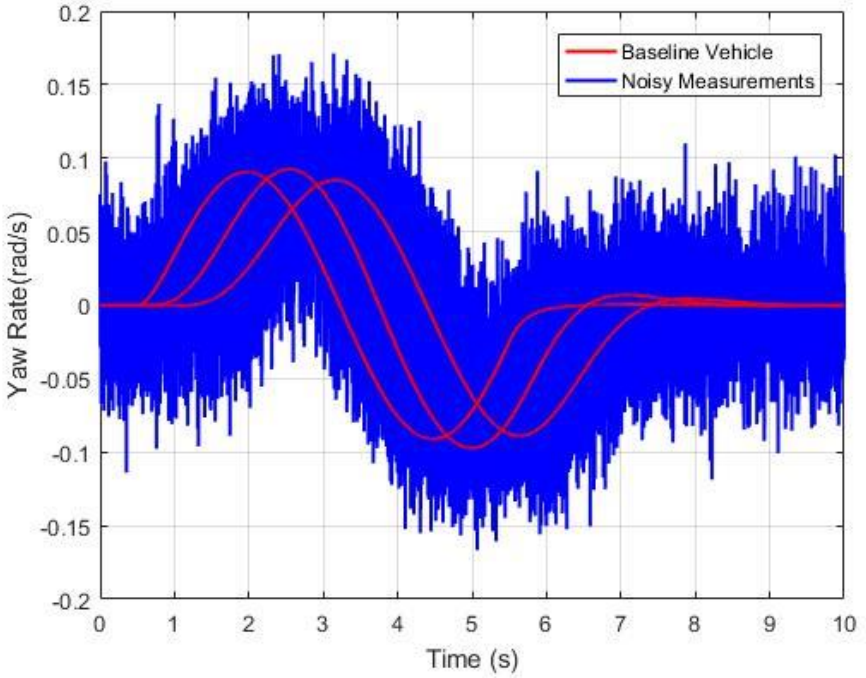

Figure 5.33: Time history of yaw rate measurements μ synthesis controller with and without sensor noise.

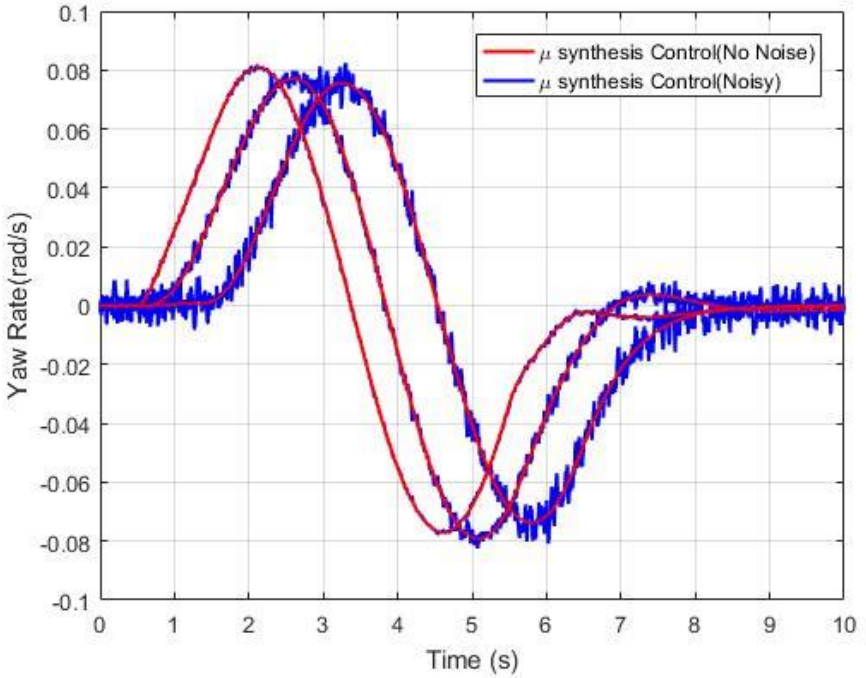

Figure 5.34: Time history of yaw rate for the μ synthesis controller with and without noise.

5.5.5. Performance of the μ synthesis Controller under Random Uncertainties

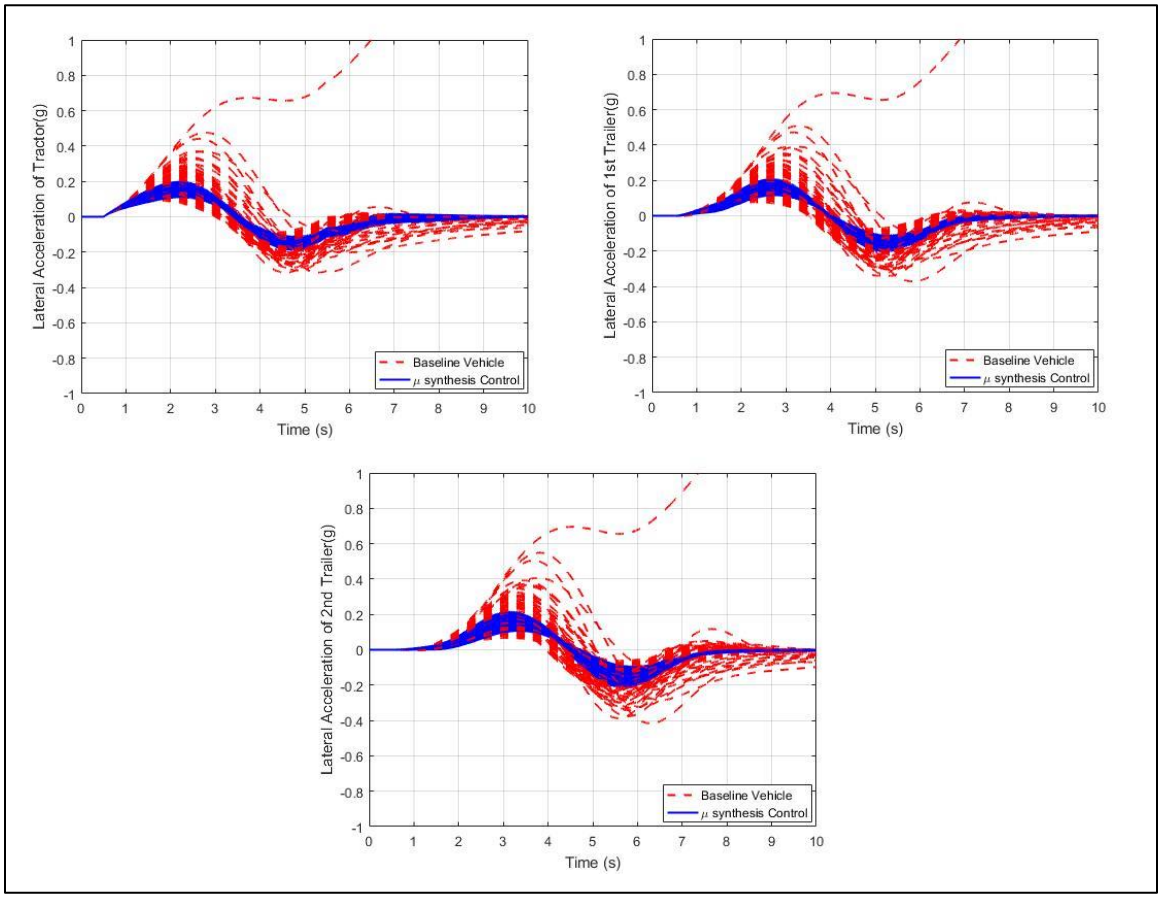

Figure 5.35: Time history of lateral accelerations of all vehicle units for baseline vehicle and μ synthesis control for 100 random cases.

To investigate the effects of the parametric uncertainties on the performance of the μ synthesis controller. Simulations are performed considering 100 random parametric uncertainties. The performance of the μ synthesis controller is demonstrated in Figures 5.35 and 5.36 using the vehicles' lateral accelerations and yaw rates response respectively. From the results, it can be observed that the baseline vehicle undergoes unstable motions in numerous conditions, whereas the robust μ synthesis controller allows the vehicle to maintain stability. Moreover, it assists the vehicle to maintain controlled motion in every given scenario.

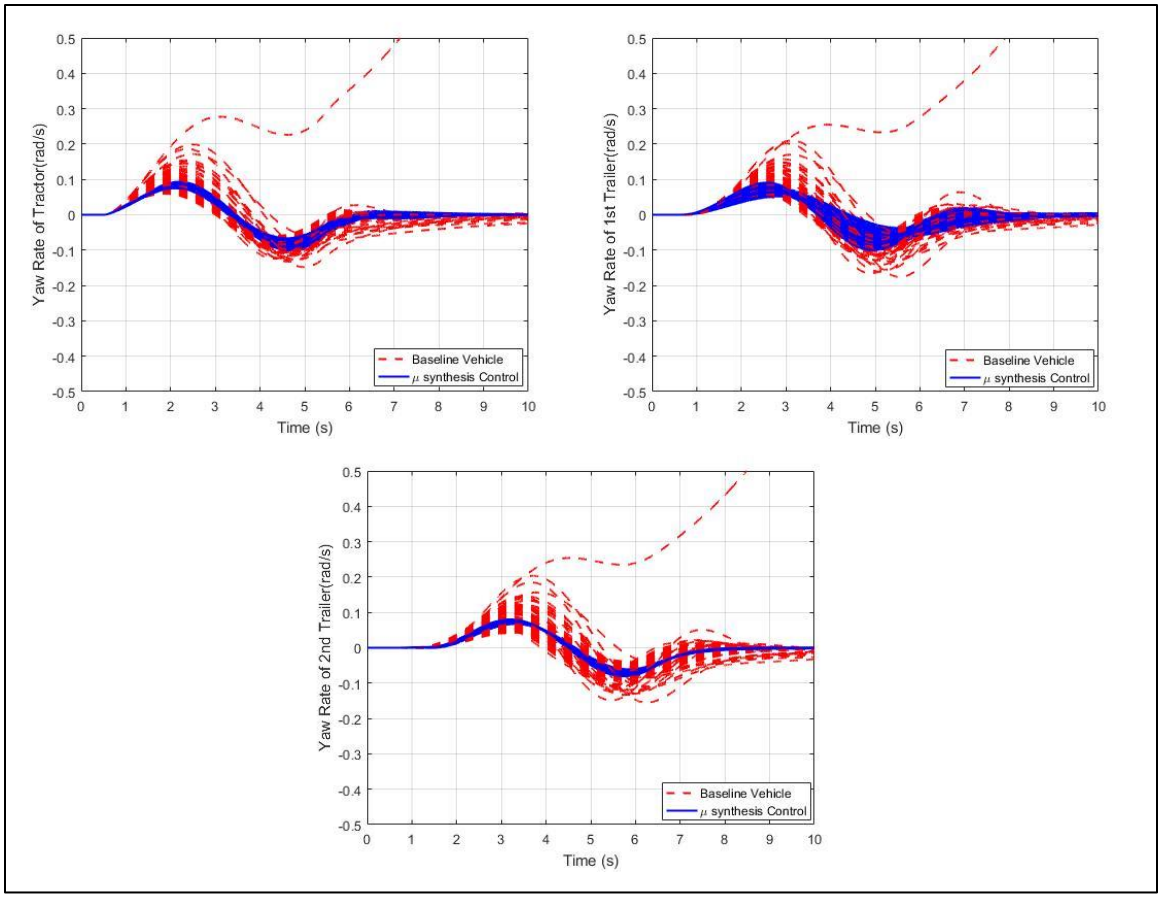

Figure 5.36: Time history of yaw rates of all vehicle units for baseline vehicle and μ synthesis control for 100 random cases

5.6. Comparative Analysis of LQR and μ synthesis Controllers

5.6.1. Influence on Path-following

Figure 5.37 compares the trajectories of baseline vehicle with the LQR and the μ synthesis controllers under the single lane-change maneuver. The figure demonstrates the behaviour of each vehicle unit. The results show that the LQR controlled model is unable to match the trajectory of the baseline model. This limitation of the LQR controller can be attributed to the absence of a reference yaw-rate model, as discussed in section 4.5.2. Conversely, the μ synthesis controller can not only match the trajectory of the bassline model but it also soothes the curves of the trajectory, resulting in a swift and smooth vehicle performance while negotiating a signal lane change maneuver.

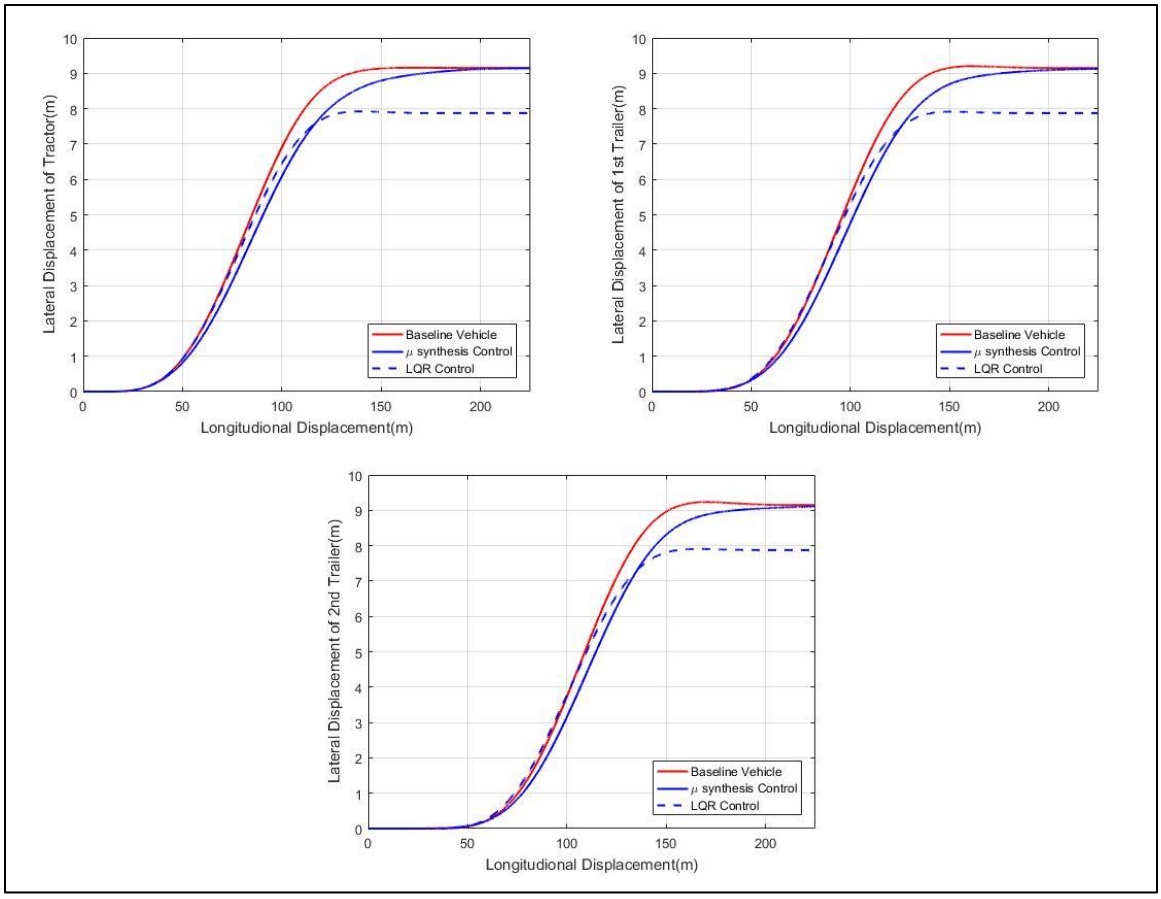

Figure 5.37: Trajectories of vehicle units for baseline vehicle, LQR control and μ synthesis control.

5.6.2. Worst Case Analysis

To compare the robustness of the controllers, their performance under the worst-case is analysed. Figures 5.38 and 5.39 compares the lateral accelerations and yaw rates of the vehicles with the LQR controller and the μ synthesis controller under a single lane-change maneuver. The baseline model demonstrates instability. Although the dynamic responses of the LQR controlled vehicle are stable, they are not satisfactory. The vehicle equipped with the μ synthesis controller demonstrates the best performance.

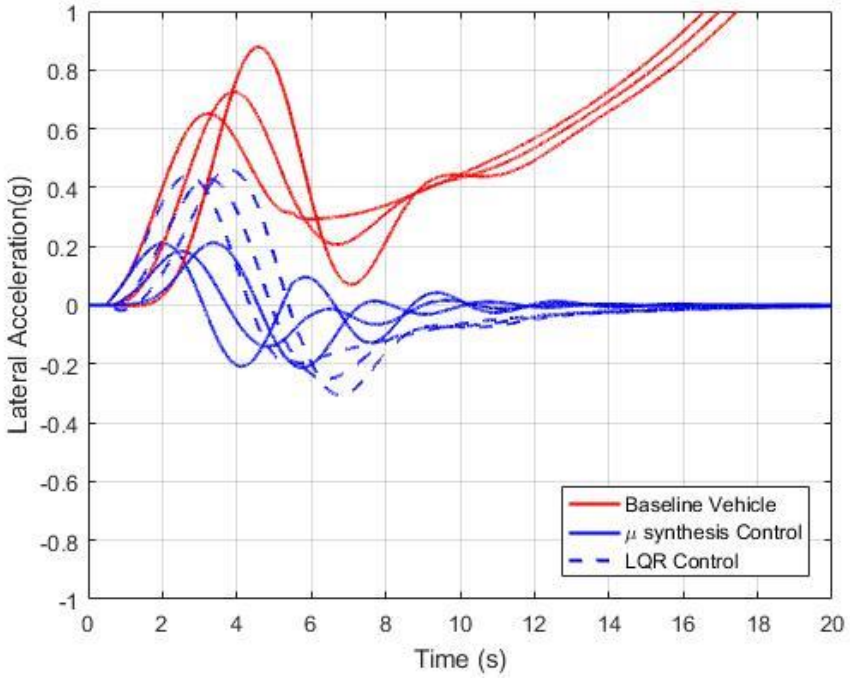

Figure 5.38: Time history of lateral accelerations for the baseline vehicle, the LQR and the μ synthesis controller with worst-case scenario.

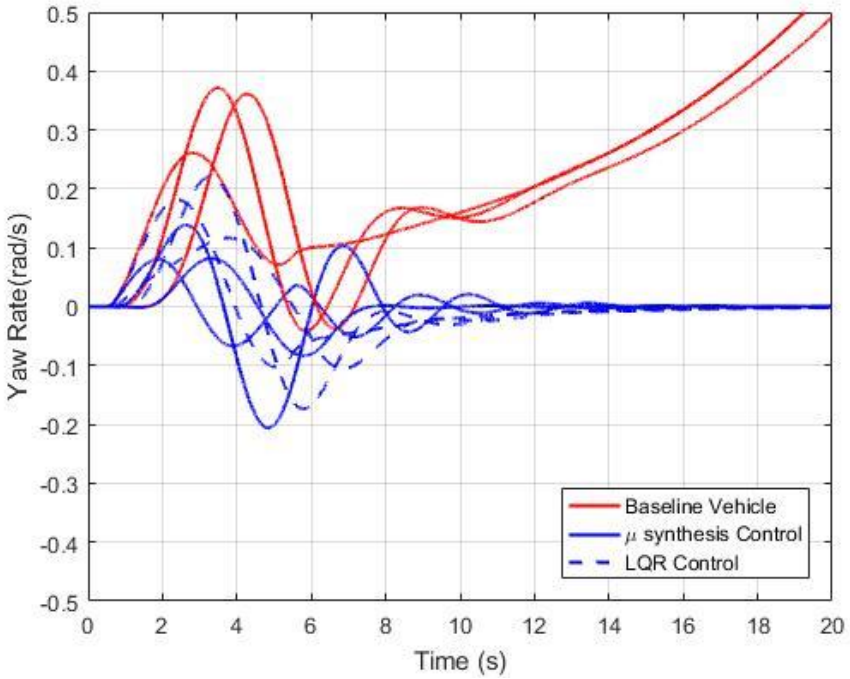

Figure 5.39: Time history of yaw rates for the baseline vehicle, the LQR and the μ synthesis controller with worst-case scenario.

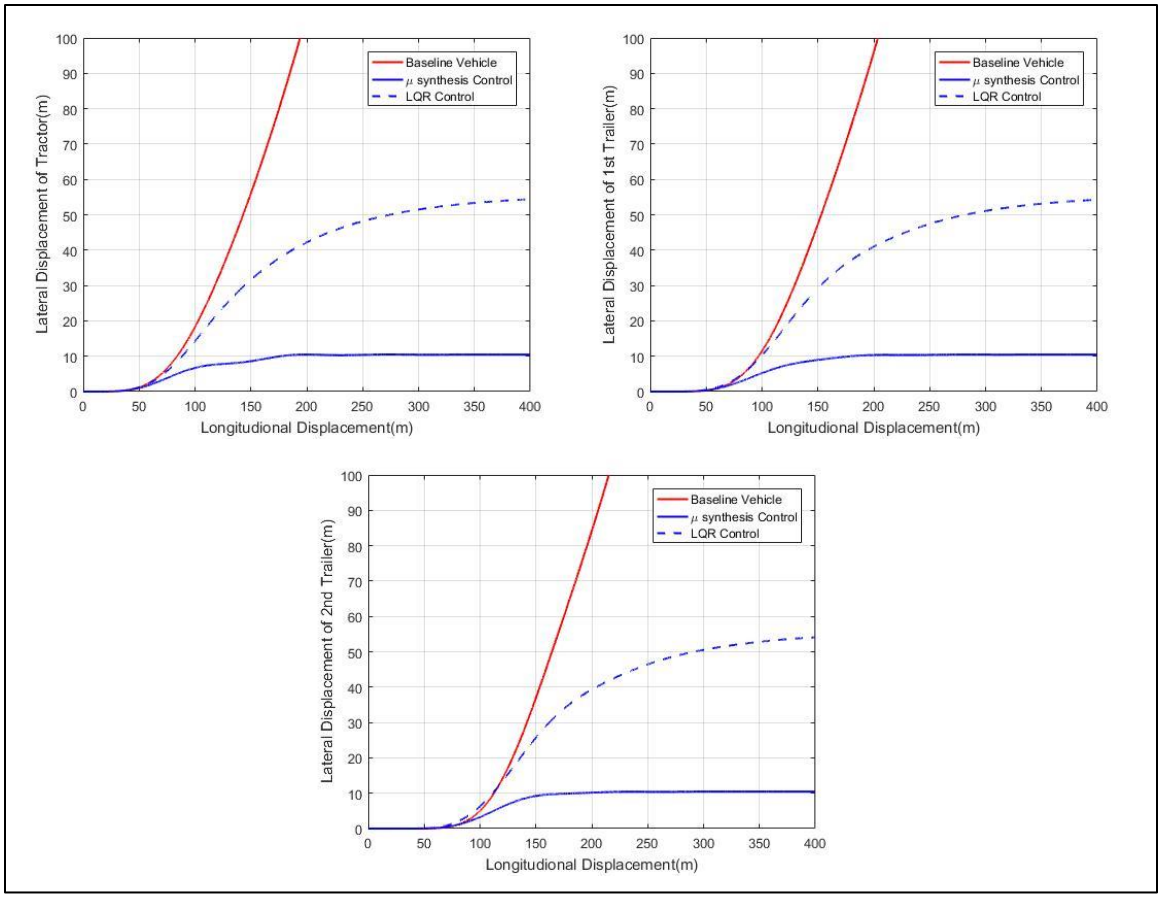

Figure 5.40: Trajectories of vehicle units for the baseline vehicle, the LQR and the μ synthesis controllers with worst-case scenario.

Figure 5.40 shows a comparison of the trajectories of the three cases, baseline vehicle model, LQR controlled vehicle model and the μ synthesis controlled vehicle model. It can be noted that only the μ synthesis controller is able to control the trajectories of all three units of the B-train double. The baseline vehicle becomes unstable, and the LQR controlled vehicle model has the trajectory around 6 times higher than that of the μ synthesis controlled vehicle model. Therefore, it can be concluded that an ATS system using the robust μ synthesis controller can improve the lateral stability of the B-train double over the wide range of parametric uncertainties.

5.7. Summary

In this chapter, initially the performance of the two-axle ATS system with the LQR control technique is evaluated. In addition, an analysis of the LQR controller's performance in the presence of system noise is conducted. It can be concluded from the results that the LQR controller, is unable to effectively reject the system noise and therefore unable to achieve desired performance. The results of the numerical simulations are validated using the TruckSim software package.

To augment the robustness of the LQR controller, Kalman filter is added. The simulation results show that the KF can effectively reject the noise and predict the required states for the LQR controller with sufficient accuracy. Moreover, in the presence of noise, the LQR controller with the assistance from KF can accurately track the system outputs. It is also, indicated that both LQR and LQG controllers can effectively reduce the peak lateral acceleration and yaw rate of the vehicle to achieve enhanced system stability.

Furthermore, a robust control strategy, μ synthesis control, is implemented to design the ATS system in the B-train double. A comparison is made between the LQR and μ synthesis based ATS controllers. It is observed that the μ synthesis controller rejects system noise efficiently, and can track its true characteristic behaviour. Moreover, the μ synthesis controller and the LQR controller are compared in the *worst case* scenario, a random combination of 13 selected parametric uncertainties, which render the system highly susceptible to unstable motion modes. It is indicated that the μ synthesis controller can not only stabilize the system but also effectively reduce the peaks of the lateral acceleration and yaw rates of the vehicle over a wide range of parameter uncertainties.

CHAPTER 6

Conclusions and Recommendations for Future Research

6.1. Conclusions

Over the course of this research, the behaviour of the B-train double was analysed with a focus on enhancing its stability and path following performance at high speeds. Moreover, its threshold performance in terms of lateral acceleration and yaw rate was analysed. Based on an extensive literature survey regarding the stability concerns in LCVs, an active safety technique, Active Trailer Steering (ATS) was adopted. A two-axle ATS system was designed and further analysed for its optimal performance based on the three presented control strategies, namely LQR, LQG and μ synthesis.

The simulation results help understand the vehicle behavior in presence of the subjected system uncertainties. It is noted that the LQR controller based ATS can effectively reduce the peaks of the lateral acceleration and the yaw rates in comparison to the baseline vehicle model.

However, in presence of noise, prominent variation in the LQR controller's performance was observed. When the system is subjected to the measurement noise, the LQR control system is unable to effectively control the vehicle's performance. Moreover, it was observed that the LQR controller exhibits degraded performance when subjected to system uncertainties. A similar trend is observed through TruckSim co-simulations, which helps validate the results obtained using the 4-DOF model.

To address the robustness concerns of the LQR controller, a Kalman filter is added as a state estimator. This combination results in the synthesis of LQG controller. It can be observed from the simulation results that the Kalman filter can capably reject the system noises. KF aids the LQR controller in enhancing the vehicle's performance in the presence of noise. Although, KF is able to reject the measurement noise, it cannot effectively account of parametric uncertainties. Therefore, a robust controller is required for dealing with noise and parametric uncertainties.

A μ synthesis controller was employed to deal with the system uncertainties and to obtain robust vehicle performance. The achieved peak μ value, a parameter for assessing the control system's robustness, was found to be 0.935, which is less than 1 and satisfies the robust performance condition. The μ synthesis controller performed remarkably well in the presence of system uncertainties in comparison to the LQR controlled and the baseline vehicle models. The reduced peaks of lateral accelerations and the yaw rates achieved through μ synthesis controller simulations can efficaciously increase both maneuverability and stability of the B-train double.

Additionally, the μ synthesis controller tracks the vehicle's intended path and smoothens the sudden movements occurring during the single lane change maneuver, thereby enhancing the vehicle's stability and performance. Whereas, the LQR controlled ATS vehicle model was unable to track the trajectories of the baseline vehicle model. Good reference tracking for all vehicle units of the B-train double was observed in the cases related to the μ synthesis controller.

To establish robust performance in random uncertain cases the controller's behavior was analysed in the *worst case*, a random combination of 13 parametric uncertainties that ensures the worst dynamics for the vehicle. As predicted, the μ synthesis controller performed exceptionally well as compared to the LQR controller, which was unable in effectively controlling the vehicle's dynamic behavior. While evaluating the performance of the vehicles for 100 random cases, it was observed that the baseline vehicle undergoes unstable motion in numerous conditions, whereas the robust μ synthesis controller allows the vehicle to maintain stability in every scenario. It can be concluded that the μ synthesis controller for ATS system enhances the vehicle's performance despite the presence of noise and wide ranging parametric uncertainties, and is the superior control technique amongst all the presented control techniques in this thesis.

6.2. Recommendations for Future Research

To improve and enhance the proposed ATS controllers, the following suggestions are recommended for future research.

1. Effective reference model generation is crucial in any reference tracking controller design. Many researchers have proposed more complex reference models that accounts of slip angles etc. Such complex models can be employed with the proposed μ synthesis controller.

2. Driver-software-in-the-loop (DSIL) and driver-hardware-in-the-loop (DHIL) real-time simulations can be applied to evaluate controllers' performance.

3. To augment the path-following performance of the LQR controller a reference yaw rate model may be employed.

Publications

Relevant

1. Lee, E., Kapoor, S., Sikder, T. and He, Y. 'An Optimal Robust Controller for Active Trailer Differential Braking Systems of Car-Trailer Combinations', Int. J. Vehicle Systems and Modelling (2017). (In Press)
2. Sikder T., Kapoor S., and He Y. "Robust Control of Active Trailer Steering Systems for Long Combination Vehicles". Proceedings of the 25th Symposium of the International Association for Vehicle System Dynamics (IAVSD 2017) (2017) (Submitted).
3. Kapoor S., Sikder T., and He Y. "Fault-Tolerant Control of Active Trailer Steering Systems for Multi-Trailer Articulated Heavy Vehicles". Proceedings of the 25th Symposium of the International Association for Vehicle System Dynamics (IAVSD 2017) (2017) (Submitted).
4. Cai, J., Kapoor, S., Sikder, T., & He, Y." Effects of Active Aerodynamic Wings on Handling Performance of High-Speed Vehicles" (No. 2017-01-1592). SAE Technical Paper (2017).

Other

Sikder, T., Kapoor, S., & He, Y. "Optimizing Dynamic Performance of High-Speed Road Vehicles Using Aerodynamic Aids", In ASME 2016 International Mechanical Engineering Congress and Exposition (pp. V007T09A060-V007T09A060). American Society of Mechanical Engineers (2016).

References

[1] Islam, Md Manjurul, He, Yuping, Zhu, Shenjin and Wang, Qiushi. "A comparative study of multi-trailer articulated heavy-vehicle models." Proceedings of the Institution of Mechanical Engineers, Part D: Journal of Automobile Engineering 229.9 (2015): 1200-1228.

[2] Government of Ontario, Ministry of Transportation,"The Ontario Ministry of Transportation Home Page", Ministry of Transportation (MOT), (2013). (Link: http://www.mto.gov.on.ca).

[3] Grislis, Aivis. "Longer combination vehicles and road safety". Transport 25.3 (2010): 336-343.

[4] Haide, Backman and Nordström, Rolf. "Improved performance of European long haulage transport". TFK-Institutet för transportforskning, 2002.

[5] Philipp, Nagl,. "Longer combination vehicles (LCV) for Asia and the Pacific region: some economic implications". United Nations Publications, 2007.

[6] Ingemar, Åkerman and Jonsson, Rikard. "European Modular System for Road Freight Transport: Experiences and Possibilities". TFK-TransportForsK AB, 2007.

[7] Ramberg, K. "Fewer trucks improve the environment: three short become two long, if the EU follows the example set by Sweden and Finland." Transport and Infrastructure, Svenskt Näringsliv (2004).

[8] Vierth, I., Berell, H., McDaniel, J., Haraldsson, M., Hammarström, U., Yahya, M.R., Lindberg, G., Carlsson, A., Ögren, M. and Björketun, U. "The effects of long and heavy trucks on the transport system: Report on a government assignment". Statens väg-och transportforskningsinstitut, 2008.

[9] Regehr, J.D., Montufar, J. and Rempel, G. "Safety performance of longer combination vehicles relative to other articulated trucks." Canadian Journal of Civil Engineering 36.1 (2008): 40-49.

[10] Kharrazi, S., Lidberg, M. and Fredriksson, J. "A generic controller for improving lateral performance of heavy vehicle combinations." Proceedings of the Institution of Mechanical Engineers, Part D: Journal of Automobile Engineering 227.5 (2013): 619-642.

[11] Cheng, C., Roebuck, R., Odhams, A. and Cebon, D. "High-speed optimal steering of a tractor–semitrailer." Vehicle system dynamics 49.4 (2011): 561-593.

[12] Odhams, A.M.C., Roebuck, R.L., Cebon, D. and Winkler, C.B. "Dynamic safety of active trailer steering systems." Proceedings of the Institution of Mechanical Engineers, Part K: Journal of Multi-body Dynamics 222.4 (2008): 367-380.

[13] Cheng, C. and Cebon, D. "Improving roll stability of articulated heavy vehicles using active semi-trailer steering." Vehicle System Dynamics 46.S1 (2008): 373-388.

[14] Abroshan, M., Taiebat, M., Goodarzi, A. and Khajepour, A. "Automatic steering control in tractor semi-trailer vehicles for low-speed maneuverability enhancement." Proceedings of the Institution of Mechanical Engineers, Part K: Journal of Multi-body Dynamics (2016): 1464419316651375.

[15] Fancher, P. and Winkler, C. "Directional performance issues in evaluation and design of articulated heavy vehicles." Vehicle System Dynamics 45.7-8 (2007): 607-647.

[16] Woodrooffe, J.H.F., Leblanc, P. and El-Gindy, M. "Development of Design and Operational Guidelines for the C-converter Dolly." International Symposium on Heavy Vehicle Weights. 1989.

[17] El-Gindy, M., Mrad, N. and Tong, X. "Sensitivity of rearward amplication control of a truck/full trailer to tyre cornering stiffness variations." Proceedings of the Institution of Mechanical Engineers, Part D: Journal of Automobile Engineering 215.5 (2001): 579-588.

[18] Di Cristoforo, R., Blanksby, C. and Germanchev, A. "Performance-based design of an innovative truck-trailer configuration: Safer and more efficient distribution of liquid fuel in Australia." Transportation Research Record: Journal of the Transportation Research Board 1966 (2006): 110-117.

[19] Yu, H., Güvenc, L. and Özgüner, Ü. "Heavy duty vehicle rollover detection and active roll control." Vehicle System Dynamics 46.6 (2008): 451-470.

[20] Frimberger, M., Wolf, F., Scholpp, G. and Schmidt, J. “Influences of parameters at vehicle rollover”. No. 2000-01-2669. SAE Technical Paper, 2000.

[21] Carsten, Oliver. "Trucks involved in fatal accidents." (1984).

[22] Kusters, L.J. "Increasing roll-over safety of commercial vehicles by application of electronic systems." Smart vehicles (1995).

[23] Winkler, C.B., Blower, D., Ervin, R.D. and Chalasani, R.M. “Rollover of heavy commercial vehicles”. No. RR-004. SAE Technical Paper, 2000.

[24] Christensen, T.C. and Blythe, W. “Offtracking: History, Analysis, and Simulation”. No. 2000-01-0465. SAE Technical Paper, 2000.

[25] He, Yuping, Khajepour, A., McPhee, J. and Wang, X. "Dynamic modelling and stability analysis of articulated frame steer vehicles." International Journal of Heavy Vehicle Systems 12.1 (2004): 28-59.

[26] Islam, Md Manjurul and He, Yuping. "Stability Optimization of Articulated Frame Steer Vehicles"." 2nd CIRP Conference on Assembly Technologies and Systems. Toronto, Canada. 2008.

[27] Rangavajhula, K. and Tsao, H.S.J. "Active trailer steering control of an articulated system with a tractor and three full trailers for tractor-track following." International Journal of Heavy Vehicle Systems 14.3 (2007): 271-293.

[28] Rangavajhula, K. and Tsao, H.S.J. "Command steering of trailers and command-steering-based optimal control of an articulated system for tractor-track following." Proceedings of the Institution of Mechanical Engineers, Part D: Journal of Automobile Engineering 222.6 (2008): 935-954.

[29] Islam, Md Manjurul. "Design synthesis of articulated heavy vehicles with active trailer steering systems". Diss. 2010.

[30] Lee, E., Kapoor, S., Sikder, T. and He, Y. (2017) 'An Optimal Robust Controller for Active Trailer Differential Braking Systems of Car-Trailer Combinations', Int. J. Vehicle Systems and Modelling (In Press)

[31] National Highway Traffic Safety Administration. "FMVSS No. 126 electronic stability control systems." Final Regulatory Impact Analysis. March (2007).

[32] Koibuchi, K., Yamamoto, M., Fukada, Y. and Inagaki, S. "Vehicle stability control in limit cornering by active brake". No. 960487. SAE Technical Paper, 1996.

[33] D'Urso, Peter. “Development of H∞ control strategy for a multi-wheeled combat vehicle”. Diss. 2016.

[34] Zhu, Shenjin. “Coordinated control of active safety systems for multi-trailer articulated heavy vehicles”. Diss. University of Ontario Institute of Technology, 2016.

[35] Wang, Qiushi, Zhu, Shenjin and He Yuping. “Model Reference Adaptive Control for Active Trailer Steering of Articulated Heavy Vehicles”. No. 2015-01-1495. SAE Technical Paper, 2015.

[36] Sweatman, Peter, and Coleman Brendan. "Productivity opportunities with steerable axles." 7th International Symposium on Heavy Vehicle Weights & Dimensions Delft, the Netherlands. 2002.

[37] Hata, N., Hasegawa, S., Ito, K. and Fujishiro, T. “A control method for 4WS truck to suppress excursion of a body rear overhang”. No. 892521. SAE Technical Paper, 1989.

[38] Gohring, E., Von Glasner, E.C., Pflug, H.C. and Povel, R. "Optimization of manoeuvrability and directional stability of commercial vehicles by an electronically controlled all-wheel steering system." Vehicle Dynamics. 25th Fisita Congress, October 1994, Beijing. Vol 2. Technical paper no. 945090. 1994.

[39] Pflug, H.C., von Glasner, E.C. and Povel, R. “Commercial vehicles with intelligent rear axle steering systems”. No. 962185. SAE Technical Paper, 1996.

[40] Notsu, I., Takahashi, S. and Watanabe, Y. “Investigation into turning behavior of semi-trailer with additional trailer-wheel steering--a control method for trailer-wheel steering to minimize trailer rear-overhang swing in short turns”. No. 912570. SAE Technical Paper, 1991.

[41] Jujnovich, Brian Anthony. “Active steering of articulated vehicles”. Diss. University of Cambridge, 2006.

[42] Islam, Md Manjurul, Ding, Xuejun and He, Yuping. "A closed-loop dynamic simulation-based design method for articulated heavy vehicles with active trailer steering systems." Vehicle system dynamics 50.5 (2012): 675-697.

[43] Ding, Xuejun, Mikaric, Steve and He, Yuping. "Design of an active trailer-steering system for multi-trailer articulated heavy vehicles using real-time simulations." Proceedings of the Institution of Mechanical Engineers, Part D: Journal of automobile engineering 227.5 (2013): 643-655.

[44] Islam, Md Manjurul, He, Yuping and Webster, Timothy D. "Automated design synthesis of articulated heavy vehicles with active trailer steering systems." ASME 2010 International Design Engineering Technical Conferences and Computers and Information in Engineering Conference. American Society of Mechanical Engineers, 2010.

[45] Tabatabaei Oreh, S.H., Kazemi, R., Azadi, S. and Zahedi, A. "A new method for directional control of a tractor semi-trailer." Australian Journal of Basic and Applied Sciences 6.12 (2012): 396-409.

[46] Kim, K.I., Guan, H., Wang, B., Guo, R. and Liang, F. "Active steering control strategy for articulated vehicles." Frontiers of Information Technology & Electronic Engineering 17 (2016): 576-586.

[47] Wang, Qiushi. “Design and validation of active trailer steering systems for articulated heavy vehicles using driver-hardware-in-the-loop real-time simulation”. Diss. University of Ontario Institute of Technology, 2015.

[48] Aurell, J. and Edlund, S. “The influence of steered axles on the dynamic stability of heavy vehicles”. No. 892498. SAE Technical Paper, 1989.

[49] Palkovics, L. and El-Gindy, M. "Examination of different control strategies of heavy-vehicle performance." Transactions of the ASME-G-Journal of Dynamic Systems Measurement and Control 118.3 (1996): 489-498.

[50] Hac, A., Fulk, D. and Chen, H. "Stability and control considerations of vehicle-trailer combination." SAE International Journal of Passenger Cars-Mechanical Systems 1.2008-01-1228 (2008): 925-937.

[51] Lee, Eungkil. “Design optimization of active trailer differential braking systems for car-trailer combinations”. Diss. University of Ontario Institute of Technology, 2016.

[52] Gu, D.W., Petkov, P. and Konstantinov, M.M. “Robust control design with MATLAB®”. Springer Science & Business Media, 2014.

[53] Bansal, A. and Sharma, V. "Design and analysis of robust H-infinity controller." Control Theory and Informatics 3.2 (2013): 7-14.

[54] Saeedi, M.A., Kazemi, R. and Azadi, S. "Improvement in the rollover stability of a liquid-carrying articulated vehicle via a new robust controller." Proceedings of the Institution of Mechanical Engineers, Part D: Journal of Automobile Engineering (2016): 0954407016639204.

[55] Levant, Arie. "Principles of 2-sliding mode design." automatica 43.4 (2007): 576-586.

[56] Hajiyev, C. and Vural, S.Y. "LQR controller with Kalman estimator applied to UAV longitudinal dynamics." Positioning 4.01 (2013): 36.

[57] Grewal, M.S. "Kalman filtering". Springer Berlin Heidelberg, 2011.

[58] Welch, Greg, and Bishop, Gary. "An introduction to the kalman filter". Proceedings of the Siggraph Course, Los Angeles (2001).

[59] Azuma, R. T. "Predictive tracking for augmented reality" (Doctoral dissertation, University of North Carolina at Chapel Hill).

[60] Cheng, C. and Cebon, D. "Parameter and state estimation for articulated heavy vehicles." Vehicle System Dynamics 49.1-2 (2011): 399-418.

[61] Sen, S. and Bhattacharya, B. "Progressive damage identification using dual extended Kalman filter." Acta Mechanica (2016): 1-11.

[62] Dinc, Mustafa, and Hajiyev, C. "Integration of navigation systems for autonomous underwater vehicles." Journal of Marine Engineering & Technology 14.1 (2015): 32-43.

[63] Yang, Y. and Gao, W. "An optimal adaptive Kalman filter." Journal of Geodesy 80.4 (2006): 177-183.

[64] Eva Wu, N., Zhang, Y. and Zhou, K. "Detection, estimation, and accommodation of loss of control effectiveness." International Journal of Adaptive Control and Signal Processing 14.7 (2000): 775-795.

[65] Chrif, L. and Kadda, Z.M. "Aircraft control system using LQG and LQR controller with optimal estimation-Kalman filter design." Procedia Engineering 80 (2014): 245-257.

[66] Piłat, A. and Włodarczyk, P. "The μ-synthesis and analysis of the robust controller for the active magnetic levitation system." Automatyka/Akademia Górniczo-Hutnicza im. Stanisława Staszica w Krakowie 15.1 (2011): 85-98.

[67] Kaiser, G. “Torque Vectoring-Linear Parameter-Varying Control for an Electric Vehicle”. Verlag Dr. Hut München, 2015.

[68] Yuan, W. and Katupitiya, J. "Design of a μ Synthesis Controller to Stabilize an Unmanned Helicopter”. 28th International Congress of the Aeronautical Sciences, 2012.

[69] Skogestad, S. and Postlethwaite, I. “Multivariable feedback control: analysis and design. Vol. 2”. New York: Wiley, 2007.

[70] Yin, G.D., Chen, N., Wang, J.X. and Wu, L.Y. "A study on μ-synthesis control for four-wheel steering system to enhance vehicle lateral stability." Journal of dynamic systems, measurement, and control 133.1 (2011): 011002.

[71] Zhou, K., Doyle, J.C. and Glover, K. “Robust and optimal control. Vol. 40”. New Jersey: Prentice hall, 1996.

[72] Corno, M., Tanelli, M., Boniolo, I. and Savaresi, S.M. "Advanced yaw control of four-wheeled vehicles via rear active differential braking". Decision and Control, 2009 held jointly with the 2009 28th Chinese Control Conference. CDC/CCC 2009. Proceedings of the 48th IEEE Conference on. IEEE, 2009

[73] Bansal, A. and Sharma, V. "Design and analysis of robust H-infinity controller". Control Theory and Informatics 3.2 (2013): 7-14.

[74] Minaker, B.P., Yang, X. and Li, S. “Design Optimization of an SAE Baja Vehicle Using the EOM Open Source Multibody Dynamics Code”. CSME International Congress 2014.

[75] Minaker, B.P. and Rieveley, R.J. "Automatic generation of the non-holonomic equations of motion for vehicle stability analysis". Vehicle System Dynamics 48.9 (2010): 1043-1063.

[76] Ellis, J., “Vehicle Dynamics”, Business Books, Ltd., London, 1969.

[77] El-Gindy, M. and Wong, J.Y. "A comparison of various computer simulation models for predicting the directional responses of articulated vehicles." Vehicle System Dynamics 16.5-6 (1987): 249-268.

[78] Sweatman, P.F. and McFarlane, S., 2000.”Investigation into the specification of heavy trucks and consequent effects on truck dynamics and drivers”. Department of Transport and Regional Services, 2000.

[79] Truck and Bus Powertrain Steering Committee. “A Test for Evaluating the Rearward Amplification of Multiarticulated Vehicles”. SAE Standard J, 2179.

[80] Bhadu, M., Senroy, N., Kar, I.N. and Sudha, G.N. "Robust linear quadratic Gaussian-based discrete mode wide area power system damping controller". IET Generation, Transmission & Distribution 10.6 (2016): 1470-1478.

[81] Mishra, S., Mallesham, G. and Sekhar, P.C. "Biogeography based optimal state feedback controller for frequency regulation of a smart microgrid". IEEE Transactions on Smart Grid 4.1 (2013): 628-637.

[82] Naik, N., Gemson, R.M.O. and Ananthasayanam, M.R. "Introduction to the Kalman filter and tuning its statistics for near optimal estimates and cramer rao bound." arXiv preprint arXiv:1503.04313 (2015)

[83] Oberoi, Dhruv. "Enhancing roll stability and directional performance of articulated heavy vehicles based on anti-roll control and design optimization". Diss. UOIT, 2011.

[84] Williams, R.L. and Lawrence, D.A. "Lawrence. Linear state-space control systems". John Wiley & Sons, 2007.

[85] Doumiati, M., Charara, A., Victorino, A. and Lechner, D. "Vehicle Dynamics Estimation using Kalman Filtering: Experimental Validation". John Wiley & Sons, 2012.

APPENDIX 1

4-DOF B-train double model system matrices A and B, where $A = M^{-1}K$ and $B = M^{-1}N$ Below mij, kij and nij represents the elements of matrices M, K and N respectively. i represents row while j represents columns.

$m11 = d * m;$

$m12 = I;$

$m13 = 0;$

$m14 = 0;$

$m15 = 0;$

$m16 = 0;$

$m21 = m;$

$m22 = 0;$

$m23 = m1;$

$m24 = 0;$

$m25 = m2;$

$m26 = 0;$

$m31 = e * m;$

$m32 = 0;$

$m33 = 0;$

$m34 = I1;$

$m35 = -f * m2;$

$m36 = 0;$

$$m41 = 0;$$

$$m42 = 0;$$

$$m43 = 0;$$

$$m44 = 0;$$

$$m45 = -j * m2;$$

$$m46 = I2;$$

$$m51 = 1;$$

$$m52 = -d;$$

$$m53 = -1;$$

$$m54 = -e;$$

$$m55 = 0;$$

$$m56 = 0;$$

$$m61 = 0;$$

$$m62 = 0;$$

$$m63 = 1;$$

$$m64 = -f;$$

$$m65 = -1;$$

$$m66 = -j;$$

$$k11 = ((C1 * (a + d)) + (C2 * (d - b1)) + (C3 * (d - b2)))/u;$$

$$k12 = (((C1 * a * (a + d)) - (C2 * b1 * (d - b1)) - ((C3 * b2 * (d - b1))))/u) - (d * m * u);$$

$$k13 = 0;$$

$$k14 = 0;$$

$$k15 = 0;$$

$$k16 = 0;$$

$$k21 = (C1 + C2 + C3)/u;$$

$$k22 = (((C1 * a) - (C2 * b1) - (C3 * b2))/u) - (m * u);$$

$$k23 = (C4 + C5 + C6)/u;$$

$$k24 = ((-(C4 * h1) - (C5 * h2) - (C6 * h) - (/u) - (m1 * u);$$

$$k25 = (C7 + C8 + C9)/u;$$

$$k26 = (((-C7 * k1) - (C8 * k2) - (C9 * k3))/u) - (m2 * u);$$

$$k31 = (e * (C1 + C2 + C3))/u;$$

$$k32 = (((e * a * C1) - (e * b1 * C2) - (e * b2 * C3))/u) - (e * m * u);$$

$$k33 = (-(C4 * h1) - (C5 * h2) - (C6 * h) - (/u;$$

$$k34 = ((C4 * h1 * h1) + (C5 * h * hhC + (C6 * h * C3))/u;$$

$$k35 = -(f * (C7 + C8 + C9))/u;$$

$$k36 = f * ((((k1 * C7) + (k2 * C8) + (k3 * C9))/u) + u * m2);$$

$$k41 = 0;$$

$$k42 = 0;$$

$$k43 = 0;$$

$$k44 = 0;$$

$$k45 = ((-((j + k) * C7) - ((j + k2) * C8) - ((j + k3) * C9)))/u;$$

$$k46 = ((((j + k1) * k1 * C7) + ((k2 * (j + k2) * C8) + (k3 * (j + k3) * C9))/u) + (j * m2 * u);$$

$$k51 = 0;$$

$$k52 = -u;$$

$k53 = 0;$

$k54 = u;$

$k55 = 0;$

$k56 = 0;$

$k61 = 0;$

$k62 = 0;$

$k63 = 0;$

$k64 = -u;$

$k65 = 0;$

$k66 = u;$

$n11 = -(a + d) * C1;$

$n21 = -C1;$

$n31 = -e * C1;$

$n41 = 0;$

$n51 = 0;$

$n61 = 0;$

APPENDIX 2

The parameter values for the linear 4-DOF yaw-plane B-train double model are given below.

Parameter		Values	
u	Vehicle Forward Speed	Minimum	55km/h
		Nominal	88km/h
		Maximum	105km/h
I	Moment of inertia of the tractor	19665kgm^2	
I_1	Moment of inertia of the first trailer	Minimum (-60%)	175996.8 kgm^2
		Nominal	439992kg kgm^2
		Maximum (+30%)	571987.6 kgm^2
I_2	Moment of inertia of the second trailer	Minimum (-60%)	175996.8 kgm^2
		Nominal	439992 kgm^2
		Maximum (+30%)	571987.6 kgm^2
a	Distance of front axle from the CG of the tractor	1.384m	
d	Distance between the CG of the tractor and the first hitch point	4.251m	
m	Total mass of the tractor	8528 kg	
m_1	Total mass of the first trailer	Minimum (-55%)	8098.65 kg
		Nominal	17997 kg
		Maximum (+25%)	22496.25kg
m_2	Total mass of the second trailer	Minimum (-55%)	8098.65 kg
		Nominal	17997 kg

		Maximum (+25%)	22496.25kg
C_1	Cornering stiffness of the front axle of the tractor	450,000N/rad	
C_2	Cornering stiffness of the rear axles of the tractor	Minimum (-28%)	259,200N/rad
		Nominal	360,000N/rad
		Maximum(+37.5%)	495,000N/rad
C_3	Cornering stiffness of the rear axles of the tractor	Minimum (-28%)	259,200N/rad
		Nominal	360,000N/rad
		Maximum(+37.5%)	495,000N/rad
C_4, C_5, C_6	Cornering stiffness of the axles of the first trailer	Minimum (-52.5%)	209,000N/rad
		Nominal	440,000N/rad
		Maximum(+18.5%)	521400N/rad
C_7, C_8, C_9	Cornering stiffness of the axles of the second trailer	Minimum (-52.5%)	209,000N/rad
		Nominal	400,000N/rad
		Maximum(+18.5%)	521,400N/rad
b_1	Distance of second axle from the CG of the tractor	3.616m	
b_2	Distance of third axle from the CG of the tractor	4.886m	
h_1	Distance between the CG of the first trailer and the fourth axle	3.845m	
h_2	Distance between the CG of the first trailer and the fifth axle	5.115m	
h_3	Distance between the CG of the first trailer and the sixth axle	6.385m	
k_1	Distance between the CG of the second trailer and seventh axle	6.385m	
k_2	Distance between the CG of the second trailer and eighth axle	5.115m	

k_3	Distance between the CG of the second trailer and the ninth axle	6.385m
k_t	understeer coefficient of the LCV combination	0.00029 s^2/m^2